XXXVI PhD course in Applied Biology and Experimental Medicine

DEPARTMENT OF CHEMICAL, BIOLOGICAL,

PHARMACEUTICAL AND ENVIRONMENTAL SCIENCES

UNIVERSITY OF MESSINA

Dr. Sarah Adriana Scuderi

SSD BIO/14

Involvement of TBK1 and PREP signalling pathways in Glioblastoma Multiforme progression: novel therapeutic perspectives

Supervisor: **Chiar.ma Prof. ssa Emanuela Esposito**

Coordinator: **Chiar.ma Prof. ssa Nunziacarla Spanò**

Anno Accademico 2022/2023

Table of contents

Part I

Abstract

Gliomas are common malignant brain tumours, among which glioblastoma multiforme (GBM) has the worst prognosis. Different studies revealed that inflammation plays a key role in GBM pathogenesis. TANK-Binding Kinase 1 (TBK1) is a serine/threonine protein kinase; it is a member of the IκB kinase (IKK) family which is involved in NF-κB pathway activation. Evidence have proven high levels of TBK1 in GBM patients, suggesting that its inhibition could represent a valid strategy to counteract cancer progression by modulating inflammatory process. Moreover, in the last years great attention was focused on the role of prolyl-endopeptidase (PREP), a serine protease involved in the release of pro-angiogenic and anti-fibrogenic molecules. Various angiogenic factors such as vascular endothelial growth factor (VEGF) and angiopoietins (Ang) are up regulated in GBM that generate highly permeable and functionally immature blood vessels, contributing to tumor growth. Thus, the modulation of angiogenesis process through PREP inhibition could represent another possible strategy to counteract GBM growth. Therefore, based on these findings, the aim of the present thesis was to investigate the key roles of TBK1 and PREP signalling pathways in GBM, and the beneficial effects of BX795, TBK1 inhibitor, and KYP-2047, PREP inhibitor, using an *in vitro, ex vivo* and *in vivo* model of GBM. *In vitro* data demonstrated that BX795, TBK1 inhibitor, at the concentrations of 1 μM and 10 μM was able to reduce GBM cell viability, exerting a cytotoxic effect in GBM cell lines. The key role of TBK1 in the pathogenesis of GBM was demonstrated by an *in vitro* and *ex vivo* model, showing that the treatment with BX795 was able to significantly reduce TBK1, as well as NIK, IKKα, TNF-α, and SOX3 expression, counteracting inflammatory process. Additionally, BX795 significantly modulated angiogenesis by a downregulation of VEGF and IRF3 levels. *In vivo* results demonstrated that KYP-2047, PREP inhibitor, at doses of 2.5 mg/kg and 5

mg/kg was able to reduce tumor growth by a significant reduction of PREP level. Moreover, KYP-2047 significantly reduced VEGF, angiopoietin, and endothelial-nitric-oxide synthase (eNOS) expression, counteracting angiogenesis. In conclusion, these findings have proven that TBK1 and PREP are involved in GBM pathogenesis, demonstrating that BX795, thanks to its anti-inflammatory effect, as well as KYP-2047, thanks to its angiogenic effect, could represent alternatives therapeutics strategies for GBM treatment, whose mortality rate is increasing.

Keywords: glioblastoma multiforme, brain tumour, TANK-Binding Kinase 1, prolyl-endopeptidase, temozolomide.

List of abbreviations:

Glioblastoma multiforme: GBM

Central nervous system: CNS

Temozolomide: TMZ

TANK-Binding Kinase: TBK1

Prolyl-endopeptidase: PREP

Prolyl-oligopeptidase: POP

IκB kinase ε: IKKε

Vascular endothelial growth factor: VEGF

Endothelial nitric oxide synthase: eNOS

Angiopoietins: Ang

Regulatory factor for interferon 3: IFN3

Interferon-β: IFN-β

Epidermal growth factor receptor: EGFR

Tumor protein p53:TP53

Phosphatase and tensin homolog: PTEN

Phosphoinositide-3-kinase catalytic alpha: PIK3Cα

Protein kinase B: AKT

Tumor necrosis factor-α: TNF-α

Chapter I: Introduction

1. Introduction

Gliomas are common malignant brain tumor that originate from glial cells [1] and represent diffusely infiltrative tumors affecting the surrounding brain tissue [2]. Gliomas are classified into: pilocytic astrocytomas (Grade I), which are benign tumours that occur primarily in children; astrocytomas, oligodendrogliomas and oligoastrocytomas which correspond to low-grade (II) or high-grade (III and IV) and can progress to glioblastoma multiforme (GBM) [2]. Among gliomas, GBM is the most common and aggressive primary tumor of the central nervous system (CNS) [1]; GBM is classified into two groups: isocitrate dehydrogenase (IDH)-wildtype GBM, which has been referred to as primary GBM and represents about 90% of cases [3], and IDH-mutant GBM, which is developed from a lower-grade diffuse glioma and represents 10% of cases [3]. The current standard treatments for GBM include surgical resection, followed by radiotherapy, and chemotherapy [4, 5]. Among chemotherapeutic agents, Temozolomide (TMZ) is the most used for the treatment of newly diagnosed GBM (ndGBM) [6]. However, current therapies have limited impact on improving the prognosis of GBM patients [7]; therefore, the research of alternative therapeutic approaches represents an important goal in the field of oncological research. Recent reports have proven that more than 140 gene mutations are involved in GBM progression, as EGFR (epidermal growth factor receptor), TP53 (tumor protein p53), PTEN (phosphatase and tensin homolog), PIK3Cα (phosphoinositide-3-kinase catalytic alpha) [7, 8]. Despite the exacts pathogenic mechanisms of GBM are not fully understood, studies revealed that inflammation significantly contribute to GBM progression [9-11]. Inflammation represents an integral component of cancer pathology [11, 12] and it has a great impact on the composition of the tumour microenvironment (TME) and on the plasticity of tumour cells, contributing to tumorigenesis [13]. One common hallmark of GBM is tissue necrosis accompanied by

microenvironment inflammation [11]. Immunosuppressive inflammation with associated necrosis is typical of GBM that display higher resistance to therapies and a worst prognosis [11]. GBM cells are able to secrete various immune suppressive chemokines and cytokines, including interleukin (IL)-6, IL-10, transforming growth factor (TGF)-β, galectin-1 and prostaglandin-E, which act on infiltrating immune cells to hijack them by inducing a protumour cellular phenotype, stimulating GBM cell proliferation, migration, angiogenesis and resistance to treatments [11, 14]. Based on these findings, particular attention was given to the role of TANK-binding kinase 1 (TBK1) in cancer progression [15, 16]. TBK1 is a serine/threonine kinase belonging to the IKB kinase (IKK) family, which plays important roles in the regulation of many cellular processes, including inflammatory cytokine production, innate immunity, apoptosis, and cell proliferation [15, 17]. Its binding with IKKε (IκB kinase ε), a key component of nuclear factor-κB (NF-κB) signalling, activates NF-κB and interferon regulatory factor (IRF) pathways, which consequently promote inflammatory process through the activation of important factors involved in cancer development, such as protein kinase B (Akt) and tumor necrosis factor (TNF) receptor associated factor-2 (TRAF2), and inhibits apoptosis by promoting Bcl-X_L activity [17]. Studies demonstrated an increased expression and/or aberrant activity of TBK1 in several cancer type [16, 18] as breast cancer, cervical cancer, colorectal cancer, and gastric cancer, demonstrating that TBK1 may promote neoplastic cell survival and tumor growth through proinflammatory cytokine production and apoptosis pathway alteration [19, 20]. The tumorigenic activities of TBK1 are not only mediated by mechanisms described above, but also by attenuating the antitumor functions of the immune system, which occurs through upregulation of immune checkpoint ligands and the maintenance of an immunosuppressive molecular signature in the tumor microenvironment [21]. Based on these findings, in the last years, several TBK1 inhibitors have been developed as BX795 [22]. BX795 was originally identified as a

potent 3-phosphoinositide-dependent protein kinase (PDK1) inhibitor, but it has been shown to inhibit mostly TBK1 and IKKε, showing anti-inflammatory effects [23]. It has been demonstrated that BX795 is able to suppress the activity of the regulatory factor for interferon 3 (IFN3) and the production of interferon-β (IFN-β) in macrophages [24]. Recently, interesting properties of BX795 have been proven by *in vivo* and *in vitro* models, suggesting its possible use for the treatment of many cancer types, including primary pancreatic ductal adenocarcinoma and melanoma [20, 25].

Furthermore, gliomas, including GBM, are highly vascular brain tumours [26]. Numerous angiogenic factors such as vascular endothelial growth factor (VEGF) and angiopoietins (Ang) are up regulated in GBM which generate highly permeable and functionally immature blood vessels, contributing to tumor growth [26]. Recently, different studies revealed the key role of prolyl-endopeptidase (PREP), a serine peptidase, in the process of carcinogenesis [27, 28]. PREP is an 80 kDa enzyme that belongs to the serine proteases family, a set of enzymes which have the ability to cleave peptides at internal proline residues[29]. PREP is widely distributed in the CNS and peripheral tissues; it has been implicated in the release of pro-angiogenic, and anti-fibrogenic molecules, and proline-containing bioactive peptides, including angiotensins, arginine-vasopressin, substance P, neurotensin and thyrotropin releasing hormone [27, 30]. PREP has also been shown to be involved in several physiological and pathological functions such as inflammation, neuronal signalling, angiogenesis, cell cycle and differentiation [30, 31]. Recently, Liu and collaborators [32] observed high protein levels of PREP in several malignant tumours, suggesting a correlation between PREP and cancer growth. Thus, in the last decade, potent substrate-like PREP inhibitors have been developed like 4-phenyl-butanoyl-L-prolyl-2(S)-cyanopyrrolidine (KYP-2047) which is one of the most effective and widely studied [33]. KYP-2047 demonstrated the ability to modulate angiogenesis

process by PREP inhibition, but also cell cycle and differentiation, showing interesting effects [28, 30, 31, 34]. However, not much is known about the exacts molecular mechanisms of TBK1 and PREP in GBM pathogenesis. Therefore, based on these findings, the aim of the present thesis was to investigate the role of TBK1 and PREP in GBM and the beneficial effects of BX795, as TBK1 inhibitor, and KYP-2047, as PREP inhibitor, to counteract cancer progression by an *in vitro, ex vivo* and *in vivo* model of GBM.

Chapter II: Glioblastoma Multiforme

2. Glioblastoma Multiforme

GBM is the most common primary brain malignancy in adults and one of the most aggressive cancers [7]. GBM, a grade IV astrocytoma, is an intrinsic brain tumor thought to originate from neuroglial stem or progenitor cells [35]. In adults, GBM occurs most often in the cerebral hemispheres, especially in the frontal and temporal lobes of the brain. It accounts for 16 % of all primary brain tumours and represents half of gliomas [35]. The incidence of GBM increases with age, and the rates are highest in the 75 to 84 years old age-group. The relative survival estimates for GBM are quite low: less than 5 % of patients survive 5 years post-diagnosis [36]. Histologically, GBM is a diffuse, grade IV glioma of the astrocytic lineage (WHO Classification of Tumors of the CNS, 4th edn, 2007) and it is characterized by the presence of pleomorphic cells, mitotic activity, intravascular microthrombi, necrosis and microvascular proliferation [37]. Based on the presence or absence of a precursor lesion, two major morphological subtypes are distinguished: primary GBM is the most common type (~90 %) which arises *de novo*, without evidence of a precursor lesion, and typically occurs in older adults (>50 years), while secondary GBM evolves from a pre-existent, lower-grade astrocytoma (WHO grades II or III) [37]. GBM is a devastating brain cancer that can result in death in six months or less, if untreated; hence, it is imperative to seek expert neuro-oncological and neurosurgical care immediately, as this can impact overall survival [35]. The current standard therapy for GBM consists of surgical resection followed by radiotherapy and chemotherapy with Temozolomide (TMZ). However, several aspects make it difficult to efficiently treat gliomas, i.e., the anatomical location, the presence of the blood-brain barrier (BBB), which hampers the delivery of therapeutic compounds to the tumor site, and the restricted immune reactivity within the CNS [38, 39]. GBM remains a cancer of a high mortality rate, low patient survival and acquired resistance to therapy. The

aggressive nature of GBM, including unconstrained growth, invasion into the normal brain parenchyma and resistance to therapy, indicates that GBM cells are able to develop mechanisms to survive and proliferate under restrictive conditions [40]. Nonetheless, despite these limitations, intense research has opened up opportunities to explore tailored therapies and to study in depth cell survival mechanisms used by GBM cells in order to develop new treatments to counteract cancer growth (Figure 1).

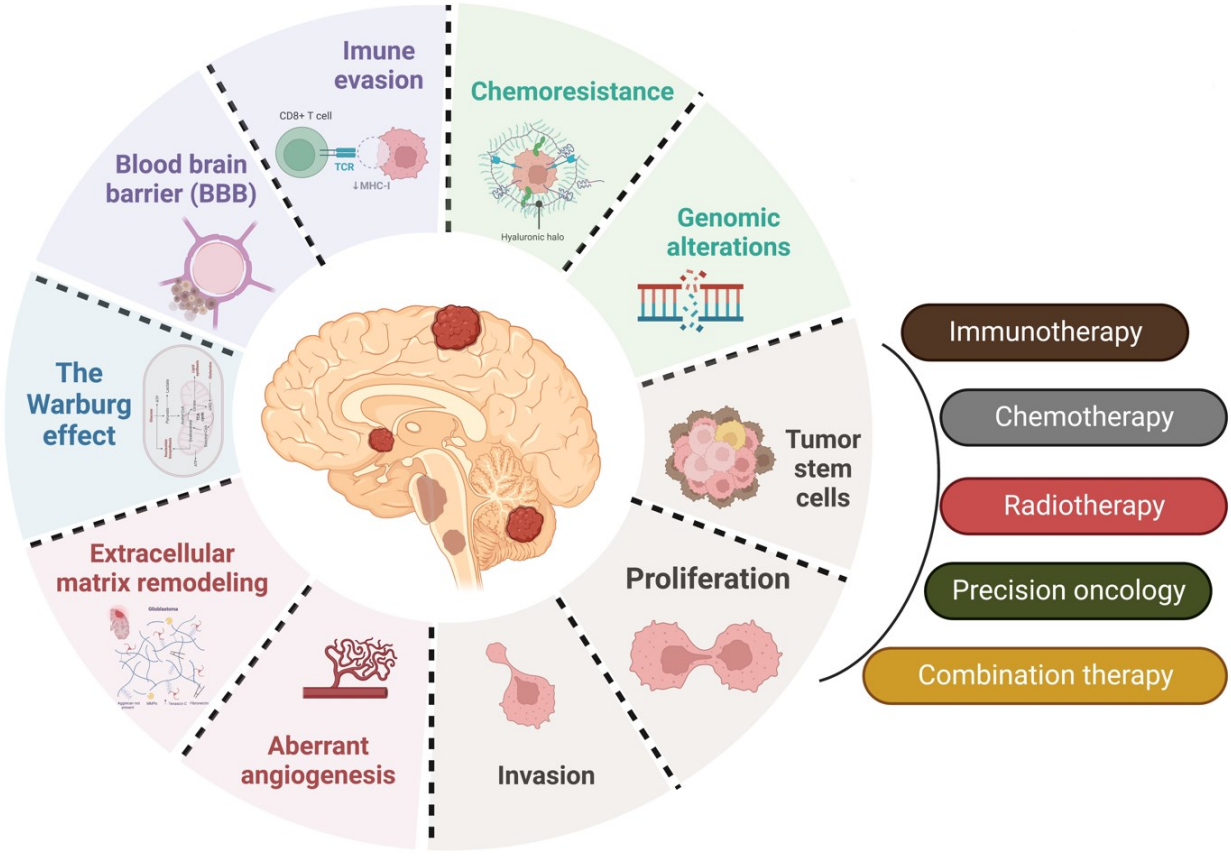

Figure 1. Hallmarks of GBM (Adapted figure from [39]).

2.1 Etiopathogenesis

The etiology of GBM remains unknown in most cases [41]. Since the 1960s more than 116 cases of GBM have been reported resulting from radiation exposure; it has been estimated that the overall risk of developing GBM following radiotherapy is 2.5% [41,

42]. It has also been reported that relatively low doses of radiation that are used to treat tinea capitis and skin haemangioma in children or infants have also been associated with relative risks for gliomas [36, 43]. Extensive retrospective cohort data also show clearly increased risk of glioma in pediatric populations after exposure to therapeutic intracranial radiation, that is both patient age- and radiation dose/volume-dependent. Furthermore, patients who received treatment for Acute lymphoid leukemia (ALL) were more prone to develop GBM, which could be a result of complications arising from the leukemia or the chemotherapeutic agents used to treat ALL [42]. However, some pesticides and other agricultural chemicals, such as organochlorides and alkylureas combined with copper sulfates, have been suspected as risk factors for brain tumors [43]. Few studies have shown the possible role of ovarian steroid hormones in development of GBM [44]. Nevertheless, there are not substantial evidence of association with lifestyle characteristics, such as cigarette smoking, alcohol consumption, drug use, or dietary exposure to nitrous compounds [41] (Figure 2).

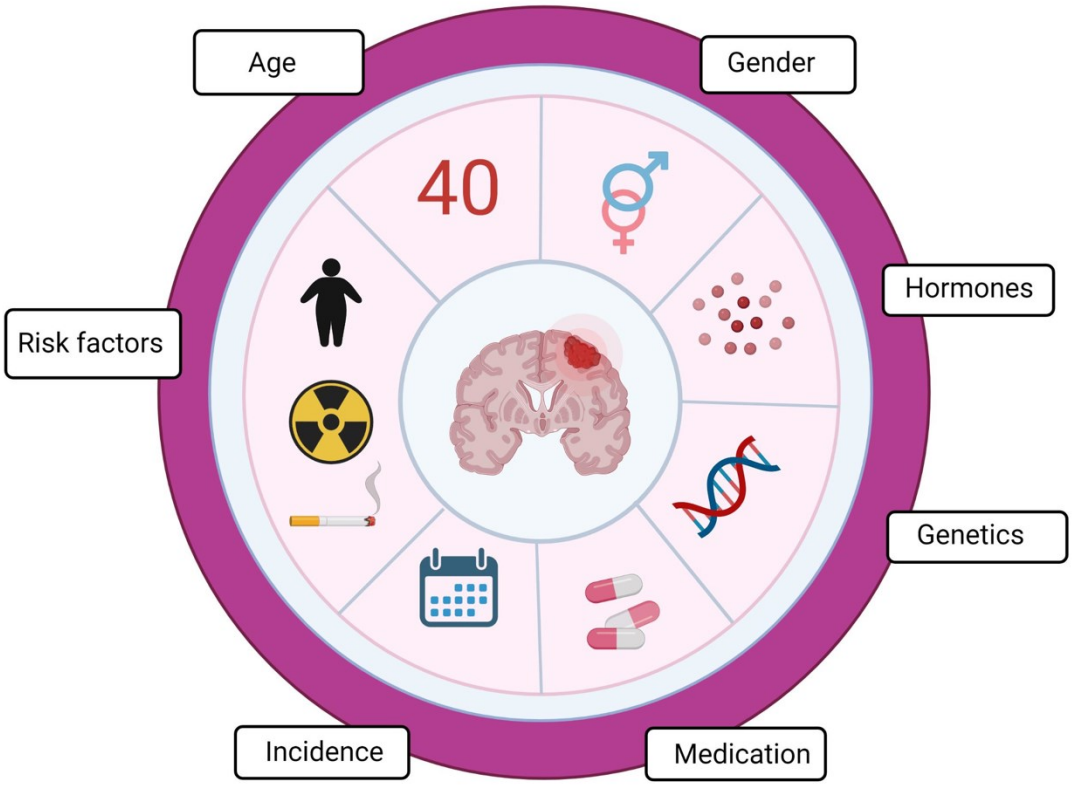

Figure 2. Etiopathogenesis of GBM (Figure from [36]).

Understanding GBM pathogenesis represents a fundamental goal not only in identifying disease biomarkers but also in designing and developing potential chemotherapeutic agents. In the last decade, significant advances have been made in the understanding of processes leading to GBM, and several important genetic defects that appear to be important for the development and progression of this tumor have been identified:

- ATRX (a-thalassemia/mental-retardation-syndrome-X-linked) mutation:

The ATRX gene located on Xq21.1 encodes a protein involved in the chromatin-rearrangement pathway, allowing histone H3.3 to be incorporated into heterochromatin. ATRX mutations occur in approximately 57% of secondary GBM; in GBM cells, ATRX mutations occur more frequently in IDH-mutant GBM than in wildtype (71% vs. exceptions) [36]. ATRX mutations are positive prognostic factors [36].

- TERT (Telomerase Reverse Transcriptase) promoter mutation:

The TERT gene encodes telomerase, an enzyme responsible for adding the missing 3′ end of a DNA strand during replication [45]. The mutation of the TERT gene promoter results in increased telomerase activity and telomere elongation, suggesting that maintaining the presence of telomeres is essential for brain tumor formation [46]. TERT mutations are present in up to 80% of GBM; they occur more frequently in IDH-wildtype GBM than IDH-mutant GBM (72% vs. 26%) [47].

- TP53 (Tumor protein P53) mutation:

The TP53 gene is located on human chromosome 17p13.1. The functional p53 protein is a homotetramer that plays a key role in the regulatory network, controlling proliferation, survival, and genome integrity. The presence of TP53 mutations is associated with the progression of GBM [36]. The inactivation of p53 correlates with increased invasiveness, decreased cell apoptosis, and increased proliferation [48]. Cell lines carrying the p53-inactivating mutation show greater resistance to DNA-damaging chemotherapeutics, such as cisplatin [50]. TP53 mutations are more common in IDH-mutant GBM than IDH-wildtype GBM (81% vs. 27%) [49]. In GBM, TP53 mutation increases malignancy of cells by promoting their proliferation, migration, invasion, metastasis, drug resistance, genome instability, and increasing survival [50].

- B-RAF V600E mutation:

B-RAF is part of the RAS-RAF-MEK-ERK MAP kinase pathway which is responsible for cell growth. Mutations that confer the constitutive B-RAF kinase activity would result in uncontrolled cell proliferation and tumor formation [36]. The V600E mutation involves the substitution of valine for glutamate at position 600 of the B-RAF protein, producing the permanently activated serine/threonine kinase B-RAF, which activates extracellular

signal-regulated kinase 1 and 2 (ERK1/2) and other mitogen-activated protein (MAP) kinases [51]. The frequency of all B-RAF mutations in GBM is estimated at 2–6% [51].

- FGFR1 (Fibroblast Growth Factor Receptor (1)):

The FGFR family of proteins is a group of transmembrane receptors with tyrosine kinase function. The exact impact of signalling by FGFR on the pathobiological aspects of individual cancers remains unknown [52]. However, it has been demonstrated that FGFR1 is associated with increased radio-resistance, invasiveness, and stemness in GBM [52].

- EGFR (epidermal growth factor receptor):

EGFR is a receptor with tyrosine kinase activity that is activated by EGF (epidermal growth factor) which promotes cell proliferation by activating the MAPK and PI3K-Akt pathways [36]. The EGFR gene is located at locus 7p12 and its amplification is observed in approximately 40% of GBM cases. The amplification of EGFR has been associated with poor prognoses. EGFR amplification is more common in IDH-wildtype GBM than IDH-mutant GBM [53]. The most common EGFR mutation is variant-III EGFR mutation (EGFRvIII), involving a deletion without a shift of the reading frame of base pair 801 extending from exon 2 to 7 [53].

- PTEN (Phosphatase and tensin homolog):

The PTEN gene is a suppressor gene located on 10q23. LOH (loss of heterozygosity) or methylation mutation disrupt the pathways that use phosphatidylinositol 3-kinase (PI3K) and are found in at least 60% of GBM cases [54]. Loss of PTEN function due to mutation or loss of heterozygosity (LOH) is associated with poor prognosis of GBM [54]. PTEN is a protein with protein phosphatase and lipid phosphatase functions, and most of the onco-suppressive properties are due to the lipid phosphatase properties [55]. The

PI3K/Akt pathway is blocked by PTEN, and loss of functional PTEN impairs the regulation of cell survival, cell growth, and proliferation [36]. According to Koul [54], loss of PTEN expression is indicative of the progression of a highly malignant tumor-PTEN is present in most low-grade tumors.

2.2 Epidemiology

GBM is one of the most aggressive malignancies of CNS, accounting for 14.5% of all central nervous system tumors and 48.6% of malignant central nervous system tumours [36]. The median overall survival (OS) of GBM patients is low, at only 15 months [36]. It is difficult to clearly define the incidence of GBM as it varies depending on the report, from 3.19 cases per 100,000 person-years to 4.17 per 100,000 person-years [36, 56]. The incidence in the pediatric population (0–18 years) is 0.85 per 100,000, where pediatric glioblastoma multiforme (p-GBM) accounts for 3–15% of primary brain tumors [36]. Dobes and co-authors [57] reported an increasing incidence of GBM in patients aged over 65 years from 2000 to 2008 in Australia with an annual percentage change (APC) of 3.0 (95% confidence interval [CI], 0.5–5.6). Besides, it has been reported an increase in the percentage (from 24 to 27%) of patients over 70 years of age with GBM between 2000 and 2013 in Finland [58]. Specifically, the 2019 report from the Central Brain Tumor Registry of the US (CBTRUS) provided the incidence rates and incidence trends of GBM by age group (0-14 years, 15-39 years and 40+ years) [59]. In the last years, some reports have proven that the western world has higher incidence of gliomas then less developed countries [60], which could be due to under reporting of gliomas cases, limited access to health care and differences in diagnostic practices. Furthermore, the ratio of incidence of GBM is higher in men compared to women [60].

2.3 Glioblastoma Multiforme subtypes

The international standard for the nomenclature and diagnosis of GBM is the World Health Organization (WHO) classification.

According to the WHO classification and the degree of malignancy, GBM is divided into the following groups:

- Isocitrate dehydrogenase (IDH)-wild type GBM (about 90% of cases) corresponding most frequently to the clinically defined primary or *de novo* without evidence of a less malignant precursor; it is predominant in patients aged over 55 years [56].

- IDH-mutant GBM (about 10% of cases) corresponding closely to the secondary GBM, which develop from initially low-grade diffuse astrocytoma (WHO grade II diffuse astrocytoma) or anaplastic astrocytoma (Grade III), and preferentially occurring in younger patients (mean age = 40 years) [56].

- Not otherwise specified GBM (NOS), which is reserved for those tumors for which full IDH evaluation cannot be performed [56].

- Not-elsewhere-classified GBM (NEC) occurring in the case of discrepancies between the clinical, histological, immunohistological, and genetic features of the tumour [56].

Genetic alterations more typical for primary GBM are EGFR overexpression, PTN mutation, and loss of chromosome 10, whereas genetic alterations commonly seen in secondary GBM include IDH1 mutations, and TP53 mutations [43, 56]. IDH1 mutation is associated with better outcome and increased overall survival. Interestingly, IDH1 mutations are also found in 80% of diffuse astrocytoma and anaplastic astrocytoma, the precursors of secondary GBM, and in less than 5% of primary GBM [56].

One provisional new variant of GBM has been added to the classification: epithelioid GBM. Epithelioid GBM features large epithelioid cells, with abundant eosinophilic cytoplasm, vesicular chromatin, prominent nucleoli (often resembling melanoma cells), and variably present rhabdoid cells. GBM with primitive neuronal component was added as a pattern in GBM [56]. This pattern, previously referred to in the literature as GBM with PNET-like component, usually comprised of a diffuse astrocytoma of any grade (or oligodendroglioma in rare cases) that has well-demarcated nodules containing primitive cells that display neuronal differentiation [49].

Recently, gene expression analyses of patient-derived tumour cells revealed three distinct GBM subtypes, classical, proneural and mesenchymal, which are classified based on their molecular genotypes [61].

All these molecular subtypes of GBM are driven by the gain-of-function of receptor tyrosine kinases (RTKs) and/or the loss of tumour suppressor activities (including PTEN, TP53, NF1 and CDKN2a). These events lead to the overactivation of the mitogen-activated protein kinase (MAPK) and phosphatidylinositol-3-kinase (PI3K) pathways, which stimulate cell growth and proliferation [61]. The classical subtype is characterized by loss of chromosomal 10, mutations in TP53 and IHD1, hyperactivation of the RTK EGFR, with the most frequent variation being the expression of EGFRvIII, a truncated mutant that lacks the extracellular ligand-binding domain and signals constitutively in the absence of growth factors [61]. In comparison, the overexpression of the RTK PDGFRA is associated with the proneural subtype, whereas the loss of NF1 is linked to the mesenchymal subtype. Moreover, the proneural subtype is associated with younger age at diagnosis [61, 62].

2.4 Morphological aspects of GBM

The current standard diagnosis of GBM is based on histopathological classification, which provides a grading of tumor malignancy.

Histologically, GBM shows significant inter-tumor and intra-tumor heterogeneity, different mutations and phenotypic states, as well as indistinct epigenetic states reflect the genomic instability that leads to therapeutic choices and variable clinical outcomes [63]. GBM commonly shows dense proliferation of highly atypical and pleomorphic cells, necrosis, and microvascular proliferation [63]. GBM cells have shown extensive variability of cell morphology that is characterized by the coexistence of small cells and multinucleated giant cell, polygonal to spindle-shaped with increased nuclear to cytoplasmic ratios, moderate nuclear pleomorphism, coarsely clumped hyperchromatic chromatin, and irregular nuclear membranes [63]. GBM presents binucleated and multinucleated cells, as well as lymphocytes, neutrophils, macrophages and necrotic cells with some intranuclear inclusions [64]. Necrotic foci are one of the most characteristic features of the GBM. Histologically, two types of necrosis are typically encountered, depending on localization and size of the necrotic area [65]. The first one consists of large areas of necrosis within the central area of the tumor, resulting from insufficient blood supply. The other type contains small, irregularly shaped necrotic foci surrounded by densely packed, somewhat radially oriented small tumour cells (‘pseudopalisading areas’) [65].

Several studies have shown that GBM shares common molecular features with metastatic cancers [66-68] like sequential switching between proliferation and invasion responsible for the formation a dense network of vessels tortuous and hyperpermeable, with increased excessive production of pro-angiogenic factors, which result in uncontrolled proliferation, infiltration and progression of tumor mass [41]. GBM cells undergo a series of molecular and conformational changes shifting the tumor towards mesenchymal traits,

including extracellular matrix (ECM) remodelling, cytoskeletal re-patterning, and stem-like trait acquisition [68]. Actually, clinical evidence suggests that some GBMs are more disseminated than others; it has been proven that mesenchymal-subtype GBM show an increased potential to invade in comparison to its neural, proneural, and classical counterparts [69]. However, in light of the overall poor outcome from current therapies, a better understanding of molecular mechanisms of GBM may provide innovative therapies for this rapidly progressing disease.

2.5 Diagnosis

One of the main problems of GBM management is related to the lack of effective diagnostic strategies. Currently, the main diagnostic methods for the detection of gliomas are based on neurological tests and neuroimaging methods [70]. Magnetic resonance imaging (MRI) is an essential tool used for detecting, characterizing and monitoring brain tumours and typically utilizes various sequence types which highlight distinct and complementary brain tissue characteristics including the tumor core, tissue necrosis and surrounding edema [71]. Late diagnosis of GBM is mainly caused by the slow dissemination process typical of brain tumors, which allows structures to gradually adapt to both compression and deformation caused by the tumor mass [71]. For this reason, even in the case of pronounced morphological signs of tumor penetration into brain tissue, clinical manifestations may be completely absent. However, a major drawback comes in patients which make use of antiangiogenic drugs or chemo-radiotherapy, that can significantly deceive the results coming from neuroimaging analyses, thus making the follow-up even more difficult [70]. The clinical presentation of GBM depends on the tumor location and size at diagnosis [70]. The most common presentation at diagnosis is a headache and/or nausea or edema [72]. Symptoms related to intracranial hypertension represent 30% of clinical signs followed by motor deficit (20%), loss of body weight

(17%), confusion (15%), visual or speech deficit (13%), epilepsy (15–20%) [72]. These symptoms are often associated and lead to a diagnosis in the weeks or months following their onset [72].

2.6 Therapeutical approaches

Conventionally, the primary therapeutic option for patients with GBM includes surgical removal followed by radiotherapy and chemotherapy with TMZ which is the most used chemotherapeutic agent in the field of GBM [65].

Despite these rigorous treatments, tumor relapse is almost inevitable due to aggressiveness of the tumor and resistance to chemo- and radiotherapy. To date, GBM remains incurable, with only a median survival of 15 months [41]. Thus, the identification and development of innovative therapeutic strategies like gene therapies, and immunotherapies, for the treatment of GBM are of critical concern.

2.6.1 Surgery

Whenever possible, the first step consists in complete macroscopic surgical resection. Literature data suggest that a resection > 90% of the contrast enhancement of the lesion in patients with no comorbidities improves the patient outcome at the time of diagnosis and recurrence [72]. Surgical resection is usually proposed to patients under the age of 70 in good condition (Karnofsky scale > 70) and a tumor accessible to complete removal [72]. Otherwise, surgical debulking or stereotactic biopsy is performed to confirm the diagnosis before adjuvant therapy. Due to the importance of a complete resection on survival, advances in surgical techniques have been made such as awake craniotomy or neuromonitoring to improve the resection quality and prevent subsequent deficits [73]. Fluorescence-guided surgery has been developed to guide the resection with better outcomes on resection and progression-free survival [74]. More recently, resection

devices have evolved with the use of Laser-Interstitial Thermal Therapy (LITT), which provides a less invasive, percutaneous approach through the insertion of an optical fiber [75]. Another technique is Mass Spectrometry Imaging (MSI) which has been studied to analyse the spatial distribution of lipids in preclinical and clinical GBM samples, suggesting a possible classification of GBM based on changes in lipid profiles between different morphological tissue regions [76].

2.6.2 Radiotherapy and Chemotherapy

The standard of care for patients aged less than 70 relies on radiotherapy (RT) which is given for a six-week period, and adjuvant TMZ [77]. TMZ, a prodrug alkylating agent, is an oral chemotherapy that crosses the blood–brain barrier (BBB). The mechanism of action of TMZ consists of add a methyl group to purine and pyrimidine in DNA, resulting in damage to cells and ultimately apoptosis [78]. During the RT and then, for six cycles of five consecutive days per month, TMZ is administered daily one per month after the end of the RT [79]. This protocol improved the overall survival in a large, randomized phase III trial [79]. However, approximately 55% of GBM patients are resistant to TMZ because of their methyl guanine methyl transferase (MGMT) DNA repair system, which transfers the methyl group from guanine, thereby repairing damaged DNA and counteracting cytotoxic effects of TMZ on tumor cells [78]. An interesting protocol by Jablonska and collaborators [80] proposed hypofractionated radiotherapy and TMZ, depending on the patient's general condition. Furthermore, it has been demonstrated that RT alone could have a positive impact on survival of GBM patients (29.1 weeks compared to 16.9 weeks in patients with supportive care alone) without any alteration of the quality of life [81]. Recently, some researches have shown that short-course RT plus TMZ was associated with longer survival (9.3 versus 7.6 months) in older patients (>65 years) [82]. However, although TMZ has slightly increased the survival of patients, it is also

responsible for inducing many side effects, such as: headache, constipation, nausea, vomiting, diarrhea, loss of appetite, hair loss.

2.6.3 Alternative therapies: Immunotherapies

Over the last decades, the use of immunotherapy for brain tumours has intensely grown. Immunostimulatory gene therapy and immune checkpoint inhibitors might prove as a promising therapeutic approach for treating patients with GBM [83]. Various preclinical studies have demonstrated the success of immunotherapy-based approaches in different *in vivo* models [83-85]. Many phase I and II clinical trials have shown immunotherapy to be safe and, in some cases, lead to improved progression-free survival (PFS) [84, 86]. Among the various types of immunotherapies, T cell immunotherapy has recently become a promising therapy to treat brain tumours [86]. Engineered T cell therapy has gained great attention as a possible effective therapeutic approach to target solid tumors, including GBM [83]. In recent years, promising anticancer effect of chimeric antigen receptor (CAR)-T cell therapy for various cancers has been shown, and Food and Drug Administration (FDA) has also permitted two CAR-T products commercially [87]. A study performed by Bagley and colleagues [88] demonstrated that CAR-T cell therapy can significantly enhance the survival of mice with glioma by targeting the epidermal growth factor receptor variant III (EGFRvIII), which is expressed in approximately 30% of patients with GBM. Moreover, EGFRvIII targeted CAR-T cells have also been developed using T cells from patients with GBM [85], confirming its therapeutic effect *in vitro* against glioma stem cell lines. However, GBM is characterized by high molecular heterogeneity which may limit the efficacy of the treatment via evading the targeted immune response; for this purpose, additional studies are needed.

Chapter III:

Role of TANK-binding kinase 1 (TBK1)

in cancer

3. Role of TANK-binding kinase 1 (TBK1) in cancer

TANK-binding kinase 1 (TBK1; also known as NF-κB-activating kinase/NAK and T2K) is a serine/threonine kinase belonging to the non-canonical inhibitor of nuclear factor-κB (IκB) kinase (IKK) family [17]. TBK1 plays important roles in the regulation of many cellular processes, including innate immunity, inflammatory cytokine production, autophagy, mitochondrial metabolism, cell survival and proliferation [17]. The biological activity of TBK1 was first recognized in innate defence against pathogens for its role in regulating the production of type I interferons (IFN), including IFN-α and IFN-β [89]. However, recent studies have demonstrated that TBK1 binds the pathogen-stimulated processes of inflammation, immunity, and proliferation involved in several human diseases, including type II diabetes, obesity, neurodegenerative diseases, and cancer [16, 33, 90]. In the context of malignancies, TBK1 acts oncogenically, promoting tumorigenesis through different cellular mechanisms [19]. The involvement of TBK1 in several cancer types such as: non-small cell lung cancer (NSCLC), pancreatic ductal adenocarcinoma (PDA), acute myeloid leukemia (AML), diffuse large B-cell lymphoma (DLBCL), melanoma, and breast cancer, has been described in detail [16, 18, 91]. However, not much is known about the molecular mechanisms of TBK1 in brain tumours including GBM. Therefore, a better knowledge of its role in cancer pathogenesis is needed to identify new molecular target and new therapeutic strategies to counteract tumor growth.

3.1 TANK-binding kinase 1 (TBK1): protein structure and related-mutations

TBK1 is a non-canonical IKK kinase encoded by *tbk1* gene located at 12q14.1 which contains 21 exons. TBK1 consists of 729 amino acids (aa), and it is constitutively expressed across all tissues; however, higher TBK1 expression has been observed in fibroblasts, CNS, skin, adipocytes, and cancer cells [19]. The kinase domains of TBK1

and IKKε share a 64% amino acid sequence identity among each other. TBK1 possesses four functionally distinct domains: a kinase domain (KD; aa1-307) at the N-terminus, two putative coiled-coil-containing regions in the C-terminal (region CCD1; aa407-657 and CCD2; aa659-713), including a C-terminal leucine zipper (LZ) and a helix-loop-helix (HLH) motif, and an ubiquitin-like domain (ULD; aa308-384) [19]. The ULD is a regulatory component of TBK1, and it is involved in the control of kinase activation, substrate presentation, and downstream signalling pathways [92]. The LZ and HLH motifs mediate dimerization, which is necessary for their functions. The KD is critical for the phosphorylation of various substrates, including IRF3 [19]. The Lys38, Asp135, and Ser172 residues within the KD constitute a key phosphorylation site for kinase activity and functioning of TBK1 through ATP binding. The ULD domain regulates kinase activity via its hydrophobic patch at Leu352/Ile353. The CCD1, also called scaffold dimerization domain (SDD), harbors a leucine zipper domain (LZ; aa499-527) and a helix-loop-helix domain (HLH; aa591-632), both of which mediate dimerization. Instead, the CCD2 at the C-terminus harbors an adaptor-binding motif which facilitates the interaction of TBK1 with adaptor proteins, such as TANK, NAK–associated protein (NAP1), TBKBP1 (TBK1-binding protein 1; also known as SINTBAD), or optineurin (OPTN) [19]. These proteins bind to TBK1 in a mutually specific manner, thus determining the ensuing subcellular localization of TBK1 and subsequent specificity of downstream signalling [19].

In the last years, an alternatively spliced form of TBK1 (named TBK1s) lacking exons 3-6 has been described in several human and mouse cells lines; it is suggested to inhibit pathways normally activated by full length TBK1 [89].

Mutations in *TBK1* were found in different diseases such as amyotrophic lateral sclerosis (ALS), frontotemporal dementia (FTD), childhood herpes encephalitis (HSE), and

normal-tension glaucoma (NTG) [92-94]. Gain-of-function mutations in TBK1 are correlated with NTG, while failure-of-function mutations affect ALS, FTD and HSE [93]. Mutations in *TBK1* are found in about 1% of patients with familial ALS and approximately 1% of patients with sporadic ALS [95]. Two different heterozygous missense mutations (p.G159A and p.D50A respectively) have been found in the KD of two unrelated European children with HSE [93]. These studies demonstrated that the patient carrying the G159A mutation developed HSE at 7 years of age and subsequently developed epilepsy and cognitive disabilities; while the patient carrying the D50A mutation developed HSE at 11 months of age and suffered from obesity, cognitive and motor dysfunctions [93]. It has been demonstrated that mutations in the KD can influence phosphorylation of substrates, while mutations within the ULD might influence employment to ubiquitinated proteins and organelles. As discussed above, CCD1 and CCD2 are essential for TBK1 functioning and for its interaction with adaptor proteins, so mutations within CCD1 and CCD2 may influence TBK1 activation and TBK1-associated signalling pathways including inflammation, apoptosis, and autophagy [93].

Despite it has been revealed that *TBK1* mutations are not common in human cancer, studies demonstrated that deletion of *TBK1* can affect several cellular processes in cancer [19]. According to this, a report demonstrated that deletion of *TBK1* in dendritic cells (DCs) causes T cell activation, autoimmune symptoms and enhances antitumor immunity in animal models of melanoma and thymoma, suggesting a role for TBK1 in restraining tumor immune response [19].

3.2 TBK1- mediated signalling pathways

TBK1 is activated downstream by pattern-recognition receptors (PRRs), such as toll-like receptor (TLR) 3 and TLR4, which initiate a signalling cascade in response to conserved molecular patterns associated to pathogens [17]. TLR3 recognises double-stranded RNA

(dsRNA) that activates the intracellular receptors retinoic acid-inducible gene I (RIG-I) and melanoma differentiation-induced protein 5 (MDA5). Consequently, MDA5 transduces the signalling through mitochondrial antiviral-signalling protein (MAVS) which activates stimulator of interferon genes (STING) by cyclic GMP-AMP synthase (cGAS), and TBK1 [96]. TLR3, MAVS and STING pathways converge on TBK1 activation, inducing the formation of TBK1 dimers or TBK1/IKKε heterodimers [96]. Once activated, TBK1 continues the signalling cascade, by phosphorylating NF-κB and interferon regulatory factor 3 and 7 (IRF3/7). The primary function of TBK1 is to induce the production of type I IFN, such as IFN-α/β, in innate immune cells by phosphorylation of IRF3 and IRF7 on multiple Ser and Thr residues [90]. The phosphorylated IRFs form homo- and/or hetero-dimers, which translocate into the nucleus, and bind IFN-stimulated response elements (ISRE) in the promoters of target genes [17]. IRF dimers control target gene expression by cooperating with other transcription factors, such as NF-κB, and SMADs. TBK1 activates NF-κB signalling by phosphorylating several members of this pathway, including RelA, cRel, and IκBα. TBK1-mediated activation of NF-κB seems highly dependent on cell- and signal-specific contexts. The activation of both IRF3 and NF-κB pathways mediates an immune defence against tumors [17]. Once activated, NF-κB cooperates with IRF3 to promote inflammation through the release of inflammatory cytokines, such as TNFα, IL-8 and IL-1β, and induce proliferation by regulating survival/proliferative genes, including Bcl-X_L, Cyclin D1, and RelB [17]. In addition to regulating the expression of important genes for immune and inflammatory responses, TBK1 through NF-κB activation also modulates apoptosis process by regulating Bcl-X_L belonging to Bcl2 proteins family [90]. The Bcl2 family consists of many proteins with an opposite role as Bcl2 and Bcl-X_L which inhibit apoptosis, and other proteins, such as Bax and Bak which promote cell death, exerting a pro-apoptotic effect [97]. Each of these

factors influences the cleavage-mediated activation of caspases, which act as the ultimate downstream effectors of the suicide program [97].

Furthermore, it has been shown that TBK1 can influence the autophagy flux by directly regulating mTOR activity [98], a serine/threonine protein kinase belonging to the PI3K-related kinase (PIKK) family. Autophagy is a fundamental biological process of self-digestion whereby a cell degrades various intracellular components, including damaged or excessive proteins and organelles, as a reactive survival mechanism or as a strategy to maintain cellular energy production [99]. Autophagy is often deregulated in human cancers; in fact, it may function as a tumor suppressor or tumor promoter depending on the tumor source and/or stage [100]. Chronic innate immune activation of TBK1 suppresses mTOR complex 1 (mTORC1) activity by phosphorylating RAPTOR, a component of mTORC1, promoting consequently autophagy [101]. Conversely, it has been demonstrated that TBK1 can activate mTOR in response to several growth factors or pathogen recognition receptors, such as TLR3, to control innate immune functions, thus suggesting that TBK1's role is cell type and context-dependent [102]. Furthermore, TBK1 has been shown to interact with others autophagy receptors and adaptor proteins, including OPTN, and p62 (SQSTM1) [103].

Another important function of TBK1 is to modulate angiogenesis process. In this context, Korherr and colleagues [104] revealed that TBK1 and IRF3 can be activated in response to hypoxia. Under hypoxic conditions, TBK1 is able to modulate the expression of hypoxia-inducible factor-1α (HIF-1α) via the NF-κB signalling pathway, thereby regulating the expression of VEGF, one of the most important proangiogenic factors. These factors stimulate tumor angiogenesis by promoting the proliferation of endothelial cells, suggesting that TBK1 may function as an angiogenic effector [104].

In summary, TBK1 acts as a central player in the processes of innate immune during the response to pathogens and inflammation, as well as in apoptosis and angiogenesis [19] (Figure 3). However, further studies are needed to better understand its role in these pathways.

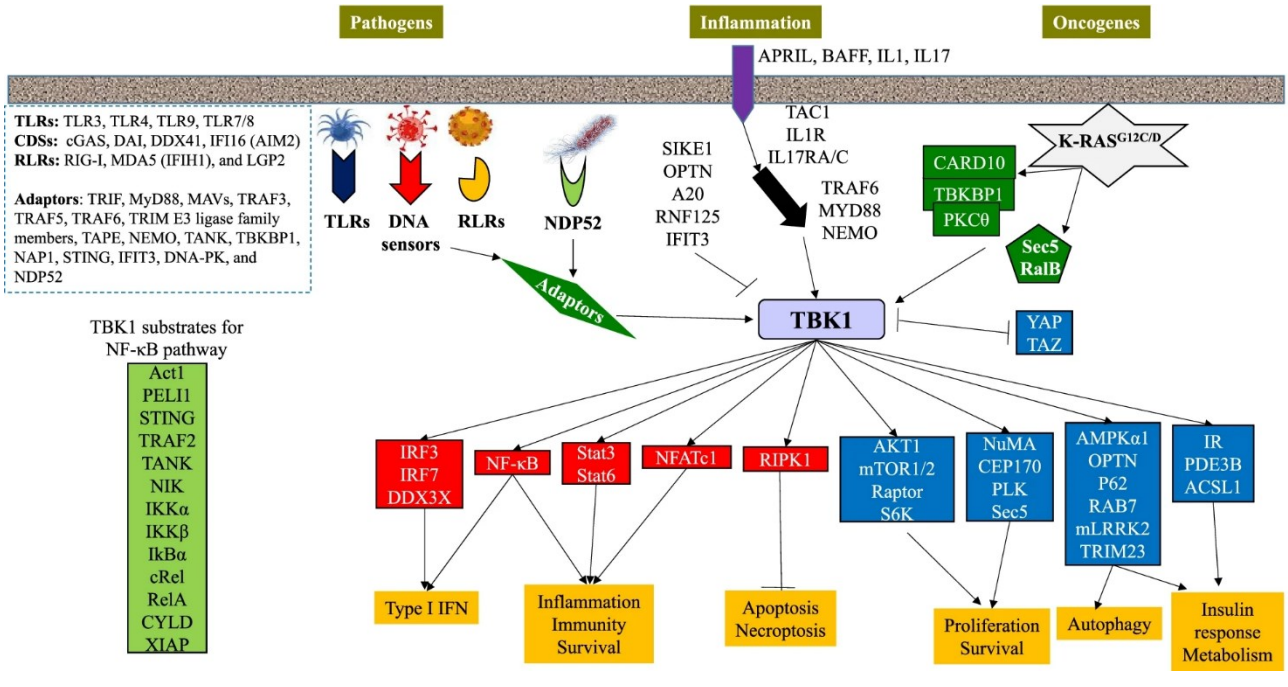

Figure 3. TBK1 mediated-signalling pathways (Figure from [19]).

3.3 TBK1 in the pathogenesis of cancer

Increasing evidence revealed that TBK1 participates to numerous signalling pathways that influence cell transformation and tumor progression [15]. Although TBK1 mutations are not common in human cancers, increased expression and/or aberrant activity of TBK1 have been reported in several cancer types such as pancreatic ductal adenocarcinoma (PDA), cholangiocarcinoma, melanoma, and breast cancer, suggesting that TBK1 could be an attractive molecular target to develop new antineoplastic drugs [16, 89]. TBK1

activation in tumor cells can be promoted by pathogen associated molecular patterns (PAMPs), damage-associated molecular patterns (DAMPs), inflammatory cytokines, oncogenic kinases, and receptor tyrosine kinases (such as K-RAS/N-RAS) [19]. TBK1 plays an important role in activating anti-apoptotic pathways in cells mutated for the proto-oncogene KRAS [19]. Accordingly, it has been demonstrated that in cancer cells harbouring a KRAS-activating mutation, TBK1 promotes cancer cell survival and proliferation by activating NF-κB and mTOR1 pathways, both of which contribute to tumorigenesis [89]. TBK1 can stimulate cancer development and progression through several mechanisms [18]:

- stimulating survival and proliferation signals in cancer cells;
- mediating the production of tumorigenic and immunosuppressive cytokines;
- suppressing anticancer functions of the immune system by upregulating the expression of immune checkpoint ligands.

In the cytoplasm of cancer cells, TBK1 drives tumor development and progression by stimulating numerous cell survival and proliferation pathways, including NF-κB, AKT-mTOR1, and p62/autophagy [105, 106].

The involvement of TBK1 in diffuse large B-cell lymphoma (DLBCL), breast cancer, K-RAS-mutant pancreatic ductal adenocarcinoma (PDA), melanoma, and non-small cell lung cancer (NSCLC) has been described in detail [19, 20, 107].

In diffuse large B-cell lymphoma (DLBCL), TBK1 mRNA levels are negatively correlated with the prognosis. In DLBCL cells, TBK1 mediates the activation of canonical NF-κB signalling via phosphorylation of p65/RelA on Ser536, which promotes the production of IL-10, CCL3, and CCL4; consequently, these cytokines promote tumorigenesis by stimulating STAT3 activation[108]. However, it has been demonstrated that treatment with the TBK1/IKKϵ inhibitor DMX3433 attenuates canonical NF-κB

signalling pathway and decreases DLBCL cell viability as revealed by Carr and colleagues [108].

In breast cancers, TBK1 expression is significantly higher compared to matched adjacent normal tissues as demonstrated by immunohistochemical staining of 171 breast cancer samples in a study performed by Wel et al [107]. Specifically, the N-terminal fragment of TBK1 (aa1-510) interacts with the DNA binding domain of estrogen receptor-α (ERα) and phosphorylates it on Ser305, which consequently modulates the transcriptional activity of Erα [107]. Increased expression of TBK1 is positively correlated with ERα and cyclin D1 expression. Patients with tumours highly expressing TBK1 respond poorly to tamoxifen treatment and show a high potential for relapse [107]. However, it has been demonstrated that TBK1 inhibition sensitizes breast cancer cells to tamoxifen-induced cell death [107].

In KRAS-mutant PDA, TBK1 supports the growth and metastasis of pancreatic cells by driving an epithelial plasticity program in tumor cells that enhances invasive and metastatic capacity [109]. Specifically, TBK1 promotes epithelial-mesenchymal transition (EMT), a process in which epithelial cancer cells lose contact with the basement membrane and neighbouring cells while gaining a more mesenchymal and invasive phenotype, typical of pancreatic cancer [109].

In primary melanoma patient samples, TBK1 is hyperactived in a subtype of BRAF/MEK inhibitor-resistant tumor cells; this subtype of melanoma displays hyperactive TLR/innate immune system signalling [110]. TBK1 activation in melanoma cells is primarily stimulated by transforming growth factor-β (TGFβ), a cytokine which consequently promotes tumor cells survival by activating AKT signalling pathway [110].

In NSCLC, Wang et al [111] demonstrated that TBK1 is expressed in 114 (80.3%) of stage I NSCLC patients, showing a relationship with poor overall survival of patients. These data suggested that TBK1 could be an effective prognostic predictor of NSCLC.

3.4 TBK1 inhibitors as novel strategies therapeutics against cancer: focus on BX795

Considering the key role of TBK1 in cancer progression, in the last years several TBK1 inhibitor have been developed, such as: MRT67307, AZ13102909, Amlexanox, Domainex compounds, SR8185 and BX795 which differ for chemical structure, selectivity and potency.

MRT67307. MRT67307 has been developed by University of Dundee, and it is an aminopyrimidine derivative similar to BX795. MRT67307 possesses an IC_{50} value of 19 nM and it doesn't inhibit related TBK1 kinases such IKKα/β, JAK and p38 MAPK up to 10 μM concentration [112]. In macrophages, MRT67307 prevents the production of IFN-β and the phosphorylation of IRF3 without suppressing the activation of NF-κB pathway.

AZ13102909. During the past years, AstraZeneca has reported more than 44 compounds as part of an azabenzimidazole derivative series. Several of these compounds inhibit TBK1 at or below 10 nM concentration. The best compound, AZ13102909, inhibits TBK1 with an IC_{50} value of 5 nM. The treatment with AZ13102909 in combination with MEK inhibitors revealed to increase cancer cell apoptosis in 3D tissue culture models [113].

Amlexanox. Amlexanox is a benzopyrano-pyridine derivative. The pyridine nitrogen and amine in the structure of this compound are responsible for inhibiting TBK1. Amlexanox is an anti-inflammatory drug approved by the FDA to treat recurrent aphthous ulcers of the mouth in the US [114]. Recently, amlexanox demonstrated to have marked anticancer

effects in multiple models of xenografted tumors in mice, including breast, colon, lung, and gastric cancers by inhibiting TBK1 and IKKε [115].

Domainex compounds. The Domainex TBK1 inhibitors, whose name refers to the manufacturing company, are pyrimidinyl compounds with IC_{50} values of 1–2 nM. They inhibit TBK1 but also other kinases such as IKKβ and JAK. These compounds have been tested in animal models of inflammatory disease, showing that they are able to inhibit the production of inflammatory cytokines without exerting any toxicity [116].

SR8185-related compounds. The Scripps Research Institute developed SR8185 with phenylpyrimidine scaffold as a Janus kinase (JAK) inhibitor. However, modification of SR8185 generated SR8185-related compounds able to inhibit TBK1 with an IC_{50} value below 1 nM concentration. These compounds have low molecular weight and high metabolic stability. Their anticancer activity has been demonstrated by several *in vitro* and *in vivo* studies [116].

BX795. Among TBK1 inhibitors, BX795 is the most well-known and widely used compound for its pharmacokinetics properties. BX795 is a weakly basic compound with an aminopyrimidine backbone which is available as a free base and hydrochloride salt [23]. The compound BX795 was originally developed as a small molecule ATP-competitive inhibitor of 3-phosphoinositide-dependent protein kinase 1 (PDK1), but it has been demonstrated to inhibit mostly the catalytic activity of TBK1 and IKKε by blocking their phosphorylation at low nanomolar concentrations *in vitro* [23]. Compared to other TBK1 inhibitors, pharmacokinetics studies about BX795 demonstrated that this compound is able to cross BBB [117]. Increasing evidence has shown that BX795 is a suppressor of phosphorylation, nuclear translocation, and transcriptional activity of IRF3 [118]. BX795 also suppresses the production of IFN-β in macrophages stimulated with polyinosinic:polycytidylic acid (poly(I:C)) or lipopolysaccharide (LPS). Recent studies

revealed that BX795 is able to inhibit other kinases such as JNK (c-Jun N-terminal kinase), p38 MAPK (mitogen-activated protein kinase), ERK8 (extracellular signal-regulated kinase 8), and protein kinase B (AKT) [23, 119]. In particular, it has been proved that BX795 exerts antiviral activity against ocular infection of multiple strains of herpes simplex virus (HSV)-1 by blocking AKT phosphorylation [119]. In the context of cancer, BX795 has been tested in models of neuroblastoma and oral squamous cell carcinoma (OSCC) [120-122]. Chilamakuri and colleagues [120] demonstrated that BX795 significantly inhibited neuroblastoma cell proliferation, and induced apoptosis, by blocking PDK1 activation and AKT phosphorylation. Moreover, they demonstrated that BX795 is able to sensitize neuroblastoma cells to chemotherapy, suggesting that combination of BX795 with current therapies could be a novel, less toxic, and more effective therapeutic strategy to counteract cancer growth [120]. Furthermore, in a model of OSCC, BX795 exhibited a significant antiproliferative effect on OSCC cells by promoting apoptosis through Poly (ADP-ribose) Polymerase (PARP) cleavage [122]. Moreover, BX795 arrested OSCC cells in the mitotic phase, and increased autophagy process by inhibiting AKT and NF-κB signalling pathways [122].

Chapter IV:

Role of Prolyl-endopeptidase (PREP) in cancer

4. Role of Prolyl-endopeptidase (PREP) in cancer

Prolyl-endopeptidase (PREP), also called prolyl oligopeptidase (POP), was first described 50 years ago as an oxytocin cleaving enzyme and it was further characterized as a peptidase able to cleave short peptides at the C-side of an internal proline [123]. PREP is involved in the hydrolysis of under 30-mer proline-containing bioactive peptides, such as: angiotensins, arginine-vasopressin, substance P, neurotensin and thyrotropin releasing hormone [123]. Because of its specificity, and the occurrence of internal proline residues in several neuropeptides, PREP is considered as a peptidase relevant in neuropeptide metabolism [123]. It has been demonstrated that PREP is involved in several physiological and pathological processes such as: inflammation, neuronal signalling, angiogenesis, apoptosis, cell cycle and differentiation [28, 31, 34]. Accordingly, synthesis and testing of PREP inhibitors have gained the attention of industry, especially since evidence demonstrated that PREP inhibition improved cognitive decline and dementia in animal models [124]. However, in the last years, studied revealed a marked increase of PREP expression in several cancer types, suggesting that it plays a key role also in cancer pathogenesis [125].

4.1 Prolyl-endopeptidase (PREP): protein structure and related-mutations

PREP is an 80 kDa enzyme that belongs to the serine proteases family, a set of enzymes which have the ability to cleave peptides at internal proline residue [126, 127]. Mammalian PREP is encoded by *Prep* gene that contains 15 exons. PREP belongs to the family of α/β hydrolase of serine peptidase (S9 in MEROPS), which also includes dipeptidyl peptidase IV (DPP, S9B), acylaminoacyl peptidase (ACC, S9C) and oligopeptidase B (OPB, S9A). PREP hydrolyses peptides at the carboxyl side of proline residue, while DPP liberates dipeptides where penultimate amino acid is proline, OPB

cleaves at arginine and lysine bonds and ACC remove N-acetylated amino acids from blocked peptides [126].

PREP family is different from the classical serine proteases based on their specificity for peptide substrates and their different catalytic triad which contains Ser, His and Asp in carboxy terminal region [126]. Structurally, PREP is composed of two domains, one is a peptidase which is α/β-folds while the other one is β-propeller domain which is based upon seven folds representing the repeats of four stranded anti-parallel β sheets. The N-terminal comprises of β-propeller domain while the α/β folds represent the C-terminal of the protease. The β-propeller domain appears to play a regulatory role, acting as a filter to control the access of specific and not large substrate to the active site of the enzyme [126]. The specificity of PREP in cleaving short peptides and exclusion of large proteins makes it unique.

In peripheral mammal tissues, PREP protein is widely distributed in many organs [30]. Generally, the highest peripheral PREP activities have been found in the kidney, liver, and lungs; however, PREP activities in peripheral tissues are lower than those found in the brain [30]. PREP activity has also been detected from human body fluids, although the activities are low compared to the tissue levels.

Mutations in *PREP* gene have been associated with rare genetic disorder as hypotonia-cystinuria syndrome (HCS), also known as the 2p21 deletion syndrome, and congenital myasthenic syndrome which is a recessive metabolic disorder [128, 129]. Chabrol et al [130] observed respiratory chain deficiency, especially partial cytochrome c oxidase deficiency, in all patients with 2p21 deletion syndrome, suggesting that PREP also exerts a mitochondrial function. Furthermore, *PREP* deletion is associated with growth hormone (GH) deficiency, which usually is related to HCS [131]. However, not much is known about *PREP* mutations in cancer.

4.2 PREP-mediated signalling pathways

Although PREP is present in all organs, it is mostly found in specific cells and cell layers across the brain and peripheral tissues. In the mature healthy brain, PREP is highly expressed in a certain group of neurons in well-defined areas such as the striatum, cortex, hippocampus, and cerebellum [132]. Over the last decade, many studies indicated that PREP has not just one physiological distinctive role, but many roles, depending on the environment in which PREP is located: inside or outside the cell, the type of cell or tissue, or the metabolic or pathological conditions in cells [123, 133]. These roles could be also determined by the kind of interaction with physiological peptides (cleavage substrates or inhibitors) or with other protein partners. Subcellularly, PREP is detected primarily in the perinuclear space closely associated with the microtubulin cytoskeleton, growth cones, and membranes of cell organelles known to be involved in protein synthesis [133]. This subcellular localization reflects regulatory functions of PREP in protein secretion, trafficking, and processing [133].

Many of PREP's functions are mediated through its interactions with some proteins including, thymosin-ß4 (Tß4), VEGF, α-tubulin, and Bax [134-136].

An interesting recent discovery in the biology of PREP concerns its association with Tß4, the most abundant ß-thymosin in mammals [134]. Tß4 is a 43 amino acid peptide which has been proposed to possess cardioprotective properties. Indirect evidence of the involvement of Tß4 in angiogenesis emerges from the observation that it is overexpressed in numerous human cancers [136, 137]. Tß4 is involved in the release of antifibrotic tetrapeptide acetyl-N-Ser-Asp-Lys-Pro (acetyl-SDKP) which is rapidly inactivated in plasma by angiotensin-converting-enzyme (ACE) [138]. It has been shown *in vitro* that PREP is the main enzyme responsible for the cleavage of Ac-SDKP from Tß4 which consequently regulates the dynamics of globular monomeric form of actin (G-actin) and

the transcription of various genes, including VEGF, one of the most important proangiogenic factors [30, 134]. According to this, the study performed by Myöhänen et al [134] demonstrated that PREP has a pro-angiogenic role via the release of Ac-SDKP from its precursor Tß4 and via VEGF regulation, suggesting that PREP inhibitors might prevent the release of Ac-SDKP and modulate angiogenesis process.

On the other hand, it has been suggested that PREP may be implicated also in apoptosis process by cleaving an apoptosis rescue peptide, humanin, at the carboxyl side of a cysteine [139, 140]. Humanin, a peptide of 24 amino acids, prevents the translocation of Bcl2 associated X protein (Bax) from cytosol to mitochondria, inhibiting apoptosis [140]. Humanin, bearing two potential PREP cleavage sites, was shown to be cleaved by PREP, modulating consequently apoptosis pathway [140].

The peptide prolyl-glycyl-proline (PGP), which is a neutrophil activator, has been described to be related with PREP levels in inflammatory lung diseases as chronic obstructive pulmonary disease, and cystic fibrosis, by activating neutrophils thorough CXC receptors [141]. In another report, Jiang et al [142] hypothesized that PREP inhibition would ameliorate disorders of lipid metabolism and hepatic inflammation to prevent non-alcoholic fatty liver disease (NAFLD) progression to non-alcoholic steatohepatitis (NASH), reducing visceral adipose tissue, and improving *de novo* lipogenesis. Authors, in part, relate these findings to previous reports on changes in mitochondrial protein turnover due to PREP inhibition, but also invoke to a possible gene expression control mediated by this peptidase, through a mechanism which involves peroxisome proliferator-activated receptor γ (PPAR-γ) expression modulation, a key gene in the regulation of lipid metabolism [142] (Figure 4).

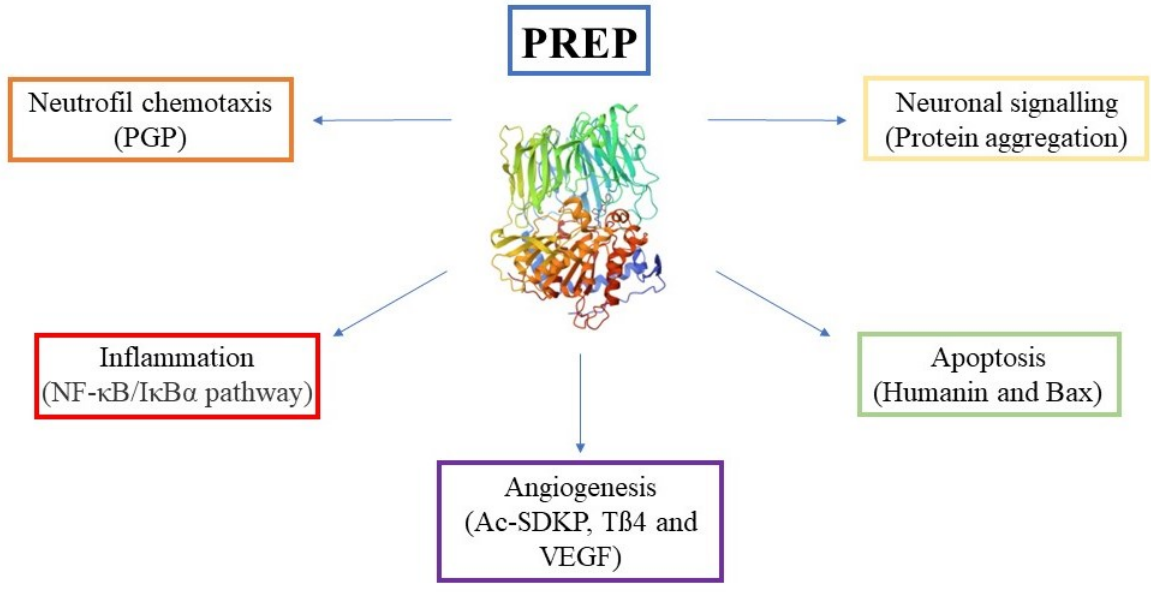

Figure 4. PREP-mediated signalling pathways.

Furthermore, PREP is involved in immune system. Studies revealed that PREP activity is higher in immature thymocytes than in mature thymocytes or in peripheral T-cells, hypothesizing that PREP enzyme activity may be used as a marker to define T cells maturation [143].

However, changes of PREP activity have been found in pathologies where neuroinflammation has a fundamental role, such as multiple sclerosis, depression, and neurodegenerative diseases (NDs) [144-146].

4.3 PREP in the pathogenesis of cancer

Altered expression and catalytic function of peptidases may contribute to several diseases processes, such as neoplastic transformation, local invasion, metastasis, and tumor progression.

Initially discovered in the human uterus, PREP activity and expression has been demonstrated throughout human and other mammalian tissues [27]. Although it has been described as a predominantly cytosolic enzyme, PREP is also found in cell membranes and nucleus. In particular, its nuclear localization in proliferating (peripheral) tissues appears to be associated with proliferation and differentiation of tissues [123]. In the last years, the potential role of PREP in cancer has been suggested. Studies demonstrated an elevated PREP expression in numerous carcinoma types, assuming it may promote cancer development through several mechanisms [27]. Increased cytosolic PREP activity has been proven in head and neck squamous cell carcinoma (HNSCC), squamous cell lung carcinoma (SCLC), colorectal adenoma, and adenocarcinoma [147, 148].

As previously discussed, PREP has been shown to play a key role in the release of the extracellular neutrophil chemoattractant, PGP [141]. Once activated, neutrophils release multiple proteinases such as metalloproteinases (MMPs) which are involved in pathological processes, including carcinogenesis. During the carcinogenesis, tumor cells participate in several interactions with the tumor microenvironment involving the extracellular matrix (ECM), growth factors, ECM-associated cytokines, and surrounding cells (endothelial cells, fibroblasts, macrophages, mast cells, neutrophils, pericytes and adipocytes) which consequently modulate tumor cells migration, invasion, and metastasis [149]. In these processes, MMPs have a central role as they degrade various cell adhesion molecules, modulating cell-cell, and cell-ECM interactions, thus hypothesizing that MMPs, and PGP activation might be associated with high PREP levels in cancer [141].

The expression of several proteases, including MMPs and peptidases, has been reported to play an important role in the development and progression of colorectal adenoma and adenocarcinoma [147]. MMPs, including matrilysin-1 (MMP-7), are overexpressed in the early stages of the colorectal adenoma and adenocarcinoma [147]. Accordingly, highest

activities of PREP were founded in precancerous lesions (adenomatous polyps), suggesting that PREP plays a key role in the early phase of colorectal neoplastic development through MMPs modulation [147, 150].

Since cancer progression depends on tumor neovascularization, proangiogenic factors have a central role in neoplastic diseases. The levels of the proangiogenic peptide Ac-SDKP and VEGF are elevated in numerous malignancies, which may be related to high PREP levels, as reported in a study by Liu and colleagues [32].

Furthermore, another interesting report demonstrated that PREP modulates pancreatic cancer progression through PI3K/AKT/mTOR pathway which is one of the most aberrantly activated signalling pathway in human cancer cells affecting a wide spectrum of cellular functions such as metabolism, proliferation, motility, and survival [151]. Specifically, they demonstrated that depletion or inhibition of PREP blocked feedback activation of PI3K/AKT and enhanced cytotoxicity in mTOR inhibitor (rapamycin)-treated pancreatic cancer cells, reducing cancer progression [151]. Together, these results suggested that PREP plays a central role in pancreatic cancer cells proliferation through PI3K/AKT/mTOR pathway modulation, and that PREP inhibitors could be a valid strategy to counteract cancer growth [151].

4.4 PREP inhibitors as novel strategies therapeutics against cancer: focus on KYP-2047

Changes in PREP expression levels, protein distribution, and activity have been reported in many studies of cancer. Based on the involvement of PREP in numerous cancer types, several PREP inhibitors have been developed, such as: Z-Pro-prolinal, SUAM-14746, JTP-4819, J94, and KYP-2047.

Z-Pro-prolinal. Z-Pro-prolinal (ZPP) is a potent and specific, cell-permeable dipeptide aldehyde inhibitor of PREP with an IC_{50} of 0.4 nM. It has been reported that ZPP is a

putative transition-state analogue for PREP and forms a tetrahedral complex with the enzyme at the active serine site. It has also been shown to inhibit the cleavage of arginine-vasopressin (ARG-Vasopressin), gonadotropin-releasing hormone (GnRH I), and other peptides. Duan et al [151] demonstrated that ZPP is able to reduce pancreatic cancer cell proliferation by modulating AKT-mTORC1 signalling pathway.

SUAM-14746. SUAM-14746 is a specific peptide that inhibits PREP; however, it has been shown to be an activator of the receptor for nerve growth factor (NGF), and an inhibitor of the activity of ion channels. Tanaka et al [152] revealed that SUAM-14746 reduced human breast cancer cell lines proliferation by decreasing cyclin D1 and D3, cyclin-dependent kinase 4 (CDK4), E2F1, and retinoblastoma protein (pRb) expression.

JTP-4819. JTP-4819 is a potent and specific inhibitor of PREP. JTP-4819 exhibited a strong and durable *ex vivo* inhibitory effect on PREP in various regions of the rat brain. In addition, JTP-4819 inhibited the degradation of substance P, arginine-vasopressin, thyrotropin-releasing hormone, neurotensin, oxytocin, bradykinin, and angiotensin II with IC_{50} values of 9.6, 13.9, 10.7, 14.0, 4.5, 7.6 and 10.6 nM, respectively [153].

J94. J94 is a soluble PREP inhibitor which possesses excellent aqueous solubility at neutral pH, low molecular weight, absence of cyclization in aqueous solution, and retention of inhibitory function after prolonged exposure to human plasma. J94 has low nanomolar Ki values for inhibiting PREP. Jackson et al [154] revealed that J94 inhibited growth of human colon cancer xenograft tumors in mice by causing an accumulation of irregularly arranged collagen fibers and widespread apoptosis within the tumor.

KYP-2047. KYP-2047, a pyrrolidine derivative, is currently one of the best characterized PREP inhibitors available [33]. It is a highly specific and potent PREP inhibitor that causes a conformational stabilization of PREP's active site regulating protein-protein interactions; it has a Ki value of 0.023 nM against pig PREP [155]. KYP-2047 is the only

available PREP inhibitor whose brain pharmacokinetics has been described in detail in rats and in mice [124]. It has been demonstrated that after systemic administration in rats, KYP-2047 crosses BBB and penetrates the brain in pharmacologically active concentrations, effectively inhibiting its intracellular target protein PREP [124, 156]. Considering the pharmacokinetics properties of KYP2047 and the role of PREP in NDs such as AD, Parkinson's disease (PD) and dementia, it has been suggested the use of this compound to reduce pathological signs of these diseases [33]. In this context, PREP has shown *in vitro* and *in vivo* to play a key role in α-synuclein (αSyn) protein aggregation which leads to an accumulation of toxic forms that disturb normal neuronal function and result in cell death, typical in PD, dementia with Lewy bodies and other synucleinopathies [157]. Effectively, KYP-2047 prevented the formation of αSyn aggregates in αSyn overexpressing cell lines and increased the clearance of αSyn in two mouse strains carrying the pathogenic human A30P aSyn gene, suggesting the use of this compound to treat NDs [33].

Despite several studies revealed the effects of KYP-2047 in NDs, like AD and PD, not much is known about the possible use of KYP-2047 to treat cancer. Nevertheless, encouraged by the findings about the pharmacokinetics properties of KYP-2047 and the role PREP in cancer, we decided to investigate the effects of KYP-2047 in GBM.

Chapter V: Aim of the thesis I

5. Aim of the thesis I

GBM is one of the most common and aggressive malignancies of the central nervous system (CNS) with an increasing mortality rate worldwide. Despite numerous scientific advances have been made in the field of oncological research, the survival rate of patients with GBM remains very low due to the acquired resistance to therapy and recurrence. As previously discussed, GBM is extremely resistant to most treatments because of its heterogeneous nature, which is associated with extreme clonal plasticity and the presence of cancer stem cells refractory to TMZ- and RT-induced cell death.

Therefore, the research and the development of new molecular target represent an important goal in the field of oncology research. Recent studies focused on the role of TBK1 and PREP signalling pathways in cancer, suggesting that their inhibition could be a valid strategy to counteract cancer growth. However, not much is known about the exacts mechanisms of action of TBK1 and PREP in brain tumours like GBM.

Thus, based on these considerations, the aim of my Ph.D. thesis was to investigate the role of TBK1 and PREP signalling pathways in GBM and the beneficial effects of BX795, TBK1 inhibitor, and KYP-2047, PREP inhibitor, to counteract GBM progression using an *in vitro, ex vivo* and *in vivo* model.

Chapter VI: Materials and Methods

6. Materials and Methods

6.1 In vitro model

6.1.1 GBM cell lines

The human glioblastoma cell lines: U-138 MG (U-138 MG ATCC® HTB-16™ *Homo sapiens* brain glioblastoma) and U-87 MG (U-87 MG ATCC® HTB-14™ *Homo sapiens* brain Likely glioblastomas) were purchased from the ATCC (American Type Culture Collection, Rockville, MD, USA). U-138 and U-87 cell lines are commonly used for glioblastoma studies. GBM cells lines were cultured in a 75-cm^2 flask with, respectively, ATCC-formulated Eagle's Minimum Essential Medium (Catalog No. 30-2003; ATCC) for U-138 MG and Dulbecco's modified Eagle's medium (DMEM; Catalog No. D5030; Sigma-Aldrich, St. Louis, MO, USA) for U-87 MG, both supplemented with antibiotics (penicillin, 1000 U; streptomycin, 0.1 mg/L; Catalog No. P4333; Sigma-Aldrich), l-glutamine (GlutaMAX™, Catalog No. 35050061; ThermoFisher Scientific, Waltham, MA, USA), and 10% (*v/v*) fetal bovine serum (FBS; Catalog No. 12103C; Sigma-Aldrich) in a humidified atmosphere containing 5% CO_2 at 37° C.

6.1.2 Cell treatment

U-87 MG and U-138 MG cells were cultured in six-well culture plates at a density of 2.5×10^5 cells/well. Sixteen hours after seeding, cells were treated with BX795 (Catalog No. 204001; Sigma-Aldrich) at increasing concentrations of 0.1, 0.5, 1, and 10 µM dissolved in culture medium with 0.001% of dimethyl sulfoxide (DMSO) (sc-358801; Santa Cruz Biotechnology, Dallas, TX, USA) for a time from 24 h to 72 h. The IC_{50} values were calculated by fitting the progress curves to the three parameters using GraphPad Prism software version 7.0 (GraphPad Software, La Jolla, CA, USA).

Experimental groups:

Group 1: Control (Ctr): human GBM cell lines U-87 MG and U-138 MG;

Group 2: BX795 0.1 μM: GBM cell lines U-87 MG and U-138 MG treated with 0.1 μM BX795;

Group 3: BX795 0.5 μM: GBM cell lines U-87 MG and U-138 MG treated with 0.5 μM BX795;

Group 4: BX795 1 μM: GBM cell lines U-87 MG and U-138 MG treated with 1 μM BX795;

Group 5: BX795 10 μM: GBM cell lines U-87 MG and U-138 MG treated with 10 μM BX795.

6.1.3 Cell viability assay

Cell viability was evaluated using a mitochondria-dependent dye for live cells (tetrazolium dye; MTT) (M5655; Sigma-Aldrich) as previously described [97]. U-87 MG and U-138 MG cells were pretreated with increasing concentrations of BX795 (0.1, 0.5, 1, and 10 μM) to determine high concentrations with high toxicity on cell viability. After 24 h, cells were incubated at 37°C with MTT (0.2 mg/ml) for 1 h. The medium was removed by aspiration, and the cells were lysed with DMSO (100 μl). The extent of reduction of MTT to formazan was quantified by measurement of optical density at 550 nm (OD_{550}) with a microplate reader.

6.1.4 Real-Time Quantitative Polymerase Chain Reaction (RT-qPCR) for Bax, p53, Bcl2, Caspase-3 and Caspase-9

Total RNA was isolated from U-87 cells for RT-qPCR analysis using a TRIzol Reagent Kit (Life Technologies, Monza, Italy) as previously described [97]. The first strand of cDNA was synthesized from 2.0 μg of total RNA using a high-capacity cDNA Archive kit (Applied Biosystems, Carlsbad, CA, USA). RT-qPCR was performed to evaluate the gene expression of Bcl2, Bax, p53, caspase-3, and caspase-9 using Power Up Sybr Master Mix (Applied Biosystems) and a QuantStudio 6 Flex Real-Time PCR System (Applied Biosystems). The amplified PCR products were quantified by measuring the calculated cycle thresholds (CT) of target genes and β-actin mRNA. β-Actin mRNA was used as an endogenous control to allow for the relative quantification. After normalization, the mean value of the normal control target levels was chosen as the calibrator, and the results were expressed as a fold change relative to normal controls. The oligonucleotide sequences of the used primers are reported in Table 1.

Table 1. Primer used for RT-qPCR.

Gene	***Forward Primer 5'-3'***	***Reverse Primer 3'-5'***
Bcl2	GAGGATTGTGGCCTTCTTTGAG	AGCCTCCGTTATCCTGGATC
Bax	GGACGAACTGGACAGTAACATG	GCAAAGTAGAAAAGGGCGACA
P53	AGAGTCTATAGGCCCACCCC	GCTCGACGCTAGGATCTGAC
Caspase-3	CTGAGGCATGGTGAAGAAGGA	GTCCAGTTCTGTACCACGGCA
Caspase-9	TGCGAACTAACAGGCAAGCA	GTCTGAGAACCTCTGGTTTGC
β-actin	GACTTCGAGCAAGAGATGG	AGCACTGTGTTGGCGTACAG

6.1.5 Western Blot analysis for Bax, p53, Bcl2, Caspase-3, Caspase-9, IKKα, NIK, VEGF and IRF3

Western blot analysis was performed in U-87 cell lysates as previously described [148] and reported below. U-87 cells were washed twice with ice-cold phosphate-buffered saline (PBS), harvested, and resuspended in Tris-HCl 20 mM pH 7.5, NaF 10 mM, 150

μl of NaCl, 1% Nonidet P-40, and protease inhibitor cocktail (Catalog No. 11836153001; Roche, Switzerland). After 40 minutes, cells were centrifuged at 12,000 rpm for 15 min at 4°C. Protein concentration was estimated by the Bio-Rad protein assay (Bio-Rad Laboratories, Hercules, CA, USA) using bovine serum albumin (BSA) as standard. Cell lysates were then heated at 95°C for 5 min, and equal amounts of protein were separated on a 10%–15% sodium dodecyl sulfate-polyacrylamide gel electrophoresis (SDS-PAGE) gel and transferred to a polyvinylidene difluoride (PVDF) membrane (Immobilon-P, Catalog No. 88018; ThermoFisher Scientific). The expression of the following primary antibodies were evaluated: anti-IRF3 (1:500; ab68481; Abcam, Cambridge, MA, USA), anti-VEGF (vascular endothelial growth factor) (1:500; sc-7269; Santa Cruz Biotechnology), anti-NIK (NF-κB-inducing kinase) (1:500; sc-8417; Santa Cruz Biotechnology), anti-IκB kinase α (IKKα) (1:500; sc-7606; Santa Cruz Biotechnology), anti-Bax (1:500; sc-7480; Santa Cruz Biotechnology), anti-Bcl2 (1:500; sc-7382; Santa Cruz Biotechnology), anti-p53 (1:500; sc-126; Santa Cruz Biotechnology), anti-caspase-3 (1:500; sc-7272; Santa Cruz Biotechnology), and anti-caspase-9 (1:500; sc-73548; Santa Cruz Biotechnology). Antibody dilutions were made in PBS/5% *w/v* nonfat dried milk/0.1% Tween-20 (PMT), and membranes were incubated overnight at 4°C. Membranes were then incubated with secondary antibody (1:2000; Jackson ImmunoResearch, West Grove, PA, USA) for 1 h at room temperature. To ascertain that blots were loaded with equal amounts of protein lysate, the membranes were also incubated with β-actin antibody for the cytosolic fraction (1:500; sc-47778; Santa Cruz Biotechnology) or Lamin A/C for the nuclear fraction (1:500; sc-376248; Santa Cruz Biotechnology). Signals were detected using enhanced chemiluminescence (ECL) detection system reagent according to the manufacturer's instructions (Thermo Fisher, Waltham, MA, USA). The relative expression of the protein bands was quantified by densitometry with BIORAD ChemiDocTMXRS + software. Images of blot signals (8

bit/600 dpi resolution) were imported to the analysis software (Image Quant TL, v2003). Protein signals were quantified by scanning densitometry using a bio-image analysis system (Bio-Profil, Milan, Italy); the results were expressed as % of control.

6.1.6 Enzyme-Linked Immunosorbent Assay (ELISA) Assay for TNF-α and IFN-β

The levels of TNF-α and IFN-β in U-87 cell supernatant were investigated by ELISA kit (human TNF-α ELISA kit; Cat. No. ab100654; Abcam; human IFN-β ELISA kit; Cat. No. ab252363; Abcam) according to manufacturer's instructions. In brief, cells were seeded into 96-well plates at a density of 1×10^4 cells/well and were cultured for 24 h in the incubator at 37°C and 5% CO_2. After 24 h, cells were treated with BX795 at the concentrations of 1 and 10 μM for 24 h. After 24h of treatment with BX795, the cell supernatant was collected and assayed for ELISA kit. Standards, samples, and biotinylated antibodies human TNF-α or IFN-β were added to the wells. After HRP conjugated streptavidin incubation, the TMB substrate solution was added to the wells. Absorbance detection was executed at 450 nm using a microplate reader (model 550; Bio-Rad Laboratories Inc.).

6.2 Ex vivo model

6.2.1 Primary GBM cell culture

Primary tumor GBM cells from patients were obtained according to protocol approved by the Regional Ethical Board at the University of Messina. All subjects gave their informed consent for inclusion before they participated in the study. The study was conducted in accordance with the Declaration of Helsinki, and the protocol was approved by the Ethics Committee of AOU "G. Martino," Hospital of Messina (No. 47/19 of 05/02/2019). Tumor samples were processed aseptically, and primary cell cultures were initiated using DMEM (Catalog No. D5030; Sigma-Aldrich) with 15% heat-inactivated

fetal calf serum (FCS) (Catalog No. 12103C; Sigma-Aldrich), 2 mM GlutaMAX-I (Catalog No. 35050061; ThermoFisher Scientific), 1% insulin-transferrin-selenium-X supplement (Catalog No. 41400045; ThermoFisher Scientific), and 1% penicillin-streptomycin mixture (Catalog No. 15640055; Invitrogen, Carlsbad, CA, USA). Cells were used within 7 days of plating or established as primary cell lines.

Experimental groups:

Group 1: Control (Ctr): healthy brain tissues were processed and used as negative control;
Group 2: Primary GBM cells: GBM cells obtained from patients were processed and used as positive control;
Group 3: Primary GBM cells + BX795 10 μM: GBM cells from patients were treated with BX795 at the concentration of 10 μM for 24h.

6.2.2 Cell viability assay

Primary GBM cells obtained from patients were treated with BX795 at the concentration of 10 μM for 24 h. After 24 h, primary GBM cells were incubated at 37°C with MTT (0.2 mg/ml; M5655; Sigma-Aldrich) for 1 h. Then, the medium was removed by aspiration, and the cells were lysed with 100 μl of DMSO (sc-358801; Santa Cruz Biotechnology). The extent of reduction of MTT to formazan was quantified by measurement of optical density at 550 nm (OD_{550}) with a microplate reader [158].

6.2.3 Western Blot analysis for TBK1, IRF3, IFNγ and SOX3

Protein extraction and western blot analysis in primary GBM cell culture were performed as previously described [148]. The filters were probed with specific antibodies: anti-TBK1 (1:500; sc-52957; Santa Cruz Biotechnology), anti-SOX3 (1:500; sc-101155; Santa Cruz Biotechnology), anti-IRF3 (1:500; ab68481; Abcam), and anti-IFN-γ (1:500;

sc-390800; Santa Cruz Biotechnology) in 1 × PBS, 5% *w/v* nonfat dried milk (sc-2324; Santa Cruz Biotechnology), 0.1% Tween-20 (P9416; Sigma-Aldrich) at 4°C overnight. The day after, the membranes were incubated with a specific peroxidase-conjugated secondary antibody (Pierce, Cramlington, UK) for 1 h at room temperature. To ascertain that blots were loaded with equal amounts of proteins, they were also incubated in the presence of the antibody against β-actin protein for the cytosolic fraction (1:500; sc-47778; Santa Cruz Biotechnology). Signals were detected with ECL detection system reagent according to the manufacturer's instructions (ThermoFisher Scientific). The relative expression of the protein bands was quantified by densitometry with Bio-Rad ChemiDoc XRS+ software. Images of blot signals (8 bit/600 dpi resolution) were imported to the analysis software (Image Quant TL, v2003). Protein signals were quantified by scanning densitometry using a bio-image analysis system (Bio-Profil, Milan, Italy); the results were expressed as % of control.

6.3 In vivo model

6.3.1 Cell line

The human GBM cell line U-87 (U-87 MG ATCC® HTB-14™ Homo sapiens brain Likely glioblastomas) was obtained from ATCC (American Type Culture Collection, Rockville, MD, USA). U-87 cells were cultured in 75 cm^2 flask with respectively Dulbecco's modified Eagle's medium (DMEM—Sigma-Aldrich® Catalog No. D5030; St. Louis, MO, USA) supplemented with antibiotics (penicillin 1000 units—streptomycin 0.1 mg/L, Sigma-Aldrich® Catalog No. P4333; St. Louis, MO, USA), L-glutamine (GlutaMAX™, ThermoFisher Scientific® Catalog No. 35050061; Waltham, MA, USA) and 10% (*v/v*) fetal bovine serum (FBS, Sigma-Aldrich® Catalog No. 12103C St. Louis, MO, USA) in a humidified atmosphere containing 5% CO_2 at 37 °C.

6.3.2 Animals

Wild-type C57BL/6J nude mice (male, 8-10 weeks old) were purchased from Jackson Laboratory (Bar Harbor, Hancock, ME, USA) and housed in microisolator cages under pathogen-free conditions on a 12 h light/12 h dark schedule for a week according to ARRIVE guidelines. Animals were fed a standard diet and water *ad libitum*. Animal experiments followed Italian regulations on protection of animals used for experimental and other scientific purposes (DM 116192) as well as European Union (EU) regulations (OJ of ECL358/1 18 December 1986).

6.3.3 Xenograft model

The xenograft tumor model was performed as previously described [158]. The mice were inoculated subcutaneously with 3×10^6 human glioblastoma U-87 cells in 0.2 mL of phosphate buffered saline (PBS) and 0.1 mL matrigel (BD Bioscience, Bedford, MA, USA). Animals were treated with KYP-2047 (Sigma-Aldrich®; Cat. SML0208) dissolved in PBS with 0.001% of dimethyl sulfoxide (DMSO) at doses of 1 mg/kg, 2.5 mg/kg, and 5 mg/kg by intraperitoneal injection every three days from day 7 until the sacrifice. After tumor cell inoculation, animals were monitored daily for morbidity and mortality. At the thirty-fifth day, the animals were sacrificed according to Valentim et al [159]; after, tumours were excised and processed to perform several analyses. Tumor volume was measured non-invasively by using an electronic calliper using an empirical formula, V = 1/2 × ((the shortest diameter) 2 × (the longest diameter)). The minimum number of mice for every technique was estimated with the statistical test "ANOVA: Fixed effect, omnibus one-way" with G-power software. The experiments were performed three times to verify the data, using 25 animals for each experimental group.

Experimental groups:

The mice were randomly divided into four groups, as described below:

Group 1: Control group (vehicle): weekly intravenous (iv) administration of saline.

Group 2: Control group + KYP-2047 1 mg/kg: intraperitoneal (ip) administration of KYP-2047 1 mg/kg dissolved in PBS with 0.001% of DMSO every three days from day 7.

Group 3: Control group + KYP-2047 2.5 mg/kg: intraperitoneal (ip) administration of KYP-2047 2.5 mg/kg dissolved in PBS with 0.001% of DMSO every three days from day 7.

Group 4: Control group + KYP-2047 5 mg/kg: intraperitoneal (ip) administration of KYP-2047 5 mg/kg dissolved in PBS with 0.001% of DMSO every three days from day 7.

The doses of KYP-2047 were chosen according to a previous dose-response study performed in our laboratory.

Furthermore, the control group + KYP-2047 1 mg/kg was only subjected to tumor volume, tumor weight and histological evaluation because it did not induce any beneficial effect; therefore, we decided to continue analysing only KYP-2047 2.5 mg/kg and 5 mg/kg.

6.3.4 Histological analysis

Histological evaluation was performed as previously described [158]. After the sacrifice of the animals, tumor samples were fixed with 10% (*w/v*) of PBS-buffered formaldehyde solution at 25°C for 24h. After dehydration, samples were embedded in paraffin, and sectioned at 7 μm. Sections were deparaffinized with xylene and stained with hematoxylin and eosin. The slides were analyzed by a pathologist blinded to the treatment

groups. All sections were analyzed using an Axiovision microscope (Zeiss, Milan, Italy). The images were shown at a magnification of 10× (100 μm of the bar scale) and 20× (50 μm of the bar scale).

6.3.5 Enzyme-Linked Immunosorbent Assay (ELISA) for PREP

An enzyme-linked immunosorbent assay (ELISA) kit was performed to evaluate PREP levels in serum of each mice using Mouse PREP ELISA kit (cat. Q9QUR6, RayBiotech, Peachtree Corners, GA, USA) according to manufacturer's instructions. The serum of each animal was collected every week until sacrifice and analysed by ELISA kit. Firstly, 100 μl of standard or sample were added to each well and incubated for 2.5 h at RT. After three washes, 100 μl of prepared biotin antibody were put to each well and incubated for 1 h at RT. After incubation with biotin antibody, streptavidin solution (100 μl) was added for 45 min at RT. Then, TMB substrate reagent was added to the well. Absorbance detection was executed at 450 nm using a microplate reader (model 550; Bio-Rad Laboratories Inc.).

6.3.6 Western Blot analysis for VEGF, eNOS, angiopoietins, Ki-67, Bax and Bcl2

Tumor samples from each mouse were suspended in extraction Buffer A (0.2 mM PMSF, 0.15 mM pepstatin A, 20 mM leupeptin, 1 mM sodium orthovanadate), homogenized at the highest setting for 2 min, and centrifuged at 12,000× g rpm for 4 min at 4 °C [160]. Supernatants are the cytosolic fraction, whereas the pellets, containing enriched nuclei, were resuspended in Buffer B (1% Triton X-100, 150 mM NaCl, 10 mM TrisHCl pH 7.4, 1 mM EGTA, 1 mM EDTA, 0.2 mM PMSF, 20 mm leupeptin, 0.2 mM sodium orthovanadate) and centrifuged at 12,000× g rpm for 10 min at 4 °C; supernatants are the nuclear fraction. Protein concentration was estimated by the Bio-Rad protein assay using bovine serum albumin as standard. Then, tumor samples, in equal amounts of protein,

were separated on 12% SDS-PAGE gel and transferred to nitrocellulose membrane as previously described [8]. The following primary antibodies were used: anti-vascular endothelial growth factor (VEGF) (1:500; Santa Cruz Biotechnology, Dallas, TX, USA; sc-7269); anti-endothelial nitric oxide synthase (eNOS) (1:500; Santa Cruz Biotechnology, Dallas, TX, USA; sc-376751); anti-angiopoietin 1 (Ang1) (1:500; Santa Cruz Biotechnology, Dallas, TX, USA; sc-517593); anti-angiopoietin 2 (Ang2) (1:500; Santa Cruz Biotechnology, Dallas, TX, USA; sc-74403); anti-Ki-67 (1:500; Santa Cruz Biotechnology, Dallas, TX, USA; sc-23900); anti-Bax (1:500; Santa Cruz Biotechnology, Dallas, TX, USA; sc-7480); anti-Bcl2 (1:500; Santa Cruz Biotechnology, Dallas, TX, USA; sc-7382). Antibody dilutions were made in PBS/5% *w/v* nonfat dried milk/0.1% Tween-20 (PMT) and membranes incubated overnight at 4 °C. Membranes were then incubated with secondary antibody (1:2000, Jackson ImmunoResearch, West Grove, PA, USA) for 1 h at room temperature. To ascertain that those blots were loaded with equal amounts of protein lysate, they were also incubated with β-actin antibody for the cytosolic fraction (1:500; Santa Cruz Biotechnology, Dallas, TX, USA; sc-8432) or Lamin A/C for the nuclear fraction (1:500, Santa Cruz Biotechnology, Dallas, TX, USA; sc-376248). Signals were detected with an enhanced chemiluminescence (ECL) detection system reagent according to the manufacturer's instructions (Thermo Fisher, Waltham, MA, USA). The relative expression of the protein bands was quantified by densitometry with BIORAD ChemiDocTMXRS + software. The results were expressed as % of control.

6.3.7 Immunohistochemical localization for VEGF, eNOS, CD34, Ki-67, and Bcl2

Immunohistochemical localization was performed as previously described [160]. After deparaffinization, endogenous peroxidase was blocked with 0.3% (*v/v*) hydrogen peroxide for 30 min. After washing with PBS, sections (7 μm) were placed in 0.1 M citrate buffer for one minute. Subsequently, sections were incubated with 2% (*v/v*) of normal

horse serum in PBS for 20 min, to minimize nonspecific absorption. Then, the slides were incubated overnight (O/N) using the following primary antibodies: VEGF (Santa Cruz Biotechnology, Dallas, TX, USA; 1:100 in PBS, *v/v*; sc-7269), eNOS (Santa Cruz Biotechnology, Dallas, TX, USA, 1:100 in PBS, *v/v*; sc-376751) anti-Bcl2 (1:100; Santa Cruz Biotechnology, Dallas, TX, USA; 1:100 in PBS, *v/v*; sc-7382); anti-Ki-67 (1:100; Santa Cruz Biotechnology, Dallas, TX, USA; 1:100 in PBS, *v/v*; sc-23900); anti-CD34 (1:100; Santa Cruz Biotechnology, Dallas, TX, USA; 1:100 in PBS, *v/v*; sc-74499). At the end of the incubation with the primary antibodies, the sections were abundantly washed with PBS and incubated with a secondary antibody (Santa Cruz Biotechnology, Dallas, TX, USA) for 1 h at room temperature. The reaction was revealed by a chromogenic substrate (brown DAB), and counterstaining with NUCLEAR FAST-RED. The percentage of positive staining was measured using a computerized image analysis system (Leica QWin V3, Cambridge, UK). The images were acquired using an optical microscope (Zeiss, Axio Vision, Feldbach, Schweiz). The images were shown at a magnification of 10× (100 μm of the bar scale) and 20× (50 μm of the bar scale).

6.3.8 Real-Time Quantitative Polymerase Chain Reaction (RT-qPCR) for VEGF and eNOS

Total RNA of tumor samples was isolated using TRIzol reagent (Invitrogen, Carlsbad, CA, USA) according to the manufacturer's instructions. RNA isolation was performed as previously described by Weinert et al [161]. First-strand cDNA obtained from RNA samples was stored at −80 °C until use. The mRNA expression levels of VEGF and eNOS in each sample, was measured using Power Up Sybr Master Mix (Applied Biosystems) and a QuantStudio Flex Real-Time Polymerase Chain Reaction (PCR) System (Applied Biosystems). The mRNA expression levels of VEGF and eNOS were normalized using

glyceraldehyde-3-phosphate dehydrogenase (GAPDH). The primer used for reverse transcriptase PCR for VEGF, eNOS and GAPDH are reported in Table 2.

Table 2. Primer used for RT-qPCR.

Gene	***Forward Primer 5'-3'***	***Reverse Primer 3'-5'***
VEGF	GAGCAGAAGTCCCATGAAGTGA	CACAGGACGGCTTGAAGATGT
eNOS	CCTGTGAGACCTT CTGTGTGG	GGATCAGACCTGGCAGCAACT
GAPDH	GGGCTGGCATTGCTCTCA	TGCTGTAGCGTATTCATTG

6.3.9 Immunofluorescence staining for CD34

Immunofluorescence staining was performed as previously described [162]. Briefly, at the end of the experiment, tumor samples were collected and processed. After deparaffinization and rehydration, slides of 7 μm were placed in 0.1 M citrate buffer for one minute. Nonspecific absorption was decreased by incubating the sections in a solution containing 2% (*v/v*) of normal horse serum in PBS for 20 min. Tissue sections were incubated with the following primary antibody anti-CD34 at 37 °C overnight (O/N) (1:100; Santa Cruz Biotechnology, Dallas, TX, USA; sc-74499). Then, tissue sections were washed three times with PBS and incubated with secondary antibody anti-mouse Alexa Fluor-488 antibody (1:1000 *v/v*, Molecular Probes, Altrincham, UK) for 1 h at 37 °C. For nuclear staining, 4′,6′-diamidino-2-phenylindole (DAPI; Hoechst, Frankfurt, Germany) (2 μg/mL) in PBS was added. Sections were observed and photographed at 40× magnification (20 μm of the bar scale) using a Leica DM2000 microscope. To prove the binding specificity for different antibodies, some sections were also incubated with only primary antibody or secondary antibody, no positive staining was observed in these sections.

6.4 Materials

BX795, KYP-2047 and all other chemicals were obtained by Sigma-Aldrich (Milan, Italy). BX795 and KYP-2047 stock solutions were prepared in DMSO and in non-pyrogenic saline (0.9% NaCl, Baxter, Milan, Italy).

6.5 Statistical analysis

All values are expressed as mean ± SEM of *n* observations. Each analysis for *in vitro, ex vivo* and *in vivo* models was performed three times with three samples replicates for each one. The results were analyzed by one-way ANOVA followed by a Bonferroni post hoc test for multiple comparisons. A value of $p < 0.05$ was considered significant.

Chapter VII: Results

7. Results

7.1 In vitro results of BX795

7.1.1 Effect of BX795 on GBM cell viability

BX795 cytotoxicity was evaluated incubating U-87 and U-138 cell lines with growing concentrations of BX795 (0.1, 0.5, 1 and 10 μM). BX795 treatment showed cytotoxic and antiproliferative effects at 24, 48, and 72 h from the beginning of the treatment in U-87 and U-138 cells in a concentration- and time-dependent manner (Figure 1A-B and C-D, respectively). The values of 1 and 10 μM represented the most cytotoxic concentrations of BX795 as shown in Figures 1A-B and C-D. The IC_{50} values for U-87 cells are included in the range of 3.5 to 0.32 μM, and for U-138 cells, IC_{50} values range are from 4.4 to 1.04 μM. The results of control + DMSO 0.001% alone were not shown because it did not induce any cytotoxic effect.

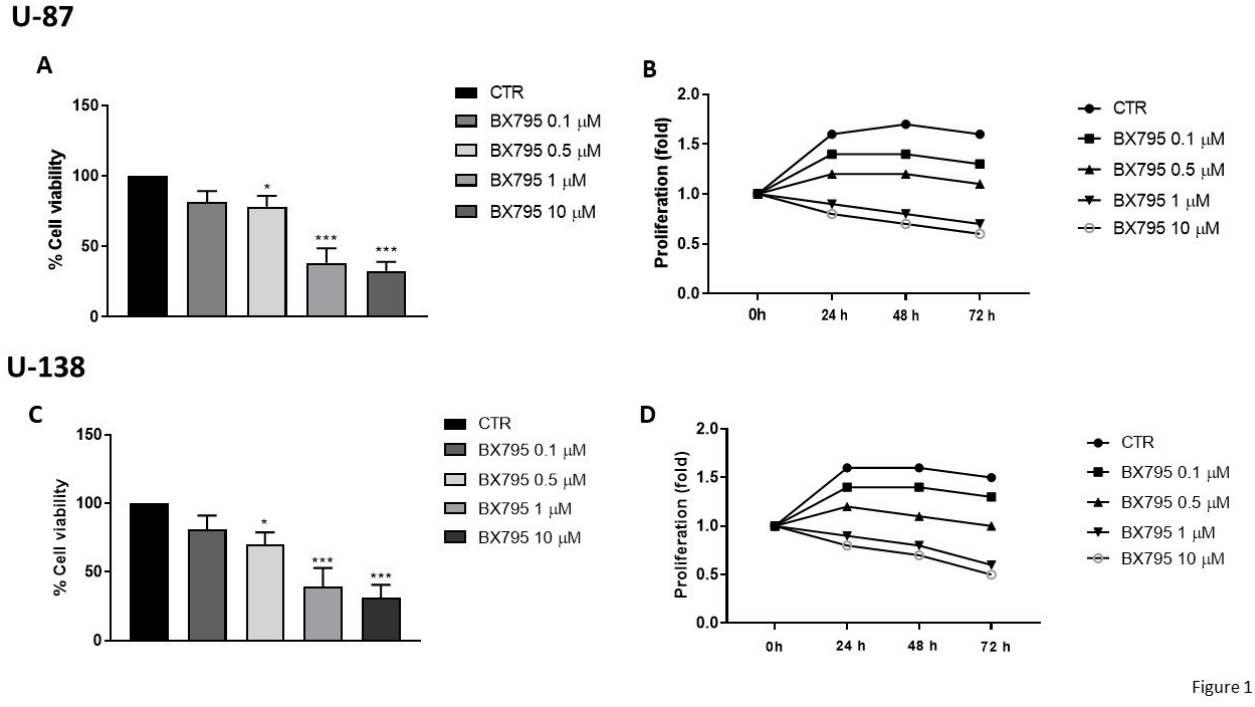

Figure 1

Figure 1. Effect of BX795 on U-87 and U-138 cell viability. Cell viability was evaluated using MTT assay 24 h after treatment with BX795 at the concentrations of 0.1, 0.5, 1 and 10 μM. BX795 showed to significantly reduce cell viability in both cell lines in a concentration-dependent

manner, mostly at the concentrations of 1 and 10 μM (A-C), exerting antiproliferative effects at different time points (B-D). Data are representative of at least three independent experiments. (Adapted figure and results from [163]); (A) $*p < 0.05$ vs the control group; $***p < 0.001$ vs the control group**;** (C) $*p < 0.05$ vs the control group; $***p < 0.001$ vs the control group.

Since BX795 showed similar effects on cell viability in both GBM cell lines, we decided to continue to analyse the effect of BX795 only in U-87 cell line, because it represented one of the most frequently used cell lines in the field of GBM [164].

7.1.2 Effect of BX795 on Bax, p53, Bcl2, Caspase-3 and Caspase-9 expression

Apoptosis-inducing therapies have gained a great interest as promising experimental treatment strategies for GBM [165, 166]. Therefore, we examined the potential effect of BX795 on apoptosis pathway, by evaluating Bax, Bcl2, p53, caspase-3, and caspase-9 expression. U-87 cells were treated with BX795 at the concentrations of 1 and 10 μM for 24h and analyzed by RT-qPCR. The results showed a significantly increase of proapoptotic Bax (Figure 2A), and tumor suppressor p53 mRNA expression (Figure 2B) and a reduction in anti-apoptotic Bcl2 mRNA expression (Figure 2C) after BX795 treatment at the concentrations of 1 and 10 μM. The results obtained were confirmed by western blot analysis, confirming an increase of Bax and p53 expression, and a decrease of Bcl2 expression after BX795 treatment in a concentration-dependent manner (Figure 2D-E-F, see densitometric analysis D1, E1, F1, respectively).

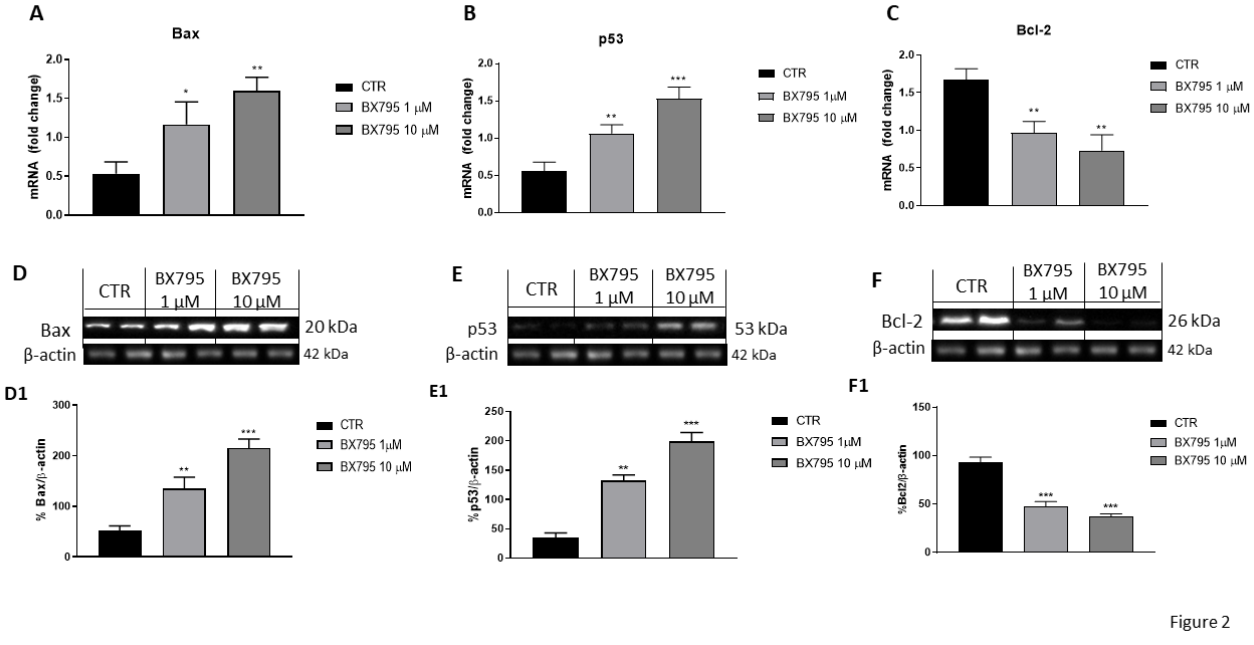

Figure 2

Figure 2. Effect of BX795 on apoptosis pathway. Treatment with BX795 at the concentrations of 1 and 10 μM significantly increased Bax and p53 mRNA expression (A, B) and reduced Bcl2 mRNA expression (C) compared to the control group. Moreover, western blot analysis confirmed an increase in Bax (D) and p53 expression (E) and a reduction in Bcl2 expression (F). Data are representative of at least three independent experiments. (Adapted figure and results from [163]); (A) $*p < 0.05$ vs the control group; $**p < 0.01$ vs the control group; (B) $**p < 0.01$ vs the control group; $***p < 0.001$ vs the control group; (C) $**p < 0.01$ vs the control group; (D) $**p < 0.01$ vs the control group; $***p < 0.001$ vs the control group; (E) $**p < 0.01$ vs the control group; $***p < 0.001$ vs the control group; (F) $***p < 0.001$ vs the control group.

Moreover, BX795 treatment for 24h at the concentration of 1 and 10 μM induced a significant increase in caspase-3 and caspase-9 mRNA expression (Figure 3A and B), highlighting an apoptosis activation. These results were confirmed also by western blot analysis as shown in the Figure 3C and D, respectively (see densitometric analysis C1 and D1).

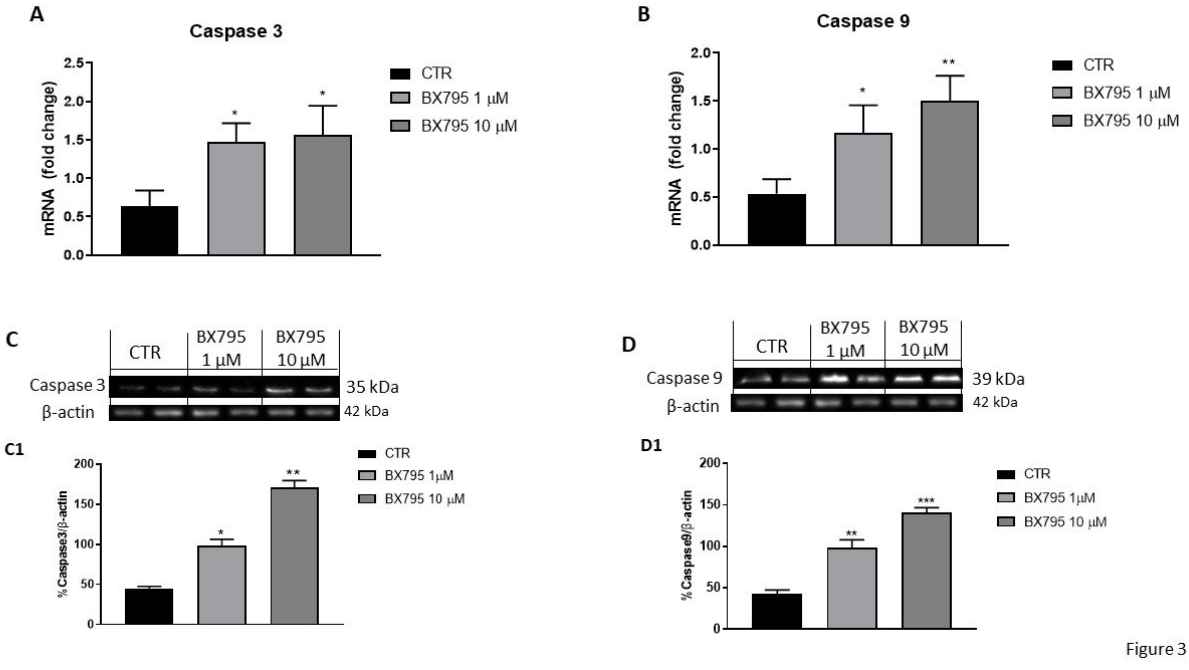

Figure 3

Figure 3. Effect of BX795 on caspase-3 and caspase-9 activation. BX795 treatment demonstrated at the concentrations of 1 and 10 μM to induce caspase-3 (A) and caspase-9 (B) mRNA expression in U-87 cells. In addition, western blots analysis confirmed an increase in caspase-3 (C) and caspase-9 expression (D) after BX795 treatment. Data are representative of at least three independent experiments. (Adapted figure and results from [163]); (A) $*p < 0.05$ vs the control group; (B) $*p < 0.05$ vs the control group; $**p < 0.01$ vs the control group; (C) $*p < 0.05$ vs the control group; $**p < 0.01$ vs the control group; (D) $**p < 0.01$ vs the control group; $***p < 0.001$ vs the control group.

7.1.3 Effect of BX795 on IKKα, NIK, TNFα and IFNβ expression

In the context of GBM, various studies have focused on the NF-κB pathway activation, which is related to IKKα and NIK (also known as MAP3K14) activation, as well as the release of proinflammatory cytokines such as TNF-α and IFN-β [10, 167]. Therefore, in this study, we investigated the anti-inflammatory effects of BX795 in U-87 cells. The results demonstrated that BX795 treatment for 24h at the concentrations of 1 and 10 μM significantly reduced IKKα and NIK expression (Figure 4A and B, see densitometric analysis A1 and B1, respectively), as well as the levels of pro-inflammatory cytokines TNF-α and IFN-β (Figure 4C and D, respectively).

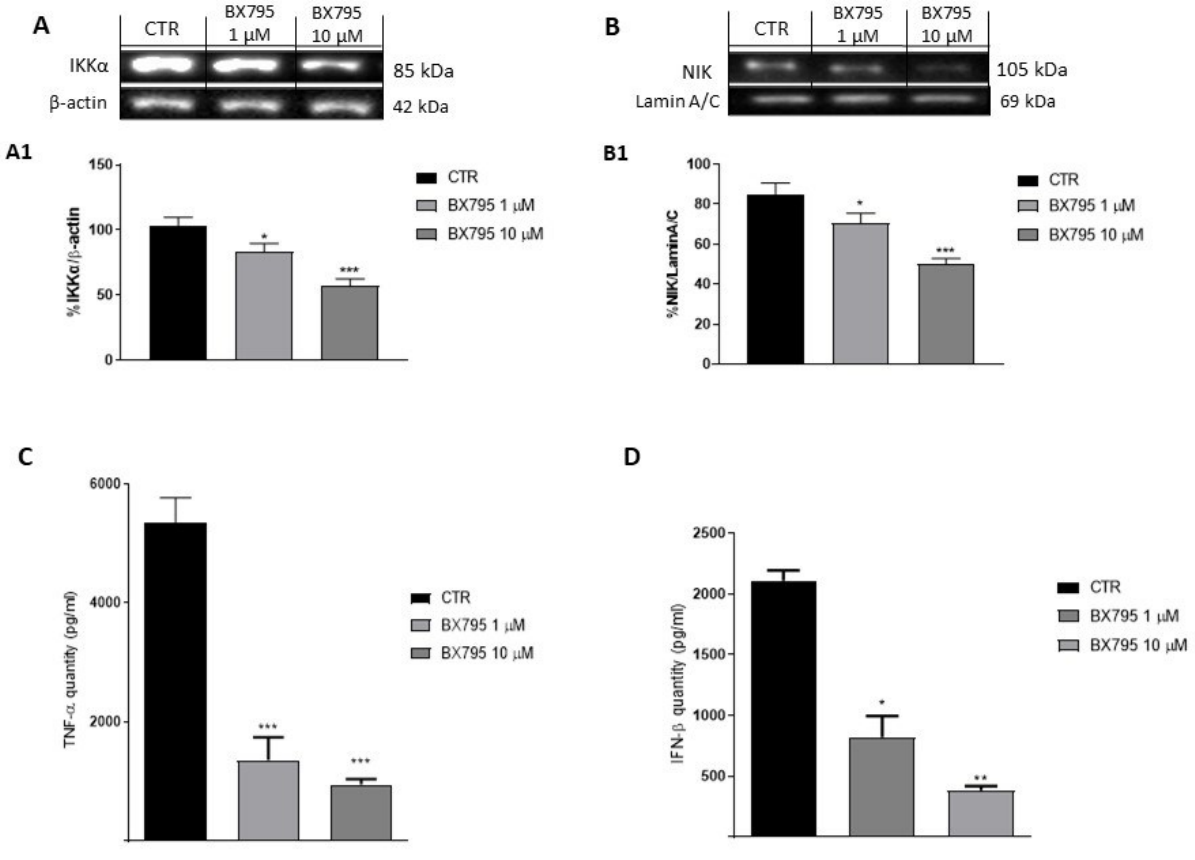

Figure 4

Figure 4. Effect of BX795 on IKKα, NIK, TNF-α and IFN-β expression. The blots revealed a significant increase in IKKα (A) and NIK (B) expression in the control group. Meanwhile, their expressions were significantly attenuated after BX795 treatment 1 μM and 10 μM. Moreover, an increase in TNF-α (C) and IFN-β (D) levels was evident in the control group, while the treatment with BX795 at the concentrations of 1 and 10 μM significantly reduced their levels, reducing inflammation. Data are representative of at least three independent experiments. (Adapted figure and results from [163]); (A) $*p < 0.05$ vs the control group; $***p < 0.001$ vs control group; (B) $*p < 0.05$ vs the control group; $***p < 0.001$ vs control group; (C) $***p < 0.001$ vs control group; (D) $*p < 0.05$ vs the control group; $**p < 0.01$ vs control group.

7.1.4 Effect of BX795 on VEGF and IRF3 expression

GBM tumours are highly vascularized; its growth depends on the formation of new blood vessels [168]. Thus, considering the key role of angiogenesis in GBM, we decided to investigate the effect of BX795 on VEGF and the transcription factor interferon regulatory factor 3 (IRF3) expression which are involved in glioma invasiveness, and production of proangiogenic mediators. The results showed a significant increase of IRF3 and VEGF expression in GBM cells, while BX795 treatment for 24h at the concentrations of 1 and 10 μM significantly reduced IRF3 and VEGF expression (Figure 5A and B; see densitometric analysis A1 and B1), counteracting angiogenesis process.

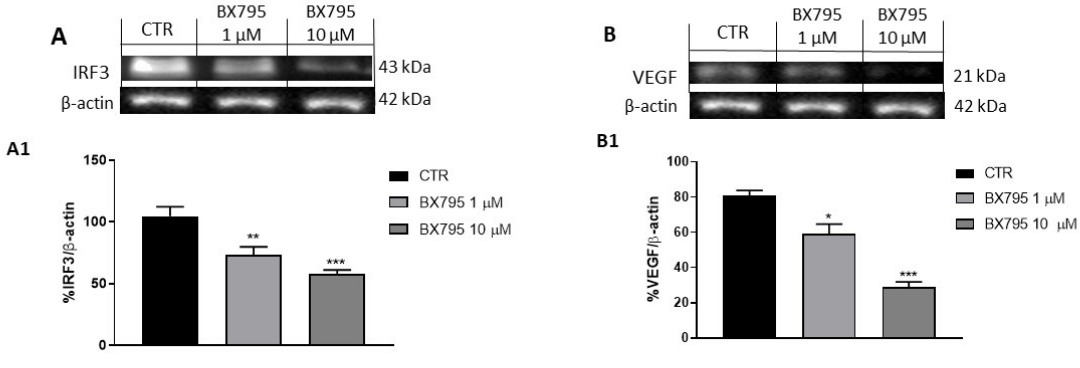

Figure 5

Figure 5. Effect of BX795 on angiogenesis. The blots revealed an increase in IRF3 (A) and VEGF (B) expression in the control group. Meanwhile, BX795 treatment at the concentrations of 1 and 10 μM significantly reduced their expression in a concentration-dependent manner. Data are representative of at least three independent experiments. (Adapted figure and results from [163]); (A) $^{**}p < 0.01$ vs the control group; $^{***}p < 0.001$ vs control group; (B) $^{*}p < 0.05$ vs the control group; $^{***}p < 0.001$ vs control group.

7.2 Ex vivo results of BX795

7.2.1 Effect of BX795 on Primary GBM cell viability

BX795 cytotoxicity was evaluated in primary GBM cell culture obtained from patients at the concentration of 10 μM, which represented the most effective concentration. BX795 treatment for 24h demonstrated to reduce primary GBM cell viability (Figure 6A) and to exert antiproliferative effect at the concentration of 10 μM for indicated time intervals (Figure 6B).

7.2.2 Effect of BX795 on TBK1, IRF3, IFNγ and SOX3 expression

To validate the effective role of TBK1 inhibitor in GBM cells obtained from patients, we assessed western blot analysis for TBK1. As shown in the Figure 6C, an increase of TBK1 expression was found in GBM primary cells extracted from patients compared to control; however, BX795 at the concentration of 10 μM for 24h was able to significantly reduce TBK1 expression (see densitometric analysis C1). To confirm the potential effect of BX795 inhibitor on primary GBM cells, we investigated by western blot analysis, IRF3 and IFN-γ expression, two key proteins phosphorylated by TBK1 [24]. The results obtained showed an increase of IRF3 and IFN-γ expression in primary GBM cells, meanwhile the treatment with BX795 10 μM significantly reduced their expression as shown in Figure 6D and E (see densitometric analysis D1 and E1).

Numerous studies have shown that some transcription factors such as SOX3 are capable of acting as oncogenes by promoting the acquisition of tumor stem cell-like phenotypes in GBM [169, 170]. Many studies demonstrated that SOX3 overexpression induces an increase in viability, proliferation, migration, and invasion of GBM cells [169, 170]. Therefore, in this study, we evaluated SOX3 expression in primary GBM cells by western blot analysis. We found that SOX3 expression in primary GBM cells was higher than that

to control group; however, BX795 treatment at the concentration of 10 μM significantly reduced its expression (Figure 6F; see densitometric analysis F1).

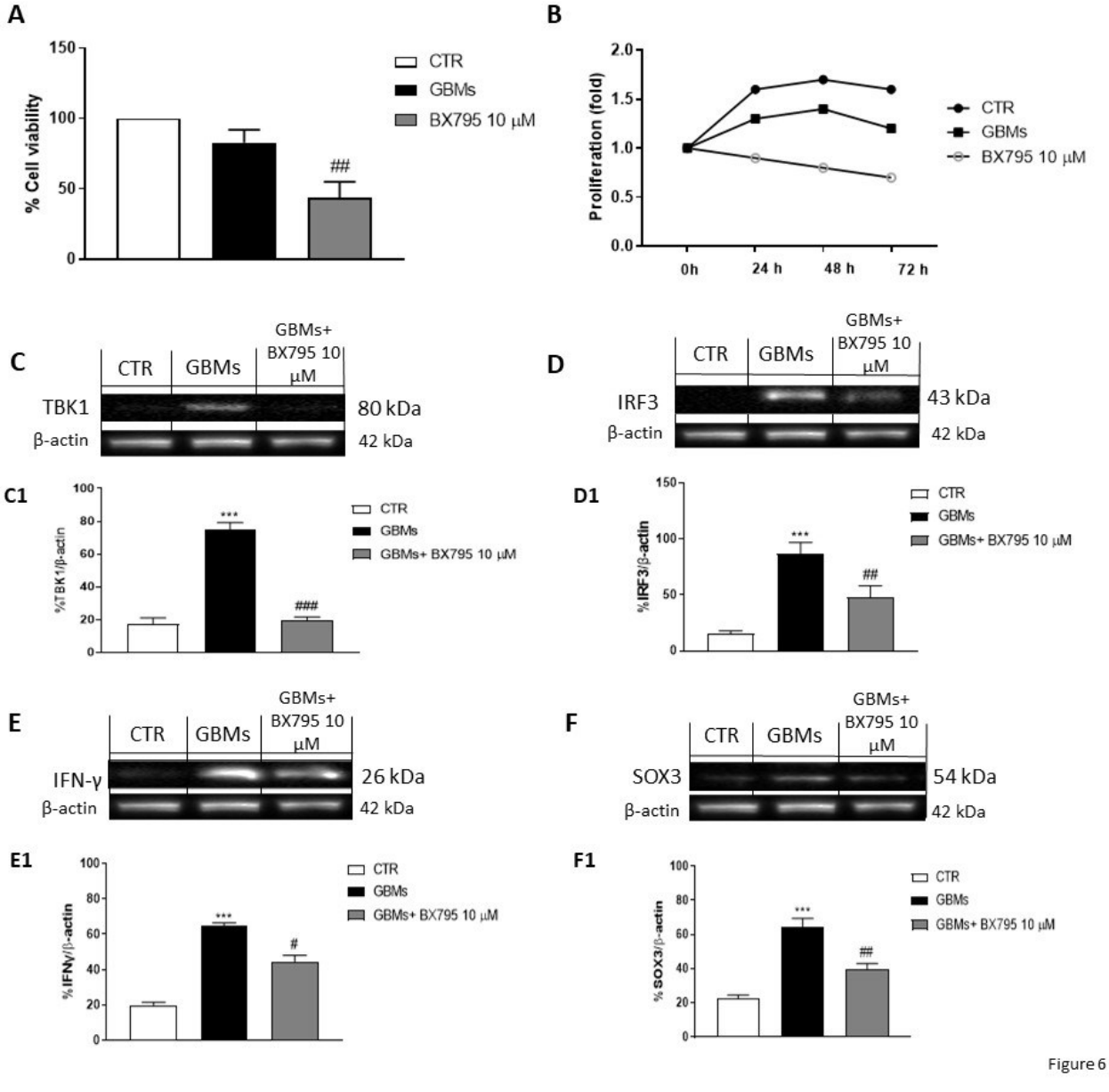

Figure 6. Effect of BX795 on primary GBM cell viability and TBK1 signalling pathway. MTT assay revealed that BX795 10 μM reduced primary GBM cell viability (A). Cell proliferation was evaluated at different times points (T0, 24, 48, and 72 h) in primary GBM cell, showing that BX795 10 μM was able to suppress GBM cell proliferation (B). The blots revealed an increase in TBK1 expression in primary GBM cells compared to the control group; meanwhile, BX795 10 μM significantly reduced its expression (C). In addition, the blots revealed an increase in IRF3, IFN-γ, and SOX3 expression in primary GBM cell compared to the control group; however, BX795 10 μM significantly reduced their expression (D-E-F). Data are representative of at least three independent experiments. (Adapted figure and results from [163]); (A) ## $p < 0.01$ vs

GBMs; (C) ***$p < 0.001$ vs control group, ###$p < 0.001$ vs GBMs; (D) ***$p < 0.001$ vs control group, ##$p < 0.01$ vs GBMs; (E) ***$p < 0.001$ vs control group, #$p < 0.05$ vs GBMs. (F) ***$p < 0.001$ vs control group; ##$p < 0.01$ vs GBMs.

7.3 In vivo results of KYP-2047

7.3.1 KYP-2047 reduces tumor growth by modulating PREP levels

The histological analysis of the control group (Figure 7A) showed a significant subcutaneous tumor mass, associated to an increase in necrosis and neutrophil infiltration; while the treatment with KYP-2047 at doses of 2.5 mg/kg and 5 mg/kg showed a reduction in tumour mass as well as neutrophil infiltration (Figure 7C-D), much more than KYP-2047 at the dose of 1 mg/kg (Figure 7B), accompanied by a reduction of mean tumor weight (E) and tumor burden (F), respectively. Furthermore, we observed a marked decrease of tumor volume following KYP-2047 treatment at doses of 2.5 mg/kg and 5 mg/kg, much more than KYP-2047 1 mg/kg (Figure 7G). To better understand if the expression levels of PREP changed during the treatment, we decided to verify the expression of PREP by ELISA kit every week until the sacrifice. The results showed that KYP-2047 at doses of 2.5 mg/kg and 5 mg/kg was able to significantly reduce PREP levels (Figure 7H). However, during the experiment, no important change in the weight of the animals was seen (Figure 7I).

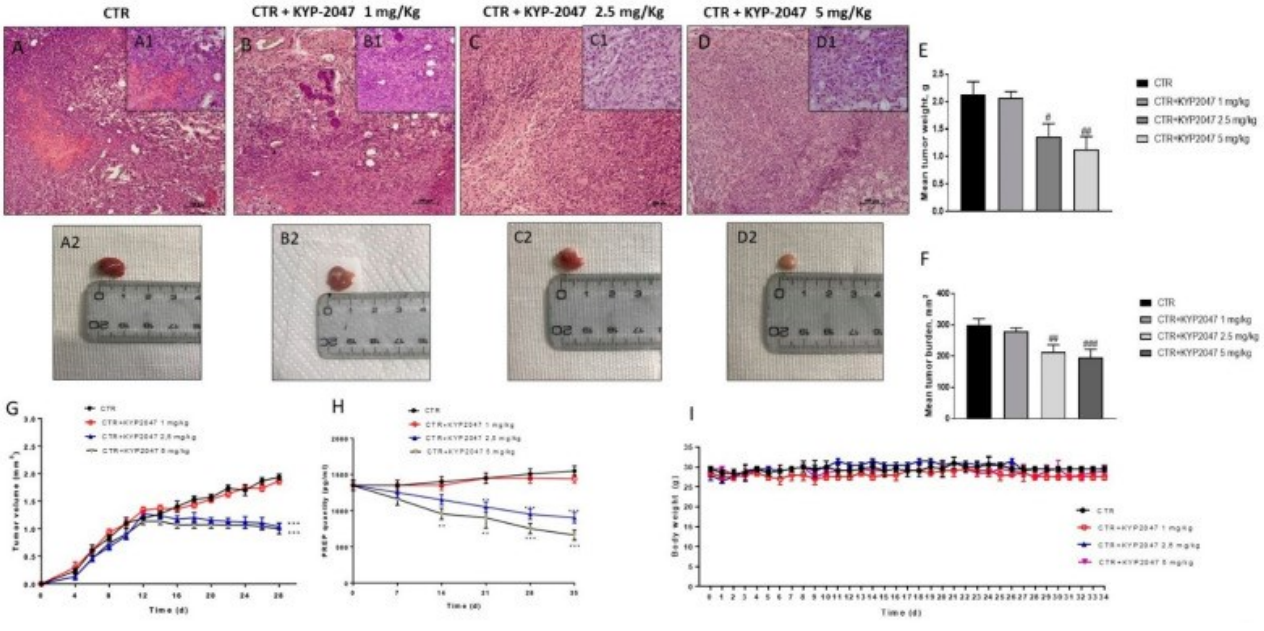

Figure 7. Effect of KYP-2047 on tumor growth. An elevated tumor mass was observed in the control group (A) while the treatment with KYP-2047 at doses of 2.5 mg/kg and 5 mg/kg significantly reduced tumor mass and neutrophil infiltration (C, D) more than KYP-2047 at dose of 1 mg/kg (B). Moreover, the panel (E, F, G) showed a reduction in tumor volume and tumor weight following KYP-2047 treatment at doses of 2.5 mg/kg and 5 mg/kg without encountering important weight differences (I). Additionally, the panel H showed a decrease of PREP expression following KYP-2047 treatment. Data are representative of at least three independent experiments. (Figure and results from [171]); Sections were observed and photographed at 10x and 20x magnification. (E) # $p < 0.05$ vs control group; ## $p < 0.01$ vs control group; (F) ## $p < 0.01$ vs control group; ### $p < 0.001$ vs control group; (G) ### $p < 0.001$ vs control group; (H) ## $p < 0.01$ vs control group; ### $p < 0.001$ vs control group.

7.3.2 KYP-2047 reduces angiogenic marker expression as VEGF, eNOS and CD34

Angiogenesis is an essential process for tumor growth [168]. GBM is characterized by a deregulation of angiogenic growth factors as VEGF and eNOS expression, which play a key role in maintaining vascular homeostasis and vessel integrity [172]. Therefore, in this study we decided to investigate by immunohistochemical staining VEGF and eNOS. Our results demonstrated a significant increase of VEGF and eNOS positive cells in the control group (Figure 8A and Figure 9A respectively); however, the treatment with KYP-2047 at doses of 2.5 mg/kg and 5 mg/kg significantly reduced them in a dose-dependent manner (Figure 8B-C, see immunohistochemistry score 8D; Figure 9B-C, see

immunohistochemistry score 9D respectively). These results were confirmed also by western blot analysis and RT-qPCR, showing a significantly reduction of VEGF and eNOS levels in the groups treated with KYP-2047 at doses of 2.5 mg/kg and 5 mg/kg compared to control (Figure 8M, see densitometric analysis 8M1; Figure 8N and Figure 9E, see densitometric analysis 9E1; Figure 9F). Additionally, we evaluated the role of CD34, a transmembrane glycoprotein involved in the process of newly forming tumors vessels by immunohistochemistry and immunofluorescence. In this context, our results showed a significant reduction of CD34 positive cells in the groups treated with KYP-2047 at doses of 2.5 mg/kg and 5 mg/kg compared to control group (Figure 8E–G; see immunohistochemistry score Figure 8H) (Figure 8I–K; see CD34 ratio positive cells score Figure 8L).

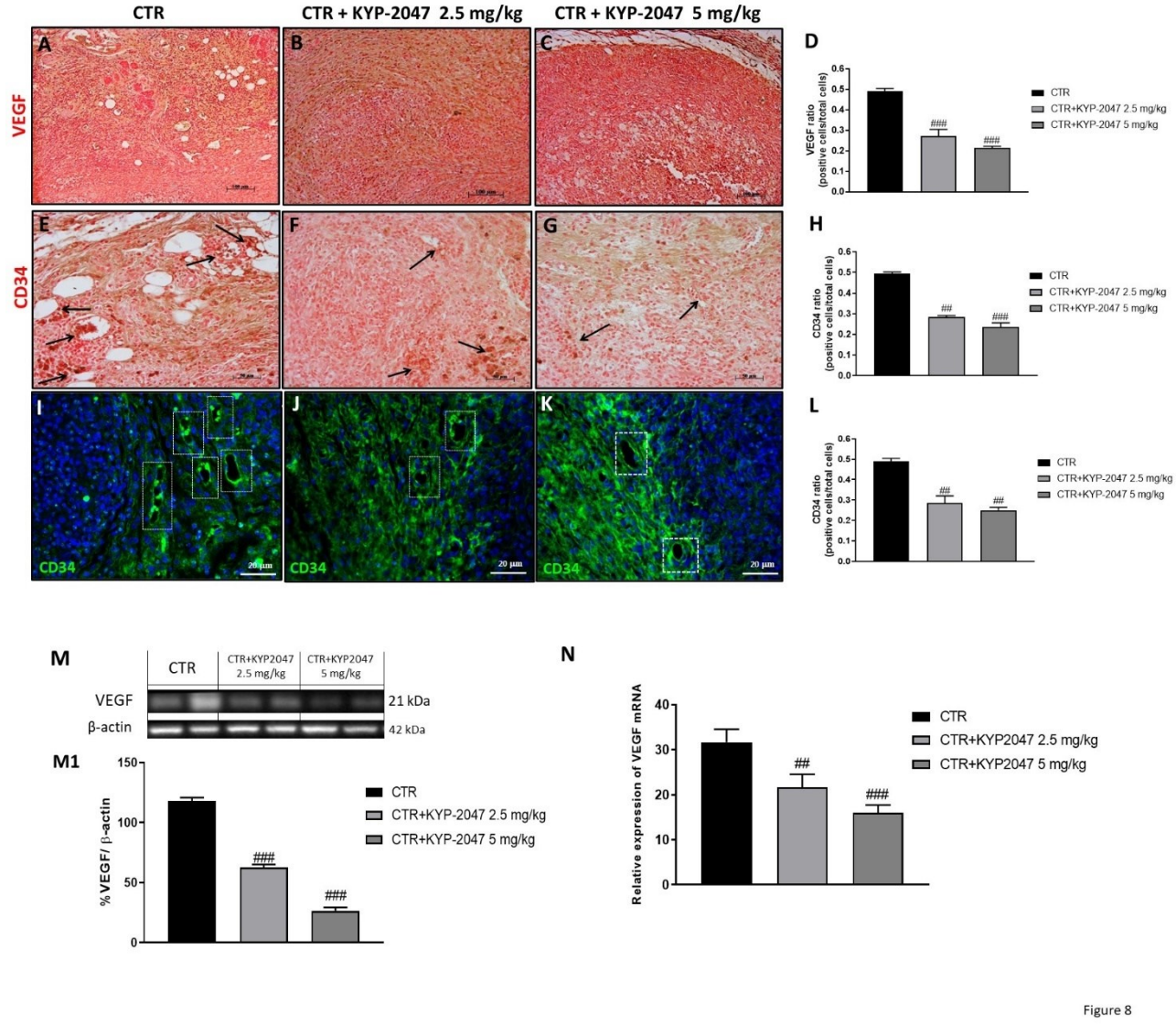

Figure 8

Figure 8. Effect of KYP-2047 on VEGF and CD34 expression. Immunohistochemical staining showed an increase of VEGF and CD34 positive cells in the control group (A, E) whereas the treatment with KYP-2047 at doses of 2.5 mg/kg and 5 mg/kg significantly reduced them (B, C, F, G). Sections were observed and photographed at 10× and 20× magnification. The data for VEGF were confirmed also by western blot analysis and RT-qPCR (M, N). Moreover, the data for CD34 were confirmed also by immunofluorescence (I, J, K). For immunofluorescence, sections were photographed at 10×, 20× and 40× magnifications. Data are representative of at least three independent experiments. (Figure and results from [171]); (D) ### $p < 0.001$ vs control group; (H) ## $p < 0.01$ vs control group; ### $p < 0.001$ vs control group; (L) ## $p < 0.01$ vs control group; (M) ### $p < 0.001$ vs control group; (N) ## $p < 0.01$ vs control group; ### $p < 0.001$ vs control group.

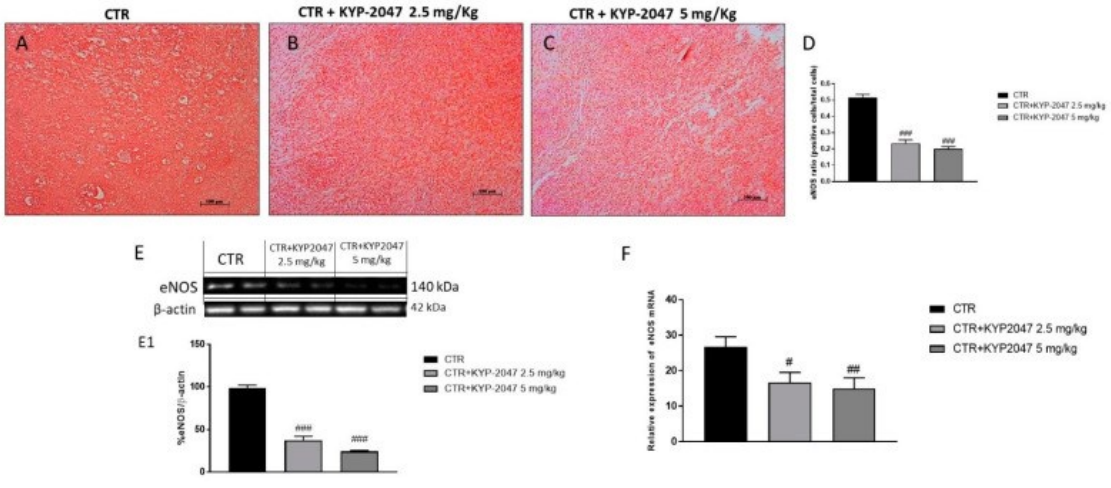

Figure 9. Effect of KYP-2047 on eNOS expression. Immunohistochemical staining showed an increase of eNOS positive cells in the control group (A) whereas the treatment with KYP-2047 at doses of 2.5 mg/kg and 5 mg/kg significantly reduced them (B, C). Sections were observed and photographed at 10× magnification. The data were confirmed by western blot analysis and RT-qPCR, showing a decrease of eNOS expression following KYP-2047 treatment (E, F). Data are representative of at least three independent experiments. (Figure and results from [171]); (D) ### $p < 0.001$ vs control group; (E) ### $p < 0.001$ vs control group; (F) # $p < 0.05$ vs control group; ## $p < 0.01$ vs control group.

7.3.3 KYP-2047 modulates angiopoietins and Ki-67 expression

Studies on angiogenesis have emphasized the importance of others angiogenic factors involved in tumor growth such as angiopoietins, in particular angiopoietin 1 (Ang1) and angiopoietin 2 (Ang2), currently proposed as biomarkers of GBM [173]. Therefore, we detected Ang1 and Ang2 expression by western blot analysis on tumor samples. Our results showed a significantly decrease of Ang1 and Ang2 levels following KYP-2047 treatment at doses of 2.5 mg/kg and 5 mg/kg compared to control (Figure 10A, see densitometric analysis 10A1; Figure 10B, see densitometric analysis 10B1) in a dose-dependent manner. Furthermore, we investigated the role of Ki-67, a nuclear protein associated with tumor proliferation and progression [174]. As shown in the Figure 10C, the blot revealed a marked expression of Ki-67 in the control group whereas the treatment with KYP-2047 at doses of 2.5 mg/kg and 5 mg/kg significantly reduced its expression (see densitometric analysis

10C1). Moreover, Ki-67 was evaluated also by immunohistochemistry confirming the previous results as shown in the Figure 10D–F (see immunohistochemistry score 10G).

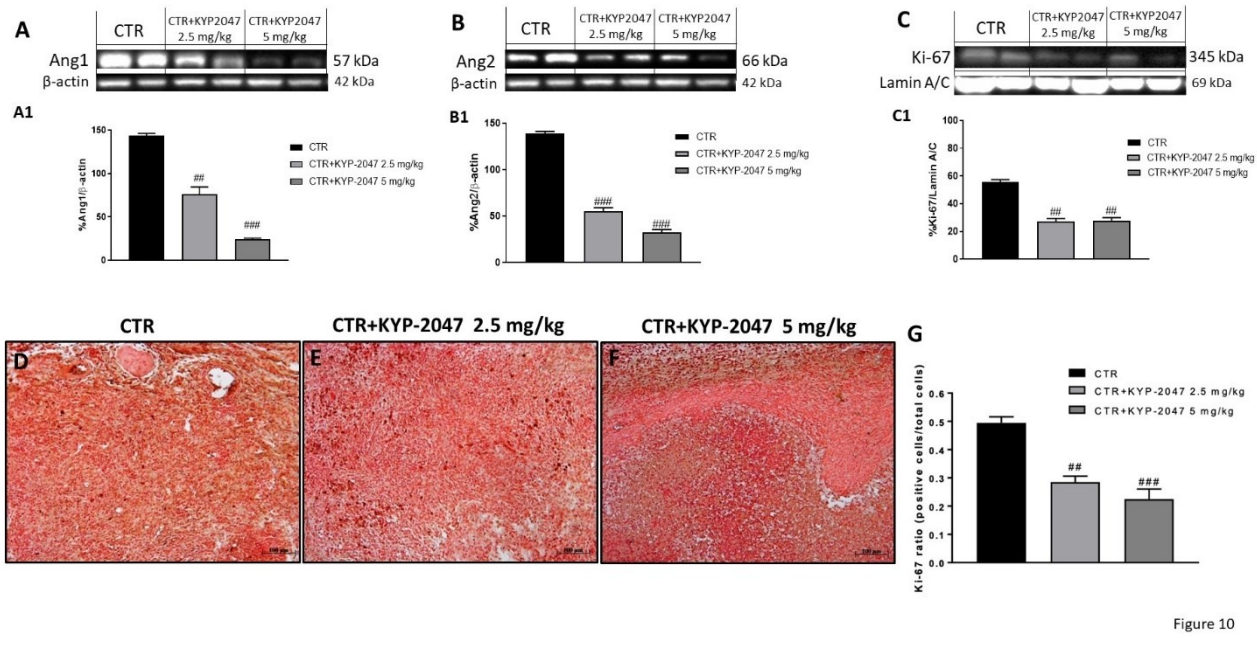

Figure 10

Figure 10. Effect of KYP-2047 on Ang1, Ang2 and Ki-67 expression. The blots revealed a significant increase of Ang1, Ang2 and Ki-67 expression in the control group while the treatment with KYP-2047 at doses of 2.5 mg/kg and 5 mg/kg significantly reduced their expression (A, B, C). The data for Ki-67 was confirmed also by immunohistochemistry (D-E-F). Sections were observed and photographed at 10× magnification. Data are representative of at least three independent experiments. (Figure and results from [171]); (A) ## $p < 0.01$ vs control group; ### $p < 0.001$ vs control group; (B) ### $p < 0.01$ vs control group; (C) ## $p < 0.01$ vs control group; (G) ## $p < 0.01$ vs control group; ### $p < 0.001$ vs control group.

7.3.4 KYP-2047 enhances apoptosis by modulating Bax and Bcl2 expression

Considering the key role of apoptosis in GBM progression, we evaluated the pro-apoptotic Bax, and anti-apoptotic Bcl2 protein by western blot analysis on tumor samples. The results showed that KYP-2047 was able to increase Bax expression and reduce Bcl2 expression (Figure 11A; see densitometric analysis 11A1; Figure 11B, see densitometric analysis 11B1). Moreover, the ability of KYP-2047 to modulate Bcl2 expression was confirmed by immunohistochemistry as shown in Figure 11C–E (see immunohistochemistry score 11F).

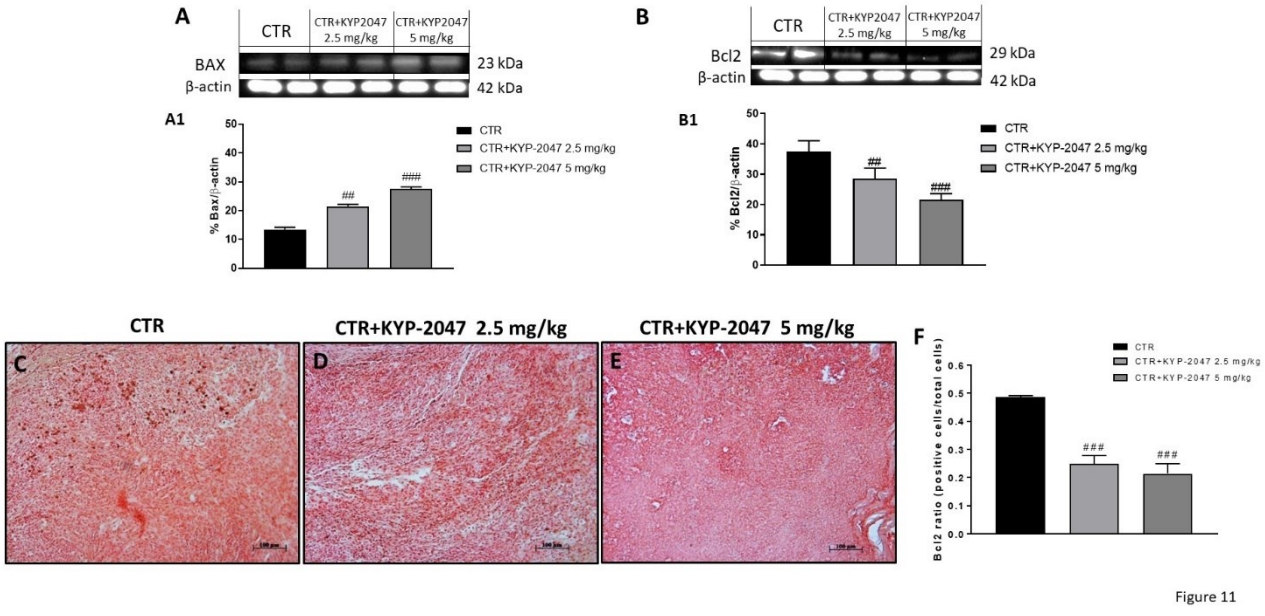

Figure 11

Figure 11. Effect of KYP-2047 on apoptosis pathway. The blots revealed an increase of pro-apoptotic Bax expression and a decrease of Bcl2 expression following KYP-2047 treatment compared to control group (A, B). Additionally, immunohistochemistry staining confirmed a decrease of Bcl2 positive cells after KYP-2047 treatment compared to control group (C-D-E). Sections were observed and photographed at 10× magnification. Data are representative of at least three independent experiments. (Figure and results from [171]); (A) ## $p < 0.01$ vs control group; ### $p < 0.001$ vs control group; (B) ## $p < 0.01$ vs control group; ### $p < 0.001$ vs control group; (F) ### $p < 0.001$ vs control group.

,

Chapter VIII: Discussion

8. Discussion

GBM is the most common and aggressive malignant tumor of the CNS [1]. GBM is characterized by diffuse infiltration of the brain tissue surrounding the bulk of the tumor [67]. Although the clinical treatment options are multiple and effective, the survival rate for patients with GBM remains low and additional therapies are needed [6]. Previous studies have demonstrated that GBMs are highly resistant to a single inhibitor, suggesting that combination approaches, involving standard chemotherapy and pathway inhibitors, might be a possible future direction for treating GBM [6, 175]. Molecular analysis of GBM revealed an overexpression of TBK1 in tumor samples, suggesting its pivotal role in cancer [18, 19]. TBK1 is a serine/threonine kinase belonging to IκB kinase family which plays important roles in the regulation of many cellular processes, such as inflammatory cytokine production, innate immunity, apoptosis, and cell proliferation [90]. The binding of IKKε, a key component of NF-κB signalling to the TBK1 leads to the activation of NF-κB and IRF3 signalling pathways which consequently promote inflammatory flux and inhibits cell death [10, 18, 19]. Reports demonstrated high levels of TBK1 in breast cancer, cervical cancer, colorectal cancer, and gastric cancer, demonstrating that TBK1 may promote neoplastic cell survival and tumor growth through proinflammatory cytokine production and apoptosis pathway alteration [16, 18]. Different *in vitro* studies demonstrated the possible use of BX795, a specific TBK1 inhibitor, for the treatment of different cancer types as primary pancreatic ductal adenocarcinoma and melanoma [20, 25]. The compound BX795 was originally developed as a potent ATP-competitive small molecule inhibitor of PDK1; however, it has been demonstrated that BX795 was able to suppress mostly TBK1 and IKKε [23]. Thus, in the present thesis, we decided to investigate the role of TBK1/IKKε signalling pathway in GBM pathogenesis and the beneficial effect of BX795, TBK1 inhibitor, by an

in vitro and *ex vivo* model of GBM. Firstly, we evaluated *in vitro* the cytotoxicity of BX795 at different concentrations using U-87 and U-138 cell lines, demonstrating that BX795 at the concentrations of 1 and 10 μM significantly reduced GBM cell viability in a concentration-dependent manner, counteracting cancer cell proliferation.

GBM is characterized by altered regulation of the apoptosis pathway, which contributes to cancer growth [176]. Apoptosis is an essential mechanism by which the homeostatic balance between cell proliferation and cell death is maintained [177]. Apoptosis occurs thanks to two main mechanisms, specifically through two apoptotic signalling pathways, one defined as intrinsic and the other one as extrinsic [177]. The intrinsic pathway, also called mitochondrial pathway, is controlled by the balance of two proteins, Bax and Bcl2; apoptotic cell death is promoted by Bax, while Bcl2 has the opposite role. On the other hand, the extrinsic pathway involves receptors of the TNF-R family that induce cell death by activating caspases [177]. However, its deregulation can promote the development of tumours by counteracting cell death [177]. For this purpose, it has been proposed that therapeutic resistance of GBM is due to an upregulation of antiapoptotic proteins and a downregulation of proapoptotic proteins, leading to genetic instability and the activation of oncogenes that favour cell survival[178]. In this context, TBK1 acts as a promoter of cancer cell survival by triggering the NF-κB pathway which promotes the expression of anti-apoptotic Bcl-X_L [90, 179]. According to this, we found a decrease of pro-apoptotic proteins as Bax and p53, and an increase of anti-apoptotic Bcl2 protein expression in GBM cells. However, BX795 significantly reduced Bcl2 and induced Bax and p53 expression, promoting apoptotic process. Furthermore, to confirm these results, we also evaluated the involvement of specific cysteine proteases, caspase-3 and caspase-9, which play a key role in apoptosis, demonstrating that BX795 induced caspase-3 and caspase-9 expression, confirming further apoptosis induction. GBM tumors are highly vascularized,

and glioma growth depends on the formation of new blood vessels through activating oncogenes and/or downregulating tumor suppressor genes [168, 173]. As known, angiogenesis is a complex process involving proliferation, migration, and differentiation of vascular endothelial cells (ECs) under the stimulation of specific signals[26]. It is controlled by the balance between its promoting and inhibiting factors [26]. In this field, TBK1 has been proposed as a putative mediator in tumor angiogenesis and tumor-associated microvascular inflammation [15]. Therefore, based on these considerations, we investigated the role of BX795 on the angiogenesis pathway by evaluating proangiogenic factors such as VEGF and IRF3, showing that BX795 reduced VEGF and IRF3 expression, contrasting the development of new blood vessels and the growth of GBM.

The molecular pathogenesis of GBM is thought to involve multiple genetic alterations that result in aberrant activity of pathways involved in proliferation and inflammation [10]. Recent studies suggest an important role for NF-κB signalling in GBM [10]. Increased expression of TBK1, which was observed in solid tumors, could be explained, in part, by inflammatory processes within the tumor and/or by infiltrating lymphocytes [18, 19]. TBK1 and IKKε have been studied extensively in relation to their functions in promoting the type I interferon response. IKKε is highly expressed in a variety of malignant tumors, and it plays an important role in tumorigenesis [16]. The binding between TBK1 and IKKε promotes interferon regulatory factor (IRF3 and IRF7) phosphorylation and NF-κB nuclear translocation, causing a substantial inflammatory response [16]. Therefore, in this context, we investigated the effect of BX795 on inflammatory pathway by analysing the expression of important regulatory factors of NF-κB pathway, as IKKα and NIK. High NIK activity is associated with different human malignancies [167]. Recent findings show that NIK promotes glioma cell invasion and

tumor-associated angiogenesis [167]. Our results clearly demonstrated that BX795 reduced NIK and IKKα expressions in GBM cells, denoting an inhibition of the inflammatory process. To confirm the anti-inflammatory effects of BX795, we also evaluated some proinflammatory cytokine levels such as TNF-α and IFN-β, demonstrating that BX795 significantly reduced their levels in GBM cells.

Despite these promising results obtained by an *in vitro* model of GBM, we conducted an *ex vivo* model on primary GBM cell obtained from patients to confirm the effects of BX795. In accordance with the *in vitro* results, our data demonstrated that BX795 exerted cytotoxic effect on primary GBM cells, confirming the antiproliferative effect. Moreover, our results confirmed the direct involvement of TBK1 in GBM pathophysiology, showing also a significantly decrease in TBK1 expression after BX795 treatment on primary GBM cell as well as a reduction of IRF3 and IFN-γ expression, two key proteins phosphorylated by TBK1. Many studies also suggested the involvement of SOX3 in tumorigenesis; SOX3 acts as an oncogene by promoting cell proliferation, migration, and invasion [170]. High levels of SOX3 expression were detected in a subset of primary glioblastoma samples compared to nontumoral brain tissues [170]. In GBM, SOX3 is able to promote cancer progression as shown in our data; however, BX795 treatment significantly reduced its expression.

As previously discussed, GBM is considered one of the most highly angiogenic solid tumor [173]. Its tumor vasculature is both structurally and functionally abnormal, characterized by a dense network of vessels tortuous with increased diameter and thickened basement membranes [26]. Recently, studies have demonstrated the involvement of PREP, a serine peptidase, in the process of carcinogenesis [32]. PREP is a proteinase constitutively expressed in all cells which is involved in the release of pro-angiogenic, and proline-containing bioactive peptides, including angiotensins, arginine-

vasopressin, substance P, and neurotensin [134]. It has been demonstrated that PREP modulates the formation of new blood vessels and cell death process; however, its alteration can contribute to cancer pathogenesis [32, 134]. According to this, a correlation between high PREP levels and cancer growth has been demonstrated [32], suggesting the development of potential PREP-inhibitors as a promising strategy for cancer treatment. In the last decade, several PREP inhibitors have been developed like KYP-2047 (4-phenylbutanoyl-L-prolyl-2(S)-cyanopyrrolidine). KYP-2047 is a highly specific and potent PREP inhibitor whose pharmacokinetics properties have been described in detail [124]. Different *in vitro* and *in vivo* studies revealed that KYP-2047 is able to modulate inflammatory pathway by reducing NF-κB/IκBα activation, and angiogenesis process through PREP inhibition [30, 34, 160]. Thus, based on these findings, the second aim of the present thesis was to investigate the role of PREP in GBM and the beneficial effects of KYP-2047, PREP inhibitor, by an *in vivo* model of GBM.

Firstly, we evaluated the ability of KYP-2047 to counteract tumour growth using the U87-xenograft model. Histological analysis showed a high-grade necrosis and neutrophil infiltration in the control group, while the treatment with KYP-2047 at higher doses significantly reduced subcutaneous tumour mass as well as neutrophil infiltration through PREP inhibition. Moreover, KYP-2047 significantly decreased tumor volume at higher doses, without encountering important weight differences. Interestingly, the treatment with KYP-2047 decreased PREP levels in serum of animals, particularly from day 14.

Various angiogenic factors and genes have been identified that stimulate glioma angiogenesis such as VEGF and CD34 [180, 181]. Therefore, in this study we decided to investigate VEGF and CD34 expression, showing that KYP-2047 at higher doses was able to reduce their expression significantly compared to the control group. Moreover, we studied the role of eNOS, a relevant endothelial enzyme that modulates vascular

homeostasis and vessel integrity, showing that the control group was characterized by an increase of eNOS expression, whereas KYP-2047 significantly reduced its expression. In addition to VEGF, other angiogenic factors are involved in cancer progression, like the angiopoietins, in particular angiopoietin 1 (Ang1) and angiopoietin 2 (Ang2) which are specific for endothelial cells [173]. Previous studies demonstrated that Ang1 and Ang2 regulate vascular development and remodelling, promoting tumor growth [182]. According to this, we found an increase of Ang1 and Ang2 expression in the control group; however, the treatment with KYP-2047 was able to significantly reduce their expression, inhibiting GBM proliferation.

An increased vascularization provides to the tumor cells more oxygen and nutrients, promoting metastatic spread and cell proliferation [183, 184]. In this context, Mastronardi and colleagues [184] evaluated the correlation between angiogenesis and proliferation processes, through Ki-67 evaluation, a nuclear protein that regulates the cell cycle. Ki-67 is considered a relevant marker of tumor proliferation in GBM [184, 185]. Thus, we decided to assess Ki-67 expression, demonstrating that the control group was characterized by an increase of Ki-67 expression, in contrast KYP-2047 treatment was able to significantly decrease its expression.

Moreover, considering the key role of apoptosis in GBM progression [165], we decided to investigate Bax and Bcl2 expression, demonstrating that KYP-2047 was able to increase pro-apoptotic Bax expression and reduce Bcl2 expression.

In summary, our results demonstrated the direct involvement of TBK1/IKKε and PREP signalling pathways in GBM, offering new insights into their role in brain tumours like GBM. Additionally, the data suggested that the use of BX795, TBK1 inhibitor, and KYP-2047, PREP inhibitor, respectively, could represent an available strategy for the treatment of GBM.

Chapter IX: Conclusions

9. Conclusions

In conclusion, the results from this thesis demonstrated the involvement of TBK1/IKKε and PREP signalling pathways in GBM, one of the most aggressive tumours of the CNS whose mortality is extremely high due to resistance to currently therapies.

As before mentioned, GBM is extremely resistant to most treatments because of its heterogeneous nature, which is associated with clonal plasticity and the presence of cancer stem cells refractory to TMZ- and RT-induced cell death. Therefore, the identification of new molecular target and of new molecules capable of overcoming these resistances represents an important goal in the field of oncological research.

According to this, in the present thesis, it is hypothesised that upregulation/overexpression of TBK1 and PREP signalling pathways increases GBM growth by modulating several pro-inflammatory and angiogenic factors which can accelerate cancer progression.

Moreover, the obtained data suggested that the use of specific TBK1/IKKε inhibitors like BX795, or PREP inhibitors like KYP-2047, could represent a potential and alternative therapeutic treatment to counteract GBM advancement thanks their abilities to modulate inflammation, angiogenesis, and apoptosis processes.

However, considering the limitations of preclinical models, further studies are needed for a fuller understanding of TBK1 and PREP mechanisms of action in GBM pathology.

Part II

Abstract

Chemotherapy, and radiotherapy may induce clinically relevant tumor-targeting immune responses. Immunogenic cell death (ICD) represents a functionally unique response pattern that is accompanied by the active secretion, or passive release of several danger-associated molecular patterns (DAMPs), which consequently promotes the recruitment and activation of immune cells. In the context of ICD, formyl peptide receptor-1 (FPR1)/Annexin-1 (AnxA-1) signalling pathway plays a key role. A loss-of-function allele of the gene coding for FPR1 was associated with poor metastasis-free and overall survival in breast and colorectal cancer patients receiving adjuvant chemotherapy, suggesting its importance in chemotherapy-induced anticancer immune response. Moreover, it has been demonstrated that TLR3 agonists compensate FPR1 deficiency, suggesting novel interesting properties of these molecules. Based on these findings, the aim of the present thesis was to evaluate the antineoplastic effect of TL-532, a new TLR3 agonist, in re-establishing immune response in *Fpr1* $^{-/-}$ fibrosarcoma-bearing mice by an *in vivo* syngeneic model. The results demonstrated that TL-532 significantly reduced tumor growth when administrated in combination with mitoxantrone (MTX) and cyclophosphamide (CTX) in WT mice bearing WT tumors compared to MTX-CTX group alone. Conversely, MTX-CTX did not exert any significant effect when either *Fpr1* (on immune cells) or its ligand *AnxA1* (on tumor cells) are absent. Nevertheless, TL-532, in combination with the chemotherapy, significantly decreased tumor growth in WT mice bearing *AnxA* $^{-/-}$ tumors and in *Fpr1* $^{-/-}$ mice bearing WT tumors, by compensating FPR1 deficiency. In conclusion, our data revealed that TL-532 could be considered an effective strategy to compensate FPR1 defect, restoring chemotherapy-immune response.

Keywords: Immunogenic cell death, formylpeptide receptor-1, Annexin-1, immunosurveillance, chemotherapy.

List of abbreviations:

Immunogenic cell death: ICD

Formylpeptide receptor 1: FPR1

Annexin-1: AnxA-1

Mitoxantrone: MTX

Cyclophosphamide: CTX

Danger-associated molecular patterns: DAMPs

Toll like receptor: TLR

Pattern recognition receptors: PRRs

Dendritic cells: DCs

Natural killer: NK

Cytotoxic T lymphocytes: CTLs

Regulatory T cells: Tregs

Major histocompatibility complex: MHC

Chapter I: Introduction

1. Introduction

Dysregulation of the regulated cell death program (RCD) represents one of the strategies adopted by cancer cells to support and increase their growth [186]. Immunogenic cell death (ICD) is a regulated form of cell death that induces the activation of innate and adaptive immune responses [187, 188]. Several chemotherapeutic agents including mitoxantrone (MTX) and cyclophosphamide (CTX), may induce ICD, which represents a functionally unique response pattern that culminates with the active secretion, or passive release of numerous danger-associated molecular patterns (DAMPs) [189]. Among DAMPs, the cytoplasmic protein annexin A1 (AnxA1) plays a key role in ICD. AnxA1, belonging to the annexin superfamily of $Ca2^{+}$ dependent phospholipid binding proteins, is expressed in many tissues and cell types, such as leukocytes, lymphocytes, and mast cells. In the context of ICD, AnxA1 mediates its effects via interaction with formylated peptide receptor-1 (FPR1), a seven-transmembrane G protein-coupled receptor expressed by myeloid cells such as dendritic cells (DCs) [190]. It has been demonstrated that lacking AnxA1 in tumor cells and/or FPR1 in immune cells, dying cancer cells are incapable to interact with DCs which are essential to recognize and lysis cancer cells [191]. Therefore, the absence of AnxA1 and/or FPR1 reduces the capacity of anthracycline-based chemotherapy to generate an effective immune response against cancer cells [191]. Epistatic analyzes demonstrated that loss-of-function allele of *Fpr1* (rs867228, E346A) is associated with poor prognosis in patients with breast and colorectal cancer treated with anthracycline-based chemotherapy [192, 193]. Recent studies explored the simultaneous effects of the single nucleotide polymorphisms (SNPs) *Fpr1* (rs867228), Toll like receptor 3 (*tlr3)* (rs3775291) and *tlr4* (rs4986790) on the survival of patients with breast cancer, proving that all three polymorphisms act on a signalling pathway, likely related to the establishment of an immune response [194]. Therefore, it has been suggested that the use of TLR3 agonists, in combination with the

chemotherapy, could overcome FPR1 deficiency, restoring immunosurveillance [191]. TLRs belong to pattern recognition receptors (PRRs) family that detect conserved molecular motifs in microbial and endogenous products, which are generally referred to as microbe- or damage-associated molecular patterns (MAMPs or DAMPs). Among TLRs, TLR3 plays a key role in pathogen recognition and activation of innate immunity; its engagement in DCs stimulates their maturation into potent immunostimulatory cells endowed with the ability to efficiently cross-prime T lymphocytes [191]. In the last years, polyinosinic: polycytidylic acid (poly(I:C)), a TLR3 agonist, have been extensively studied in several preclinical models for its antineoplastic potential [191]. Poly(I:C) is a synthetic dsRNA whose activation occurs upon binding to TLR3 leucine-rich repeats (LLR) domain. Numerous effects of poly(I:C) have been attributed to TLR3-mediated killing of cancer cells or the activation of immune effectors including DCs, natural killer (NK) cells and macrophages [191]. Recently, poly(I:C) has been introduced into clinical trials as an adjuvant for stimulating anticancer immune responses by vaccination [195]. Thus, encouraged by these findings, attempts are on the way to create new TLR3 ligands able to restore immune function. Based on these considerations, the present thesis aimed to investigate the effects of a new TLR3 agonist, TL-532, in re-establishing the anticancer immune response caused by FPR1 deficiency using an *in vivo* syngeneic model.

Chapter II: Cancer features, immunosurveillance and immunoediting

2. Cancer features, immunosurveillance and immunoediting

Cancer refers to any one of a large number of diseases characterized by the development of abnormal cells that divide uncontrollably and have the ability to infiltrate and destroy normal tissue [196]. Cellular transformation and tumor development result from an accumulation of mutational and epigenetic changes that alter normal cell growth and survival pathways [13]. According to epidemiological data from the National Cancer Institute, in 2018, there were 18.1 million new cases and 9.5 million cancer-related deaths worldwide [197]. The most common cancers are breast cancer, lung cancer, prostate cancer, colon and rectum cancer, melanoma of the skin, bladder cancer, non-Hodgkin lymphoma, kidney and renal cancer, endometrial cancer, leukemia, pancreatic cancer, thyroid cancer, and liver cancer [197]. Despite recent progresses in early diagnosis of this malignancy and in the discovery of new clinical approaches, the rate of mortality is still increasing. The treatment of cancer includes several therapeutical approaches such as surgery, immunotherapy, radiotherapy and/or chemotherapy [198]. The success of these treatments has been attributed to their ability to destroy cancerous cells or their capacity of inducing a cell cycle arrest which depend on tumor-intrinsic biological properties. Cancer possesses various recognized hallmarks, each of which influences the immunological characteristics of tumour cells [198]. Tumours can become self-sufficient for growth signals by producing autocrine and paracrine growth factors that have immunosuppressive properties [198]. Moreover, tumours can evade apoptosis by overexpressing mitochondrial cell-death inhibitors and avoiding caspase activation. Others important hallmarks of cancer are: angiogenesis alteration which involves the production of angiogenic factors, such as VEGF, that consequently inhibit dendritic-cell maturation and T-cell activation, and local invasion and metastasis [198].

In the last years, particular attention was given to the role of immune system in oncogenesis and tumor progression. Galon and colleagues [199] for the first time supported the hypothesis that adaptative immune response influences the behaviour of human cancers. In particular, data from clinical studies demonstrated the presence of specific immune cell population in neoplastic lesions, including $CD8^+$ cytotoxic T lymphocytes, helper T lymphocytes 1 (Th1), NK cells, and DCs, suggesting that could be considered prognostic markers in cancer [200]. The concept of cancer immunosurveillance predicts that the immune system can identify precursors of cancer and, in most cases, destroy these precursors before they become clinically apparent [198]. Evidence that supports the idea that immunosurveillance has a role in the suppression of human cancer is provided by the finding that immunodeficiencies predispose patients to the development of cancer [200]. Accordingly, it has been demonstrated that in patients with colorectal carcinoma, the presence of mRNA encoding molecules expressed by effector T helper 1 (Th1) cells (such as CD8α, IFN-γ and IFN-regulatory factor 1) and effector memory T cells is correlated with reduced metastatic invasion and increased survival of the patients [198]. However, immune system can exert pro- and anti-tumor effects, depending on the specific context. The immune system possesses three primary roles in the prevention of tumors [200]. Firstly, the immune system can protect the host from virus-induced tumors by eliminating or suppressing viral infections. Second, the timely elimination of pathogens and prompt resolution of inflammation can prevent the establishment of an inflammatory environment conducive to tumorigenesis. Third, the immune system can specifically identify and eliminate tumor cells based on their expression of tumor-specific antigens or molecules induced by cellular stress [198]. However, despite immunosurveillance, tumors continue to develop even in the presence of a functioning immune system. Therefore, based on these considerations, the new concept of "cancer immunoediting" was developed which refers

to the dual host-protective and tumor-promoting actions of immunity [201]. Cancer immunoediting is considered a dynamic process comprised of three distinct phases: elimination, equilibrium, and escape [201]. Elimination phase is a modern view of the older notion of cancer immunosurveillance, in which innate and adaptive immunity work together to detect and destroy transformed cells [201]. However, sometimes, tumor cell variants may not be completely destroyed but instead enter into an equilibrium phase in which the immune system controls their growth [201]. The functional dormancy of the tumor cell population may be broken, leading to progression of the cells into the escape phase, during which edited tumors of reduced immunogenicity begin to grow progressively in an immunologically unrestrained manner, establishing an immunosuppressive tumor microenvironment [201]. The elimination and equilibrium phases are mediated by cytotoxic T lymphocytes (CTLs), type I helper (Th1) $CD4^+$ T lymphocytes, and NK cells; while the escape phase is characterized by accumulation of cells that suppress anticancer immunity, such as regulatory T cells (Tregs) and immunosuppressive myeloid cells [202].

Chapter III: Chemotherapy-induced antitumor immunity

3. Chemotherapy-induced antitumor immunity

Emerging evidence suggests that the clinical success of chemotherapy is not merely due to tumor cell toxicity but also arises from the restoration of immunosurveillance [202]. Tumor development is not only driven by activation of oncogenes and inactivation of tumor suppressors, but also by alterations in the tumor microenvironment (TME) [202]. These alterations reflect the ability of tumors to generate immunosuppressive signals and foster immunosuppressive cells in the TME. In anticancer immune response, CTLs utilize T cell receptor (TCR) and CD8 to recognize antigens presented by major histocompatibility complex (MHC) class I molecules on the plasma membrane of tumor cells, leading to release of perforin-1 (PRF1) and granzyme B to induce cytotoxicity [202]. CTLs also suppress tumor growth by releasing IFNγ, an immuno-stimulatory cytokine. Th1 $CD4^+$ T lymphocytes recognize antigens presented by MHC class II molecules on the plasma membrane of target cells through TCR and CD4 and release a variety of immuno-stimulatory cytokines such as IFNγ and interleukin-2 (IL-2) [202]. Upon the activation of NK cells, cancer cells lose inhibitory signals and present ligands to NK cell-activating receptors including CD226. CTLs and Th1 $CD4^+$ T lymphocytes are actively involved in local immunosurveillance, while NK cells primarily defend against tumor metastasis [202]. An effective antitumor immune response is often triggered by a combination of lymphocytes and a subset of DCs [203]. Conventional chemotherapy may exert anti-tumor immune responses by “on-target” effect, which directly increases immunogenicity of targeted cancer cells, or through “off-target” effect on different immune cell populations, leading to alteration of the whole-body physiology, favouring anti-cancer immunosurveillance [203]. Chemotherapeutic agents may act by marked lymphodepletion or so-called ‘reset’ of the immune system, decreased immunosuppressive cells, including M2-like tumor-associated macrophages (TAMs), and Tregs, or by activation of effector cells such as CTLs and DCs [203]. Accumulating

evidence suggest that reactivation of immunosurveillance is critical for better prognosis and improved patient survival, which can be achieved by using agents that induce cellular death in tumor cells [203].

Chapter IV: Immunogenic cell death (ICD)

4. Immunogenic cell death (ICD)

Cancer is characterized by uncontrolled cell proliferation and/or evasion of cell death [189]. Dysregulation of the regulated cell death program (RCD) represents one of the strategies adopted by neoplastic cells to strengthen and enhance their growth. ICD is a type of RCD which stimulates an immune response against dead-cell antigens, in particular when they derive from cancer cells [189]. ICD involves changes in the composition of cell surface as well as the release of soluble mediators, occurring in a defined temporal sequence. It constitutes a prominent pathway for the activation of the immune system against cancer, which in turn determines the long-term success of anticancer therapies [189]. The ability of RCD including ICD, to drive adaptive immunity depends on two major parameters, neither of which is ultimately intrinsic to dying cells: antigenicity and adjuvanticity [188]. Antigenicity is conferred by the expression and presentation of antigens that fail to induce clonal deletion in the context of central tolerance in a specific host, implying that the host contains naïve T cell clones that can recognize such antigens [188]. Thus, healthy cells are limited in their ability to drive ICD, as their antigens are typically expressed by the thymic epithelium during T cell development [188]. Conversely, malignant cells, display sufficient antigenicity to drive immune responses, as they express a panel of antigenic epitopes for which naïve T cell clones are generally available [188]. Adjuvanticity is provided by the coordinated release or exposure of danger signals that are necessary for the recruitment and maturation of antigen-presenting cells (APCs), which are referred to as DAMPs [189](Figure 5).

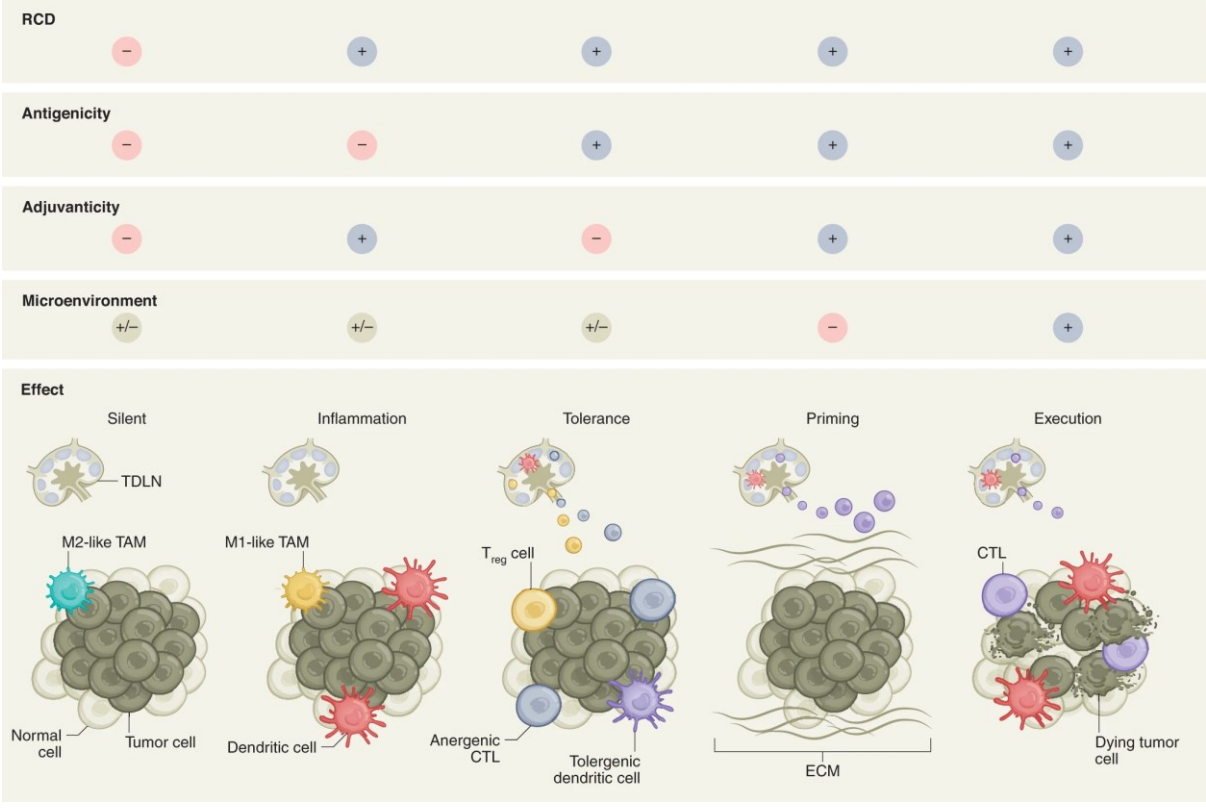

Figure 5. Hallmarks of ICD (Figure from [189]).

Dying cancer cells can stimulate different immune cells by inflammatory, chemical mediators, and DAMPs, which represent the connection between cell death induction and immune response [189]. Many of the ICD pathways have a key role in the induction of antitumour immunity, becoming of interest for biomedical research. The key mechanism triggering antitumour immune responses, especially during ICD, involves the recruitment and activation of DCs [204]. The induction of an adaptive immune response begins when DCs engulf fractions of cancer cells or interact with cancer cells promoting ICD. This process leads to the formation of tumour-associated antigens (TAAs) that will determine DC maturation and differentiation with secretion of pro-inflammatory cytokines, such as IL-1β, IL-12 and TNF-α [204]. Following migration through lymphatic vessels to lymph nodes, DCs deliver antigens to naïve T lymphocytes that instruct differentiation in $CD8^+$ cytotoxic and $CD4^+$ helper T cells [204]. Activated

Th cells proliferate and secrete additional cytokines, producing a cascade effect on B cells, which are licensed to produce specific antibodies aimed to eliminate pathogens or damaged cells [204]. Together with shaping T cell responses, DCs release cytokines, such as IL-12, IL-18, IL-15 and IFN-γ, that promote NK cell activation and their cytolytic activity. Evidence suggests that agents inducing ICD could potentially use the dying cancer cells as 'vaccines' to reactivate immune surveillance, through the maturation of DCs and activation of CTLs as well as by enhancing the cytotoxic activity of NK cells, so as to generate a more efficient antitumour response [204].

4.1 Molecular mechanisms of ICD

ICD is a cell death process characterized by the extracellular release of DAMPs-based signals, such as calreticulin (CRT), adenosine triphosphate (ATP) and high mobility group box 1 (HMGB1) which consequently promote inflammatory processes, and the activation of immune cells, including DCs, macrophages, neutrophils and NK cells [202].

4.1.1 Calreticulin (CRT) exposure and endoplasmatic reticulum (ER) stress

ICD induced by chemotherapeutics often involves endoplasmic reticulum (ER) stress, which promotes translocation of CRT from ER lumen to the outer leaflet of plasma membrane [202]. This occurs prior to membrane exposure of phosphatidylserine (PS), a marker of apoptosis. Upon treatment with the ICD-inducing chemotherapeutics such as anthracyclines, ER stress is initiated through phosphorylation of eukaryotic translation initiation factor 2α (eIF2α) by PKR-like ER kinase (PERK) [202]. This leads to subsequent signalling events including caspase-8-dependent proteolysis of the ER protein BAP31, activation of pro-apoptotic proteins BAX and BAK, translocation of CRT from the ER to Golgi apparatus, and exocytosis of CRT-containing vesicles [202]. CRT exposure is essential as an ER immunogenic signal for the induction of tumor-

associated immune responses. CRT acts on target DCs via CD91 expressed on their surface to promote the release of pro-inflammatory cytokines (e.g., TNF-α and IL-6) and modulate the activity of type 17 helper T (Th17) cells in an immunosuppressive tumor bed [202]. The binding of CRT to CD91 also facilitates the recruitment of antigen-presenting cells (e.g., DCs) into the tumor bed, and antigen presentation to T cells, leading to activation of the immune system. Therefore, it has been proven that pharmacological or genetic inhibition of the ER stress response pathway abrogates CRT translocation and attenuates the immunological effects of cytotoxic chemotherapeutics [202]. Suppression of CRT exposure and ICD also abolishes the activity of dying tumor cells as a vaccine to trigger an anticancer immune response [202].

4.1.2 HMGB1 and TLR4 axis

HMGB1, a nuclear protein, is released from dying cells that are undergoing necrosis including programmed necrosis as well as from immune cells that recognize pathogens [205]. Upon its release, HMGB1 generates a strong inflammatory response. HMGB1 activates DCs and stimulates an optimal presentation of tumor-associated antigens to T cells due to its binding to TLR4 [206]. TLR4 is associated with ICD signalling; its inactivation diminished the DC-based cross-presentation of cancer-associated antigens and caused immune deficiency. According to this, it has been proven that inhibition of HMGB1 using blocking antibodies or siRNAs suppressed anthracycline-induced anticancer immunity [206].

4.1.3 ATP and P2RX7 axis

ATP secretion from tumor cells can trigger an immune response, and it is often associated with autophagy, a physiological process in response to stress or nutrients deprivation [100]. During autophagy process, cytoplasmic content is sequestered into double-membraned organelles through a series of ordered events, including formation of

autophagosomes, lysosomal fusion, and cargo digestion, which allow recycling of building blocks of cells into energy metabolic/anabolic reactions [100]. Blocking autophagy by a pharmacological or genetic approach limited extracellular release of ATP resulted in poor recruitment of macrophages and DCs, compromised anticancer immunity and unfavourable antitumor response [202]. Extracellular ATP released from dying cancer cells causes a strong "find-me" signal for DCs and macrophages, upon its binding to P2Y2 receptors expressed on the surface of the target cells, promoting their migration to the damaged tissue [207]. ATP can also induce the maturation of myeloid-derived DCs, which is accompanied by increased expression of CD40, CD80, CD83, and CD86, promoting immune response [202].

4.2 ICD inducers

Several anticancer drugs, such as cyclophosphamide, oxaliplatin, 5-fluorouracil and mitoxantrone, induce ICD through several molecular mechanisms [204]. Cyclophosphamide has been found to elicit an antitumour response by promoting the expansion of NK and T cells in transplantable murine glioma and lymphoma [204]. Studies on mouse models have proven that cyclophosphamide also promotes an antitumour immune response, inducing the delocalization of Gram-positive bacteria of the intestinal microbiota to secondary lymphoid organs, via gap junctions, in the intestinal epithelium, stimulating the production of Th17 cells and the secretion of IL-17 and IFN-γ [208]. Oxaliplatin stimulates ICD by inducing the ER stress-dependent exposure of CRT, as shown in a murine colorectal carcinoma [209]. Moreover, oxaliplatin can promote the activation of cytotoxic T lymphocytes in both transgenic and transplantable murine models of prostate cancers [210]. 5-Fluorouracil increases the frequency of tumour-infiltrating cytotoxic T lymphocytes in colorectal cancers, activating HMGB1 and ATP secretion, promoting antigen presentation [211].

Mitoxantrone can induce exposure of CRT in human colorectal cancer cells and the autophagic process via the release of ATP and HMGB1 from necrotic cells in pancreatic and breast cancer cells [212]. However, in the last years, one of the major challenges of cancer therapy research is to find novel natural compounds able to elicit antitumour effects through ICD induction [204]. Among these, doxorubicin has gained a great interest. Doxorubicin, belonging to the anthracycline glycoside family, is an anticancer drug with ICD properties by inducing apoptotic cell death in a caspase-dependent manner in many cancer cell types, such as colorectal carcinoma and melanoma murine cells with the consequent activation of immune response mediated by DCs and $CD8^+$ T cells [213].

Chapter V: Role of formyl peptide receptor 1 (FPR1) in chemotherapy response

5. Role of formyl peptide receptor 1 (FPR1) in chemotherapy response

FPR1 is a seven-transmembrane G protein-coupled receptor that is expressed by myeloid cells such as DCs [192]. Studies demonstrated that FPR1 could mediate various cellular processes including cell chemotaxis [192, 214]. FPR1 is also involved in the processes of tumors progression, migration, and invasion. In the context of ICD, FPR1 and his ligand AnxA1 play a key role [191]. AnxA1 is a 37 kDa cytoplasmatic protein which belongs to the annexin superfamily of Ca^{2+} dependent phospholipid binding proteins. AnxA1 is expressed in many tissues and cell types, such as leukocytes, lymphocytes, mast cells, and endothelial cells [215]. It regulates several cellular processes, including acute and chronic inflammation, intracellular vesicle trafficking, and leukocyte migration [215]. Despite the exact molecular mechanisms involved in the release of AnxA1 by cancer cells succumbing to ICD remain still unknown, it has been demonstrated that AnxA1 assists DCs activity via interaction with FPR1 [191]. The crosstalk between dying tumor cells and DCs, mediated by AnxA1 and FPR1, chemotactically guides immature DCs towards dying cells, facilitating the phagocytotic uptake of portions of tumor cells by DCs [216]. Lacking AnxA1 in tumor cells and/or FPR1 in immune cells, dying cancer cells are unable to interact with DCs which are essential to recognize and lysis cancer cells [191]. Therefore, the absence of AnxA1 and/or FPR1 reduces the capacity of chemotherapeutic agents like anthracycline to generate an effective immune response against neoplastic cells [194].

5.1 Clinical relevance of FPR1

The success of anticancer chemotherapy is linked to a durable tumor-targeting immune response. The presence of tumor infiltrating DCs and $CD8^+$ T lymphocytes at diagnosis increases the likelihood of breast cancer patients to respond to anthracyclines [194]. One

mechanism through which anthracyclines can stimulate an antitumor immunity is by inducing ICD, which also includes the involvement of TLR3 and TLR4 [194]. Vacchelli et al [194] designed a screen for identifying candidate genetic defects that negatively affect chemotherapeutic responses in DNA samples from breast cancer patients treated with adjuvant anthracycline-based chemotherapy. It has been demonstrated that only one SNP, rs867228, was significantly associated with overall survival (OS) in patient cohorts [194]. This SNP (1037A>C) affects exon 2 of the gene coding for FPR1, which provokes an amino acid substitution (E346A) that suppresses FPR1 signalling. A loss-of-function allele of *Fpr1* (rs867228, E346A) that has a high prevalence across all ethnic groups (between 20% and 30%) is associated with poor prognosis in patients with breast cancer treated with anthracycline-based adjuvant chemotherapy [194]. DCs from individuals bearing rs867228 either in heterozygosity or in homozygosity show a reduced interaction with dying tumor cells [194, 217]. Recent studies investigated the simultaneous effects of the SNPs *Fpr1* (rs867228), *tlr3* (rs3775291) and *tlr4* (rs4986790) on the survival of patients with breast cancer [194]. The negative impact of the *Fpr1* polymorphism on OS was only evident in patients with normal *tlr3* and *tlr4*, suggesting that all three polymorphisms act on a signalling pathway, likely related to the establishment of an immune response [194]. The use of TLR agonists to restore or increase immunosurveillance has demonstrated real effects as vaccine adjuvants or in combination with anti-cancer therapies [191, 194]. Thus, it has been hypothesized that the use of TLR3 agonists, in combination with chemotherapy, could overcome FPR1 deficiency, restoring immunosurveillance [191]. TLRs are an evolutionarily conserved family of pattern recognition receptors (PRRs) that detect conserved molecular motifs in microbial and endogenous products, which are generally referred to as microbe-associated molecular patterns (MAMPs) or DAMPs [218]. Among TLRs, TLR3 plays a key role in pathogen recognition and activation of innate immunity. TLR3 recognizes

double-stranded RNA (dsRNA) and its engagement in DCs stimulates their maturation into potent immunostimulatory cells endowed with the ability to efficiently cross-prime T lymphocytes [191]. In this context, several immunostimulatory molecules have been tested to compensate for the loss of FPR1 function. Accordingly, a recent study conducted by Le Naour and colleagues [191] demonstrated that immunotherapy with polyinosinic:polycytidylic acid (poly (I:C)), a synthetic dsRNA whose activation occurs upon binding to TLR3 leucine-rich repeats (LLR) domain, can overcome the functional consequence of FPR1 defect, restoring the immune response to chemotherapy. Thus, based on these considerations, attempts are on the way to create new TLR3 ligands.

Chapter VI: Aim of the thesis II

6. Aim of the thesis II

The emergence and progression of human tumors strongly depends on the interaction between cancer cells and their microenvironment, especially in its immunological components. In the last years, various immunostimulatory molecules have been developed to restore immunosurveillance and chemotherapy-immune response.

Kromer's team has proven for the first time that DCs from patients with breast and colon cancer bearing *Fpr1* mutation, rs867228, either in heterozygosity or in homozygosity, show a reduced interaction with dying tumor cells and consequently poor prognosis [194]. Considering the key role of FPR1/AnxA1 signalling in chemotherapy-immune response, the research for new compounds that can restore FPR1 deficiency represents a critical concern. Accordingly, several TLR agonists, including poly(I:C), have been studied for their abilities to restore immunosurveillance and to overcome FPR1 defect.

Thus, based on these findings, the aim of the Ph.D. thesis was to investigate the antineoplastic effect of TL-532, a new TLR3 agonist, to re-establish the anticancer immune response caused by FPR1 deficiency by an *in vivo* syngeneic model.

Chapter VII: Materials and methods

7. Materials and methods

7.1 Cell line

Murine fibrosarcoma MCA205 cells (class I MHC haplotype H-2b, syngeneic for C57BL/6 mice) were cultured in Roswell Park Memorial Institute medium (RPMI)-1640 medium supplemented with 10% (*v/v*) fetal bovine serum (FBS), 100 IU/mL, penicillin G sodium salt, 100 µg/mL streptomycin sulfate and 1 mM HEPES buffer in the incubator at 37°C and 5% CO_2.

7.2 Animals

Six- to 7-week-old female wild-type C57Bl/6 mice were obtained from Envigo (Indianapolis, IN, USA). Mice were bred and maintained in the animal facilities of the Centre de Recherche des Cordeliers in specific pathogen–free conditions in a temperature-controlled environment with 12 h light/12 h dark cycles and received food and water *ad libitum*. Animal experiments followed the Federation of European Laboratory Animal Science Association (FELASA) guidelines and followed EU Directive 63/2010. Protocol #34928–2022012015416724-v7 was approved by the Ethical Committee of the CRC (registered C2EA–05 at the French Ministry of Research).

7.3 Syngeneic model

The syngeneic solid was performed by subcutaneously injection of 3×10^5 wildtype (WT) or *AnxA1*$^{-/-}$ murine fibrosarcoma MCA205 cells into WT or *Fpr1*$^{-/-}$ mice [191]. Tumor surface (longest dimension × perpendicular dimension) was monitored every two days non-invasively using a digital caliper. When the tumor surface reached 35–60 mm^2, mice received 5.17 mg/kg i.p. MTX in 200 µl PBS and 50 mg/kg i.p. CTX in 200 µl PBS or an equivalent volume of vehicle (PBS). When appropriate, mice also received 50 µg/mice i.p. poly(I:C) or 150 µg/mice i.p. poly(A:U) or 200 µg/mice i.p. TL-532 or 2 mg/mice i.p.

TL-532 in 50 µl of PBS (injected at day 1, 4 and 7 after the other treatments). poly(I:C) and poly(A:U) are used as positive control.

7.4 Materials

Mitoxantrone dihydrochloride (MTX), cyclophosphamide (CTX), sodium chloride 0.9%, polyadenylic:polyuridylic acid (poly(A:U)) and polyinosinic:polycytidylic acid (poly(I:C)) were purchased by Sigma Aldrich (St. Louis, MO, USA). Synthesis of TL-532 and TL-532-Cy5 was executed by Horizon Discovery (Waterbeach, UK) and NittoAVECIA (Milford, MA, USA), respectively. Powders were resuspended in apyrogenic, nuclease-free, sterile 0.9% NaCl (InvivoGen, San Diego, CA, USA).

7.5 Statistical analysis

Longitudinal analysis of tumor growth data was executed. Wald test was used to compute *p* values by testing jointly that both tumor growth slopes and intercepts (on a log scale) were the same between treatment groups of interest (https://kroemerlab.shinyapps.io/TumGrowth). Tumor growth curves are represented either as: individual curves from all measurements of each mouse and group-averaged tumor size alongside its SEM computed at each time point.

Chapter VIII: Results

8. Results

8.1 TL-532 compensates FPR1$^{-/-}$ deficiency

Considering the role of FPR1 in chemotherapy response, we decided to investigate the effect of TL-532, a new TLR3 agonist, by an *in vivo* syngeneic model. The data performed into WT mice bearing WT tumors demonstrated that chemotherapy with MTX-CTX as well as poly(I:C) and poly(A:U) significantly reduced tumor growth compared to vehicle group. However, TL-532 at both doses of 200 μg/mice and 2 mg/mice further decreased tumor growth when administered in combination with MTX-CTX (Figure 12), suggesting that TL-532 could overcome FPR1 defect. Moreover, to confirm the previous results, we decided to evaluate the effects of TL-532 in WT mice bearing *AnxA1* $^{-/-}$ tumors and in *Fpr1* $^{-/-}$ mice bearing WT tumors. The results demonstrated that chemotherapy with MTX-CTX failed to yield significant effects when either *Fpr1* (on the host) or its ligand *AnxA1* (on tumor cells) were absent from the system. However, TL-532, at both doses, in combination with MTX-CTX, significantly reduced tumor growth compared to vehicle and MTX-CTX groups alone, even if the tumors lacked *AnxA1* or the host was deficient for *Fpr1* (Figure 12).

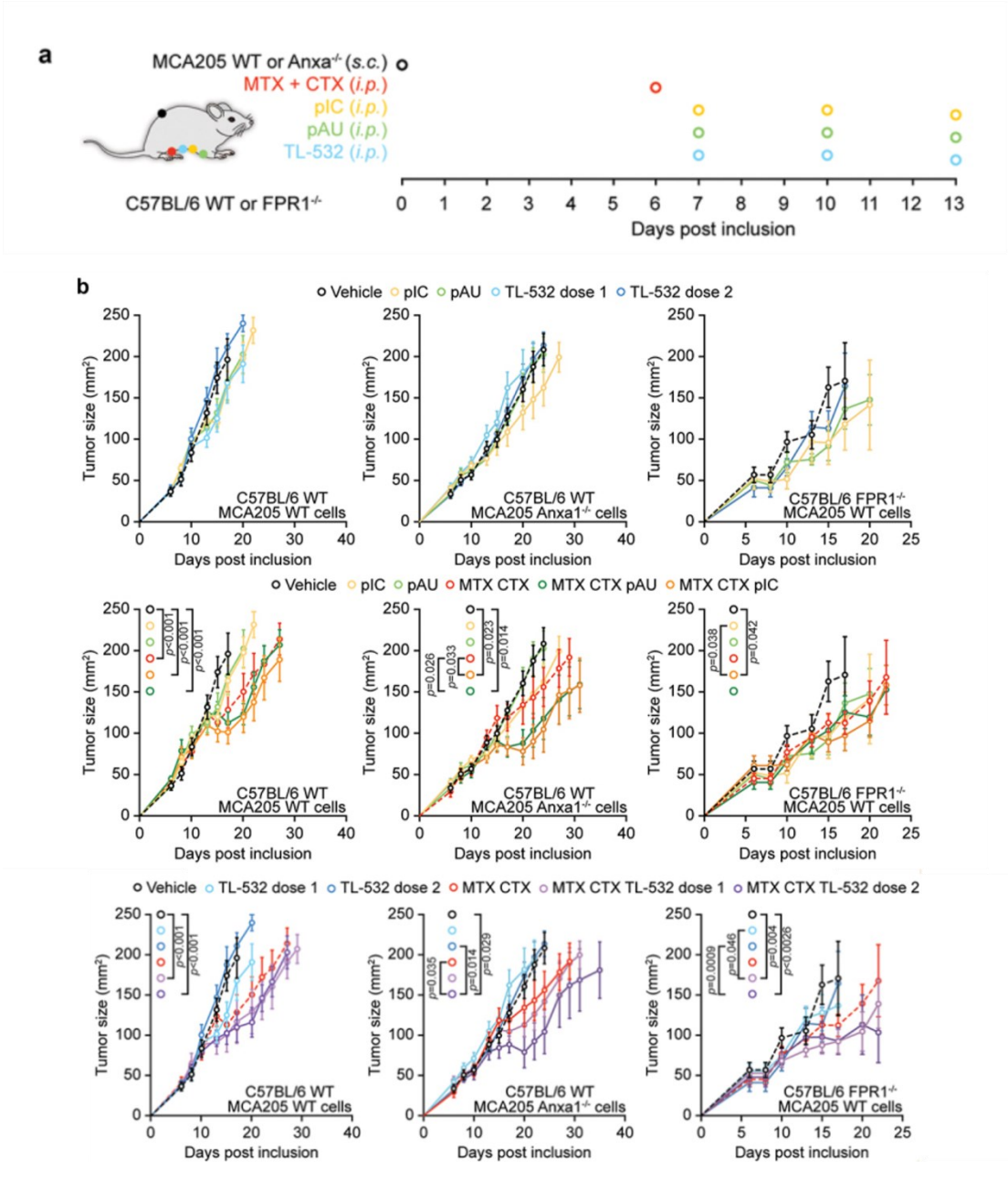

Figure 12. TL-532 restores the efficacy of chemotherapy in defective AnxA1/Fpr1 signalling mice. (A) Scheme of the in *vivo* experiment. (B) TL-532 at doses of 200 µg/mice and 2 mg/mice decreased tumor growth in WT mice bearing WT tumors when administered in combination with MTX-CTX compared to MTX-CTX group alone. Moreover, TL-532, at both doses, in combination with MTX-CTX, significantly reduced tumor growth compared to vehicle and MTX-CTX alone, even if the tumors lacked *AnxA1* or the host was deficient for *Fpr1* (Figure and results from [195]).

Chapter IX: Discussion

9. Discussion

ICD results from exposure to various agents of chemical, physical or infective origin which trigger intracellular stress mediated by reactive oxygen species (ROS) and structural alterations to the ER, leading to the sequential release of DAMPs, which, in turn promote immune system activation[188]. Among DAMPs, the cytoplasmic protein AnxA1 plays a key role in the context of ICD. AnxA1 exerts its effects via interaction with FPR1, a seven-transmembrane G protein-coupled receptor expressed by DCs [192]. Lacking AnxA1 in tumor cells and/or FPR1 in immune cells, dying cancer cells are incapable to interact with DCs which are essential to recognize and lysis cancer cells [194]. Therefore, the absence of AnxA1 and/or FPR1 reduces the capacity of anthracycline-based chemotherapy to generate an immune response against cancer cells [194]. Based on epistatic analyzes on the survival of patients with breast cancer, it has been proven that *Fpr1, tlr3* and *tlr4* polymorphisms seem to act on a signalling pathway, probably related to the establishment of an immune response [194, 217]. Therefore, since TLR3 and TLR4 act on the same immune-therapeutic pathway of FPR1, the use of TLR agonists, in combination with chemotherapy, could be a valid strategy to overcome FPR1 deficiency, restoring immunosurveillance [191]. Among TLRs, TLR3 plays a key role in ICD as its engagement in DCs stimulates their maturation into potent immunostimulatory cells endowed with the ability to efficiently cross-prime T lymphocytes. In the last years, numerous TLR agonists, including poly(I:C), have been developed to investigate their immunological and antineoplastic potential [191]. Currently, several trials are evaluating the antineoplastic effects of numerous TLR3 agonists, mostly in combination with immunotherapy or chemotherapy [195]. Therefore, based on these considerations, we decided to investigate the effects of a new TLR3 agonist, TL-532, in re-establishing the anticancer immune response caused by FPR1 deficiency. TL-532 is a chemically synthesized double-stranded RNA composed by blocks of poly(I:C) and poly(A:U)

(polyadenylic – polyuridylic acid) with interesting pharmacokinetics properties. TL-532 demonstrated to exert a significant antineoplastic effect by reducing tumor progression when administrated in combination with the chemotherapy MTX-CTX in WT mice bearing WT tumors compared to the chemotherapy group alone. Conversely, the chemotherapy with MTX-CTX failed to produce significant effects when either *Fpr1* (on the host) or its ligand *AnxA1* (on tumor cells) were absent from the system, highlighting the importance of FPR1/AnxA1 signalling in chemotherapy immune response; however, TL-532, in combination with MTX-CTX, significantly compensated FPR1 deficiency, reducing tumor growth.

Chapter X: Conclusions

10. Conclusions

In conclusion, the results of my Ph.D. thesis demonstrated that TL-532, a synthetic TLR3 agonist, is able to restore chemotherapy-induced immunosurveillance despite the defective FPR1/AnxA1 signalling pathway. These findings suggested that TL-532 could be considered a valid and alternative approach to compensate FPR1 deficiency and to re-establish chemotherapy immune response. However, further studies are needed to better understand the clinical utility of TL-532 or similar TLR3 agonists.

References

1. Omuro, A. and L.M. DeAngelis, *Glioblastoma and other malignant gliomas: a clinical review.* JAMA, 2013. **310**(17): p. 1842-50.
2. Ohgaki, H. and P. Kleihues, *Epidemiology and etiology of gliomas.* Acta Neuropathol, 2005. **109**(1): p. 93-108.
3. Ohgaki, H., P. Burger, and P. Kleihues, *Definition of primary and secondary glioblastoma--response.* Clin Cancer Res, 2014. **20**(7): p. 2013.
4. Oike, T., et al., *Radiotherapy plus concomitant adjuvant temozolomide for glioblastoma: Japanese mono-institutional results.* PLoS One, 2013. **8**(11): p. e78943.
5. Minniti, G., et al., *Radiotherapy plus concomitant and adjuvant temozolomide for glioblastoma in elderly patients.* J Neurooncol, 2008. **88**(1): p. 97-103.
6. Mallick, S., A.K. Gandhi, and G.K. Rath, *Therapeutic approach beyond conventional temozolomide for newly diagnosed glioblastoma: Review of the present evidence and future direction.* Indian J Med Paediatr Oncol, 2015. **36**(4): p. 229-37.
7. Cai, X. and M.E. Sughrue, *Glioblastoma: new therapeutic strategies to address cellular and genomic complexity.* Oncotarget, 2018. **9**(10): p. 9540-9554.
8. Scuderi, S.A., et al., *GSK343, an Inhibitor of Enhancer of Zeste Homolog 2, Reduces Glioblastoma Progression through Inflammatory Process Modulation: Focus on Canonical and Non-Canonical NF-kappaB/IkappaBalpha Pathways.* Int J Mol Sci, 2022. **23**(22).
9. Soubannier, V. and S. Stifani, *NF-kappaB Signalling in Glioblastoma.* Biomedicines, 2017. **5**(2).
10. Friedmann-Morvinski, D., et al., *Targeting NF-kappaB in glioblastoma: A therapeutic approach.* Sci Adv, 2016. **2**(1): p. e1501292.
11. Roesler, R., S.A. Dini, and G.R. Isolan, *Neuroinflammation and immunoregulation in glioblastoma and brain metastases: Recent developments in imaging approaches.* Clin Exp Immunol, 2021. **206**(3): p. 314-324.
12. Chen, L., et al., *Inflammatory responses and inflammation-associated diseases in organs.* Oncotarget, 2018. **9**(6): p. 7204-7218.
13. Greten, F.R. and S.I. Grivennikov, *Inflammation and Cancer: Triggers, Mechanisms, and Consequences.* Immunity, 2019. **51**(1): p. 27-41.
14. Zhao, H., et al., *Inflammation and tumor progression: signalling pathways and targeted intervention.* Signal Transduct Target Ther, 2021. **6**(1): p. 263.
15. Czabanka, M., et al., *Influence of TBK-1 on tumor angiogenesis and microvascular inflammation.* Front Biosci, 2008. **13**: p. 7243-9.
16. Durand, J.K., Q. Zhang, and A.S. Baldwin, *Roles for the IKK-Related Kinases TBK1 and IKKepsilon in Cancer.* Cells, 2018. **7**(9).
17. Yu, T., et al., *The pivotal role of TBK1 in inflammatory responses mediated by macrophages.* Mediators Inflamm, 2012. **2012**: p. 979105.
18. Jiang, Y., et al., *TANK-Binding Kinase 1 (TBK1) Serves as a Potential Target for Hepatocellular Carcinoma by Enhancing Tumor Immune Infiltration.* Front Immunol, 2021. **12**: p. 612139.
19. Runde, A.P., et al., *The role of TBK1 in cancer pathogenesis and anticancer immunity.* J Exp Clin Cancer Res, 2022. **41**(1): p. 135.
20. Vu, H.L. and A.E. Aplin, *Targeting TBK1 inhibits migration and resistance to MEK inhibitors in mutant NRAS melanoma.* Mol Cancer Res, 2014. **12**(10): p. 1509-19.
21. Zhu, L., et al., *TBKBP1 and TBK1 form a growth factor signalling axis mediating immunosuppression and tumourigenesis.* Nat Cell Biol, 2019. **21**(12): p. 1604-1614.
22. Thaimattam, R., et al., *Protein kinase inhibitors: structural insights into selectivity.* Curr Pharm Des, 2007. **13**(27): p. 2751-65.

23. Clark, K., et al., *Use of the pharmacological inhibitor BX795 to study the regulation and physiological roles of TBK1 and IkappaB kinase epsilon: a distinct upstream kinase mediates Ser-172 phosphorylation and activation.* J Biol Chem, 2009. **284**(21): p. 14136-46.
24. Guinn, Z.P. and T.M. Petro, *Interferon regulatory factor 3 plays a role in macrophage responses to interferon-gamma.* Immunobiology, 2019. **224**(4): p. 565-574.
25. Choi, E.A., et al., *A pharmacogenomic analysis using L1000CDS(2) identifies BX-795 as a potential anticancer drug for primary pancreatic ductal adenocarcinoma cells.* Cancer Lett, 2019. **465**: p. 82-93.
26. Ahir, B.K., H.H. Engelhard, and S.S. Lakka, *Tumor Development and Angiogenesis in Adult Brain Tumor: Glioblastoma.* Mol Neurobiol, 2020. **57**(5): p. 2461-2478.
27. Myohanen, T.T., et al., *Distribution of prolyl oligopeptidase in human peripheral tissues and in ovarian and colorectal tumors.* J Histochem Cytochem, 2012. **60**(9): p. 706-15.
28. Moreno-Baylach, M.J., et al., *Prolyl endopeptidase is involved in cellular signalling in human neuroblastoma SH-SY5Y cells.* Neurosignals, 2011. **19**(2): p. 97-109.
29. Venalainen, J.I., R.O. Juvonen, and P.T. Mannisto, *Evolutionary relationships of the prolyl oligopeptidase family enzymes.* Eur J Biochem, 2004. **271**(13): p. 2705-15.
30. Casili, G., et al., *The Inhibition of Prolyl Oligopeptidase as New Target to Counteract Chronic Venous Insufficiency: Findings in a Mouse Model.* Biomedicines, 2020. **8**(12).
31. Casili, G., et al., *The protective role of prolyl oligopeptidase (POP) inhibition in acute lung injury induced by intestinal ischemia-reperfusion.* Oncotarget, 2021. **12**(17): p. 1663-1676.
32. Liu, J.M., et al., *Overexpression of the angiogenic tetrapeptide AcSDKP in human malignant tumors.* Anticancer Res, 2008. **28**(5A): p. 2813-7.
33. Myohanen, T.T., et al., *A prolyl oligopeptidase inhibitor, KYP-2047, reduces alpha-synuclein protein levels and aggregates in cellular and animal models of Parkinson's disease.* Br J Pharmacol, 2012. **166**(3): p. 1097-113.
34. Casili, G., et al., *The Protective Role of Prolyl Oligopeptidase (POP) Inhibition in Kidney Injury Induced by Renal Ischemia-Reperfusion.* Int J Mol Sci, 2021. **22**(21).
35. Iacob, G. and E.B. Dinca, *Current data and strategy in glioblastoma multiforme.* J Med Life, 2009. **2**(4): p. 386-93.
36. Grochans, S., et al., *Epidemiology of Glioblastoma Multiforme-Literature Review.* Cancers (Basel), 2022. **14**(10).
37. Olar, A. and K.D. Aldape, *Using the molecular classification of glioblastoma to inform personalized treatment.* J Pathol, 2014. **232**(2): p. 165-77.
38. Alghamri, M.S., et al., *Targeting Neuroinflammation in Brain Cancer: Uncovering Mechanisms, Pharmacological Targets, and Neuropharmaceutical Developments.* Front Pharmacol, 2021. **12**: p. 680021.
39. Yalamarty, S.S.K., et al., *Mechanisms of Resistance and Current Treatment Options for Glioblastoma Multiforme (GBM).* Cancers (Basel), 2023. **15**(7).
40. Oliver, L., et al., *Drug resistance in glioblastoma: are persisters the key to therapy?* Cancer Drug Resist, 2020. **3**(3): p. 287-301.
41. Hanif, F., et al., *Glioblastoma Multiforme: A Review of its Epidemiology and Pathogenesis through Clinical Presentation and Treatment.* Asian Pac J Cancer Prev, 2017. **18**(1): p. 3-9.
42. Salvati, M., et al., *Radiation-induced gliomas: report of 10 cases and review of the literature.* Surg Neurol, 2003. **60**(1): p. 60-7; discussion 67.
43. Wrensch, M., et al., *Epidemiology of primary brain tumors: current concepts and review of the literature.* Neuro Oncol, 2002. **4**(4): p. 278-99.
44. Kabat, G.C., A.M. Etgen, and T.E. Rohan, *Do steroid hormones play a role in the etiology of glioma?* Cancer Epidemiol Biomarkers Prev, 2010. **19**(10): p. 2421-7.

45. Udroiu, I., J. Marinaccio, and A. Sgura, *Many Functions of Telomerase Components: Certainties, Doubts, and Inconsistencies.* Int J Mol Sci, 2022. **23**(23).
46. Reitman, Z.J., C.J. Pirozzi, and H. Yan, *Promoting a new brain tumor mutation: TERT promoter mutations in CNS tumors.* Acta Neuropathol, 2013. **126**(6): p. 789-92.
47. Olympios, N., et al., *TERT Promoter Alterations in Glioblastoma: A Systematic Review.* Cancers (Basel), 2021. **13**(5).
48. Wang, T.J., et al., *Comparisons of tumor suppressor p53, p21, and p16 gene therapy effects on glioblastoma tumorigenicity in situ.* Biochem Biophys Res Commun, 2001. **287**(1): p. 173-80.
49. Louis, D.N., et al., *The 2016 World Health Organization Classification of Tumors of the Central Nervous System: a summary.* Acta Neuropathol, 2016. **131**(6): p. 803-20.
50. Oren, M. and V. Rotter, *Mutant p53 gain-of-function in cancer.* Cold Spring Harb Perspect Biol, 2010. **2**(2): p. a001107.
51. Behling, F., et al., *Frequency of BRAF V600E mutations in 969 central nervous system neoplasms.* Diagn Pathol, 2016. **11**(1): p. 55.
52. Jimenez-Pascual, A. and F.A. Siebzehnrubl, *Fibroblast Growth Factor Receptor Functions in Glioblastoma.* Cells, 2019. **8**(7).
53. Ekstrand, A.J., et al., *Amplified and rearranged epidermal growth factor receptor genes in human glioblastomas reveal deletions of sequences encoding portions of the N- and/or C-terminal tails.* Proc Natl Acad Sci U S A, 1992. **89**(10): p. 4309-13.
54. Koul, D., *PTEN signalling pathways in glioblastoma.* Cancer Biol Ther, 2008. **7**(9): p. 1321-5.
55. Liu, A., et al., *PTEN Dual Lipid- and Protein-Phosphatase Function in Tumor Progression.* Cancers (Basel), 2022. **14**(15).
56. Tamimi, A.F. and M. Juweid, *Epidemiology and Outcome of Glioblastoma*, in *Glioblastoma*, S. De Vleeschouwer, Editor. 2017: Brisbane (AU).
57. Dobes, M., et al., *Increasing incidence of glioblastoma multiforme and meningioma, and decreasing incidence of Schwannoma (2000-2008): Findings of a multicenter Australian study.* Surg Neurol Int, 2011. **2**: p. 176.
58. Korja, M., et al., *Glioblastoma survival is improving despite increasing incidence rates: a nationwide study between 2000 and 2013 in Finland.* Neuro Oncol, 2019. **21**(3): p. 370-379.
59. Ostrom, Q.T., et al., *CBTRUS Statistical Report: Primary Brain and Other Central Nervous System Tumors Diagnosed in the United States in 2012-2016.* Neuro Oncol, 2019. **21**(Suppl 5): p. v1-v100.
60. Thakkar, J.P., et al., *Epidemiologic and molecular prognostic review of glioblastoma.* Cancer Epidemiol Biomarkers Prev, 2014. **23**(10): p. 1985-96.
61. Steponaitis, G. and A. Tamasauskas, *Mesenchymal and Proneural Subtypes of Glioblastoma Disclose Branching Based on GSC Associated Signature.* Int J Mol Sci, 2021. **22**(9).
62. Behnan, J., G. Finocchiaro, and G. Hanna, *The landscape of the mesenchymal signature in brain tumours.* Brain, 2019. **142**(4): p. 847-866.
63. Becker, A.P., et al., *Tumor Heterogeneity in Glioblastomas: From Light Microscopy to Molecular Pathology.* Cancers (Basel), 2021. **13**(4).
64. Schultz, S., et al., *Fine needle aspiration diagnosis of extracranial glioblastoma multiforme: Case report and review of the literature.* Cytojournal, 2005. **2**: p. 19.
65. Urbanska, K., et al., *Glioblastoma multiforme - an overview.* Contemp Oncol (Pozn), 2014. **18**(5): p. 307-12.
66. D'Alessio, A., et al., *Pathological and Molecular Features of Glioblastoma and Its Peritumoral Tissue.* Cancers (Basel), 2019. **11**(4).
67. Lemee, J.M., et al., *Characterizing the peritumoral brain zone in glioblastoma: a multidisciplinary analysis.* J Neurooncol, 2015. **122**(1): p. 53-61.

68. Liu, C.A., et al., *Migration/Invasion of Malignant Gliomas and Implications for Therapeutic Treatment.* Int J Mol Sci, 2018. **19**(4).
69. Vollmann-Zwerenz, A., et al., *Tumor Cell Invasion in Glioblastoma.* Int J Mol Sci, 2020. **21**(6).
70. Silantyev, A.S., et al., *Current and Future Trends on Diagnosis and Prognosis of Glioblastoma: From Molecular Biology to Proteomics.* Cells, 2019. **8**(8).
71. Buchlak, Q.D., et al., *Machine learning applications to neuroimaging for glioma detection and classification: An artificial intelligence augmented systematic review.* J Clin Neurosci, 2021. **89**: p. 177-198.
72. Gilard, V., et al., *Diagnosis and Management of Glioblastoma: A Comprehensive Perspective.* J Pers Med, 2021. **11**(4).
73. Hoosein, S., *Eyes wide open: the awake craniotomy for tumour resection: a review.* Axone, 2006. **28**(1): p. 15-8.
74. Sun, R., H. Cuthbert, and C. Watts, *Fluorescence-Guided Surgery in the Surgical Treatment of Gliomas: Past, Present and Future.* Cancers (Basel), 2021. **13**(14).
75. Patel, B. and A.H. Kim, *Laser Interstitial Thermal Therapy.* Mo Med, 2020. **117**(1): p. 50-55.
76. Roncevic, A., et al., *MALDI Imaging Mass Spectrometry of High-Grade Gliomas: A Review of Recent Progress and Future Perspective.* Curr Issues Mol Biol, 2023. **45**(2): p. 838-851.
77. Fernandes, C., et al., *Current Standards of Care in Glioblastoma Therapy*, in *Glioblastoma*, S. De Vleeschouwer, Editor. 2017: Brisbane (AU).
78. Singh, N., et al., *Mechanisms of temozolomide resistance in glioblastoma - a comprehensive review.* Cancer Drug Resist, 2021. **4**(1): p. 17-43.
79. Faustino, A.C., G.A. Viani, and A.C. Hamamura, *Patterns of recurrence and outcomes of glioblastoma multiforme treated with chemoradiation and adjuvant temozolomide.* Clinics (Sao Paulo), 2020. **75**: p. e1553.
80. Jablonska, P.A., et al., *Hypofractionated radiation therapy and temozolomide in patients with glioblastoma and poor prognostic factors. A prospective, single-institution experience.* PLoS One, 2019. **14**(6): p. e0217881.
81. Asmaa, A., et al., *Management of elderly patients with glioblastoma-multiforme-a systematic review.* Br J Radiol, 2018. **91**(1088): p. 20170271.
82. Perry, J.R., et al., *Short-Course Radiation plus Temozolomide in Elderly Patients with Glioblastoma.* N Engl J Med, 2017. **376**(11): p. 1027-1037.
83. Luksik, A.S., et al., *CAR T Cell Therapy in Glioblastoma: Overcoming Challenges Related to Antigen Expression.* Cancers (Basel), 2023. **15**(5).
84. Riley, R.S., et al., *Delivery technologies for cancer immunotherapy.* Nat Rev Drug Discov, 2019. **18**(3): p. 175-196.
85. Morgan, R.A., et al., *Recognition of glioma stem cells by genetically modified T cells targeting EGFRvIII and development of adoptive cell therapy for glioma.* Hum Gene Ther, 2012. **23**(10): p. 1043-53.
86. Zhao, L. and Y.J. Cao, *Engineered T Cell Therapy for Cancer in the Clinic.* Front Immunol, 2019. **10**: p. 2250.
87. Jogalekar, M.P., et al., *CAR T-Cell-Based gene therapy for cancers: new perspectives, challenges, and clinical developments.* Front Immunol, 2022. **13**: p. 925985.
88. Bagley, S.J., et al., *CAR T-cell therapy for glioblastoma: recent clinical advances and future challenges.* Neuro Oncol, 2018. **20**(11): p. 1429-1438.
89. Revach, O.Y., S. Liu, and R.W. Jenkins, *Targeting TANK-binding kinase 1 (TBK1) in cancer.* Expert Opin Ther Targets, 2020. **24**(11): p. 1065-1078.
90. Delhase, M., et al., *TANK-binding kinase 1 (TBK1) controls cell survival through PAI-2/serpinB2 and transglutaminase 2.* Proc Natl Acad Sci U S A, 2012. **109**(4): p. E177-86.
91. Kim, J.Y., et al., *Dissection of TBK1 signalling via phosphoproteomics in lung cancer cells.* Proc Natl Acad Sci U S A, 2013. **110**(30): p. 12414-9.

92. Oakes, J.A., M.C. Davies, and M.O. Collins, *TBK1: a new player in ALS linking autophagy and neuroinflammation.* Mol Brain, 2017. **10**(1): p. 5.
93. Ahmad, L., et al., *Human TBK1: A Gatekeeper of Neuroinflammation.* Trends Mol Med, 2016. **22**(6): p. 511-527.
94. Herhaus, L., *TBK1 (TANK-binding kinase 1)-mediated regulation of autophagy in health and disease.* Matrix Biol, 2021. **100-101**: p. 84-98.
95. Freischmidt, A., et al., *Haploinsufficiency of TBK1 causes familial ALS and fronto-temporal dementia.* Nat Neurosci, 2015. **18**(5): p. 631-6.
96. Zhang, M., et al., *Inhibitory targeting cGAS-STING-TBK1 axis: Emerging strategies for autoimmune diseases therapy.* Front Immunol, 2022. **13**: p. 954129.
97. Paterniti, I., et al., *Poly (ADP-Ribose) Polymerase Inhibitor, ABT888, Improved Cisplatin Effect in Human Oral Cell Carcinoma.* Biomedicines, 2021. **9**(7).
98. Tooley, A.S., et al., *The innate immune kinase TBK1 directly increases mTORC2 activity and downstream signalling to Akt.* J Biol Chem, 2021. **297**(2): p. 100942.
99. Van Limbergen, J., et al., *Autophagy: from basic science to clinical application.* Mucosal Immunol, 2009. **2**(4): p. 315-30.
100. Kroemer, G., G. Marino, and B. Levine, *Autophagy and the integrated stress response.* Mol Cell, 2010. **40**(2): p. 280-93.
101. Antonia, R.J., et al., *TBK1 Limits mTORC1 by Promoting Phosphorylation of Raptor Ser877.* Sci Rep, 2019. **9**(1): p. 13470.
102. Bodur, C., et al., *The IKK-related kinase TBK1 activates mTORC1 directly in response to growth factors and innate immune agonists.* EMBO J, 2018. **37**(1): p. 19-38.
103. Matsumoto, G., et al., *TBK1 controls autophagosomal engulfment of polyubiquitinated mitochondria through p62/SQSTM1 phosphorylation.* Hum Mol Genet, 2015. **24**(15): p. 4429-42.
104. Korherr, C., et al., *Identification of proangiogenic genes and pathways by high-throughput functional genomics: TBK1 and the IRF3 pathway.* Proc Natl Acad Sci U S A, 2006. **103**(11): p. 4240-5.
105. Cooper, J.M., et al., *TBK1 Provides Context-Selective Support of the Activated AKT/mTOR Pathway in Lung Cancer.* Cancer Res, 2017. **77**(18): p. 5077-5094.
106. Chien, Y., et al., *RalB GTPase-mediated activation of the IkappaB family kinase TBK1 couples innate immune signalling to tumor cell survival.* Cell, 2006. **127**(1): p. 157-70.
107. Wei, C., et al., *Elevated expression of TANK-binding kinase 1 enhances tamoxifen resistance in breast cancer.* Proc Natl Acad Sci U S A, 2014. **111**(5): p. E601-10.
108. Carr, M., et al., *IKKepsilon and TBK1 in diffuse large B-cell lymphoma: A possible mechanism of action of an IKKepsilon/TBK1 inhibitor to repress NF-kappaB and IL-10 signalling.* J Cell Mol Med, 2020. **24**(19): p. 11573-11582.
109. Cruz, V.H., et al., *Axl-mediated activation of TBK1 drives epithelial plasticity in pancreatic cancer.* JCI Insight, 2019. **5**(9).
110. Eskiocak, B., et al., *Biomarker Accessible and Chemically Addressable Mechanistic Subtypes of BRAF Melanoma.* Cancer Discov, 2017. **7**(8): p. 832-851.
111. Wang, X., et al., *Expression and prognostic role of IKBKE and TBK1 in stage I non-small cell lung cancer.* Cancer Manag Res, 2019. **11**: p. 6593-6602.
112. Lork, M., et al., *Importance of Validating Antibodies and Small Compound Inhibitors Using Genetic Knockout Studies-T Cell Receptor-Induced CYLD Phosphorylation by IKKepsilon/TBK1 as a Case Study.* Front Cell Dev Biol, 2018. **6**: p. 40.
113. Wang, T., et al., *Discovery of azabenzimidazole derivatives as potent, selective inhibitors of TBK1/IKKepsilon kinases.* Bioorg Med Chem Lett, 2012. **22**(5): p. 2063-9.
114. Reilly, S.M., et al., *An inhibitor of the protein kinases TBK1 and IKK-varepsilon improves obesity-related metabolic dysfunctions in mice.* Nat Med, 2013. **19**(3): p. 313-21.
115. Bailly, C., *The potential value of amlexanox in the treatment of cancer: Molecular targets and therapeutic perspectives.* Biochem Pharmacol, 2022. **197**: p. 114895.

116. Hasan, M. and N. Yan, *Therapeutic potential of targeting TBK1 in autoimmune diseases and interferonopathies.* Pharmacol Res, 2016. **111**: p. 336-342.
117. Yadavalli, T., et al., *Tolerability, pharmacokinetics, and anti-herpetic activity of orally administered BX795.* Biomed Pharmacother, 2023. **165**: p. 115056.
118. Yu, T., et al., *The kinase inhibitor BX795 suppresses the inflammatory response via multiple kinases.* Biochem Pharmacol, 2020. **174**: p. 113797.
119. Madavaraju, K., et al., *Prophylactic treatment with BX795 blocks activation of AKT and its downstream targets to protect vaginal keratinocytes and vaginal epithelium from HSV-2 infection.* Antiviral Res, 2021. **194**: p. 105145.
120. Chilamakuri, R., et al., *BX-795 inhibits neuroblastoma growth and enhances sensitivity towards chemotherapy.* Transl Oncol, 2022. **15**(1): p. 101272.
121. Pai, S., et al., *PDK1 Inhibitor BX795 Improves Cisplatin and Radio-Efficacy in Oral Squamous Cell Carcinoma by Downregulating the PDK1/CD47/Akt-Mediated Glycolysis Signalling Pathway.* Int J Mol Sci, 2021. **22**(21).
122. Bai, L.Y., et al., *BX795, a TBK1 inhibitor, exhibits antitumor activity in human oral squamous cell carcinoma through apoptosis induction and mitotic phase arrest.* Eur J Pharmacol, 2015. **769**: p. 287-96.
123. Garcia-Horsman, J.A., *The role of prolyl oligopeptidase, understanding the puzzle.* Ann Transl Med, 2020. **8**(16): p. 983.
124. Jalkanen, A.J., J.V. Leikas, and M.M. Forsberg, *KYP-2047 penetrates mouse brain and effectively inhibits mouse prolyl oligopeptidase.* Basic Clin Pharmacol Toxicol, 2014. **114**(6): p. 460-3.
125. Christiansen, V.J., et al., *Targeting inhibition of fibroblast activation protein-alpha and prolyl oligopeptidase activities on cells common to metastatic tumor microenvironments.* Neoplasia, 2013. **15**(4): p. 348-58.
126. Long, J.Z. and B.F. Cravatt, *The metabolic serine hydrolases and their functions in mammalian physiology and disease.* Chem Rev, 2011. **111**(10): p. 6022-63.
127. Szeltner, Z. and L. Polgar, *Structure, function and biological relevance of prolyl oligopeptidase.* Curr Protein Pept Sci, 2008. **9**(1): p. 96-107.
128. Yang, Q., et al., *PREPL Deficiency: A Homozygous Splice Site PREPL Mutation in a Patient With Congenital Myasthenic Syndrome and Absence of Ovaries and Hypoplasia of Uterus.* Front Genet, 2020. **11**: p. 198.
129. Towheed, A., et al., *Hypotonia-cystinuria 2p21 deletion syndrome: Intrafamilial variability of clinical expression.* Ann Clin Transl Neurol, 2021. **8**(11): p. 2199-2204.
130. Chabrol, B., et al., *Deletion of C2orf34, PREPL and SLC3A1 causes atypical hypotonia-cystinuria syndrome.* BMJ Case Rep, 2009. **2009**.
131. Sayol-Torres, L., et al., *Prolyl Endopeptidase-like Deficiency Associated with Growth Hormone Deficiency.* J Clin Res Pediatr Endocrinol, 2023. **15**(2): p. 205-209.
132. Tenorio-Laranga, J., et al., *The expression levels of prolyl oligopeptidase responds not only to neuroinflammation but also to systemic inflammation upon liver failure in rat models and cirrhotic patients.* J Neuroinflammation, 2015. **12**: p. 183.
133. Garcia-Horsman, J.A., P.T. Mannisto, and J.I. Venalainen, *On the role of prolyl oligopeptidase in health and disease.* Neuropeptides, 2007. **41**(1): p. 1-24.
134. Myohanen, T.T., et al., *Prolyl oligopeptidase induces angiogenesis both in vitro and in vivo in a novel regulatory manner.* Br J Pharmacol, 2011. **163**(8): p. 1666-78.
135. Mannisto, P.T. and J.A. Garcia-Horsman, *Mechanism of Action of Prolyl Oligopeptidase (PREP) in Degenerative Brain Diseases: Has Peptidase Activity Only a Modulatory Role on the Interactions of PREP with Proteins?* Front Aging Neurosci, 2017. **9**: p. 27.
136. Kumar, N., et al., *The anti-inflammatory peptide Ac-SDKP is released from thymosin-beta4 by renal meprin-alpha and prolyl oligopeptidase.* Am J Physiol Renal Physiol, 2016. **310**(10): p. F1026-34.

137. Zhang, Y., et al., *Thymosin Beta 4 is overexpressed in human pancreatic cancer cells and stimulates proinflammatory cytokine secretion and JNK activation.* Cancer Biol Ther, 2008. **7**(3): p. 419-23.
138. Wang, W., W. Jia, and C. Zhang, *The Role of Tbeta4-POP-Ac-SDKP Axis in Organ Fibrosis.* Int J Mol Sci, 2022. **23**(21).
139. Matsuda, T., et al., *Prolyl oligopeptidase is a glyceraldehyde-3-phosphate dehydrogenase-binding protein that regulates genotoxic stress-induced cell death.* Int J Biochem Cell Biol, 2013. **45**(4): p. 850-7.
140. Bar, J.W., et al., *Prolyl endopeptidase cleaves the apoptosis rescue peptide humanin and exhibits an unknown post-cysteine cleavage specificity.* Adv Exp Med Biol, 2006. **575**: p. 103-8.
141. O'Reilly, P.J., et al., *Neutrophils contain prolyl endopeptidase and generate the chemotactic peptide, PGP, from collagen.* J Neuroimmunol, 2009. **217**(1-2): p. 51-4.
142. Jiang, D.X., et al., *Prolyl endopeptidase gene disruption attenuates high fat diet-induced nonalcoholic fatty liver disease in mice by improving hepatic steatosis and inflammation.* Ann Transl Med, 2020. **8**(5): p. 218.
143. Odaka, C., et al., *Murine T cells expressing high activity of prolyl endopeptidase are susceptible to activation-induced cell death.* FEBS Lett, 2002. **512**(1-3): p. 163-7.
144. Hannula, M.J., et al., *Prolyl oligopeptidase colocalizes with alpha-synuclein, beta-amyloid, tau protein and astroglia in the post-mortem brain samples with Parkinson's and Alzheimer's diseases.* Neuroscience, 2013. **242**: p. 140-50.
145. Williams, R.S., et al., *Loss of a prolyl oligopeptidase confers resistance to lithium by elevation of inositol (1,4,5) trisphosphate.* EMBO J, 1999. **18**(10): p. 2734-45.
146. Julku, U.H., et al., *Prolyl Oligopeptidase Regulates Dopamine Transporter Oligomerization and Phosphorylation in a PKC- and ERK-Independent Manner.* Int J Mol Sci, 2021. **22**(4).
147. Perez, I., et al., *Altered Activity and Expression of Cytosolic Peptidases in Colorectal Cancer.* Int J Med Sci, 2015. **12**(6): p. 458-67.
148. Scuderi, S.A., et al., *Beneficial effect of KYP-2047, a propyl-oligopeptidase inhibitor, on oral squamous cell carcinoma.* Oncotarget, 2021. **12**(25): p. 2459-2473.
149. Gong, Y., U.D. Chippada-Venkata, and W.K. Oh, *Roles of matrix metalloproteinases and their natural inhibitors in prostate cancer progression.* Cancers (Basel), 2014. **6**(3): p. 1298-327.
150. Larrinaga, G., et al., *Prolyl endopeptidase activity is correlated with colorectal cancer prognosis.* Int J Med Sci, 2014. **11**(2): p. 199-208.
151. Duan, L., et al., *The prolyl peptidases PRCP/PREP regulate IRS-1 stability critical for rapamycin-induced feedback activation of PI3K and AKT.* J Biol Chem, 2014. **289**(31): p. 21694-705.
152. Tanaka, S., K. Suzuki, and M. Sakaguchi, *The prolyl oligopeptidase inhibitor SUAM-14746 attenuates the proliferation of human breast cancer cell lines in vitro.* Breast Cancer, 2017. **24**(5): p. 658-666.
153. Toide, K., et al., *JTP-4819: a novel prolyl endopeptidase inhibitor with potential as a cognitive enhancer.* J Pharmacol Exp Ther, 1995. **274**(3): p. 1370-8.
154. Jackson, K.W., et al., *Suppression of tumor growth in mice by rationally designed pseudopeptide inhibitors of fibroblast activation protein and prolyl oligopeptidase.* Neoplasia, 2015. **17**(1): p. 43-54.
155. Toppila, M., et al., *The Prolyl Oligopeptidase Inhibitor KYP-2047 Is Cytoprotective and Anti-Inflammatory in Human Retinal Pigment Epithelial Cells with Defective Proteasomal Clearance.* Antioxidants (Basel), 2023. **12**(6).
156. Jalkanen, A.J., et al., *Brain pharmacokinetics of two prolyl oligopeptidase inhibitors, JTP-4819 and KYP-2047, in the rat.* Basic Clin Pharmacol Toxicol, 2011. **109**(6): p. 443-51.

157. Savolainen, M.H., et al., *Prolyl oligopeptidase enhances alpha-synuclein dimerization via direct protein-protein interaction.* J Biol Chem, 2015. **290**(8): p. 5117-5126.
158. Campolo, M., et al., *TAK1 Inhibitor Enhances the Therapeutic Treatment for Glioblastoma.* Cancers (Basel), 2020. **13**(1).
159. Valentim, A.M., et al., *Euthanasia using gaseous agents in laboratory rodents.* Lab Anim, 2016. **50**(4): p. 241-53.
160. Casili, G., et al., *Therapeutic Potential of BAY-117082, a Selective NLRP3 Inflammasome Inhibitor, on Metastatic Evolution in Human Oral Squamous Cell Carcinoma (OSCC).* Cancers (Basel), 2023. **15**(10).
161. Weinert, B.T., et al., *Real-time PCR analysis of genes encoding tumor antigens in esophageal tumors and a cancer vaccine.* Cancer Immun, 2009. **9**: p. 9.
162. Campolo, M., et al., *Co-Ultra PEALut Enhances Endogenous Repair Response Following Moderate Traumatic Brain Injury.* Int J Mol Sci, 2021. **22**(16).
163. Scuderi, S.A., et al., *TBK1 Inhibitor Exerts Antiproliferative Effect on Glioblastoma Multiforme Cells.* Oncol Res, 2021. **28**(7): p. 779-790.
164. Clark, M.J., et al., *U87MG decoded: the genomic sequence of a cytogenetically aberrant human cancer cell line.* PLoS Genet, 2010. **6**(1): p. e1000832.
165. Forte, I.M., et al., *Targeted therapy based on p53 reactivation reduces both glioblastoma cell growth and resistance to temozolomide.* Int J Oncol, 2019. **54**(6): p. 2189-2199.
166. Hsu, F.T., I.T. Chiang, and W.S. Wang, *Induction of apoptosis through extrinsic/intrinsic pathways and suppression of ERK/NF-kappaB signalling participate in anti-glioblastoma of imipramine.* J Cell Mol Med, 2020. **24**(7): p. 3982-4000.
167. Duran, C.L., et al., *NIK regulates MT1-MMP activity and promotes glioma cell invasion independently of the canonical NF-kappaB pathway.* Oncogenesis, 2016. **5**(6): p. e231.
168. Hundsberger, T., D.A. Reardon, and P.Y. Wen, *Angiogenesis inhibitors in tackling recurrent glioblastoma.* Expert Rev Anticancer Ther, 2017. **17**(6): p. 507-515.
169. Stevanovic, M., et al., *SOX transcription factors and glioma stem cells: Choosing between stemness and differentiation.* World J Stem Cells, 2021. **13**(10): p. 1417-1445.
170. Marjanovic Vicentic, J., et al., *SOX3 can promote the malignant behavior of glioblastoma cells.* Cell Oncol (Dordr), 2019. **42**(1): p. 41-54.
171. Scuderi, S.A., et al., *KYP-2047, an Inhibitor of Prolyl-Oligopeptidase, Reduces GlioBlastoma Proliferation through Angiogenesis and Apoptosis Modulation.* Cancers (Basel), 2021. **13**(14).
172. Peleli, M., A. Moustakas, and A. Papapetropoulos, *Endothelial-Tumor Cell Interaction in Brain and CNS Malignancies.* Int J Mol Sci, 2020. **21**(19).
173. Groblewska, M. and B. Mroczko, *Pro- and Antiangiogenic Factors in Gliomas: Implications for Novel Therapeutic Possibilities.* Int J Mol Sci, 2021. **22**(11).
174. Rautiola, J., et al., *Association of Angiopoietin-2 and Ki-67 Expression with Vascular Density and Sunitinib Response in Metastatic Renal Cell Carcinoma.* PLoS One, 2016. **11**(4): p. e0153745.
175. Mao, H., et al., *Deregulated signalling pathways in glioblastoma multiforme: molecular mechanisms and therapeutic targets.* Cancer Invest, 2012. **30**(1): p. 48-56.
176. Valdes-Rives, S.A., et al., *Apoptotic Signalling Pathways in Glioblastoma and Therapeutic Implications.* Biomed Res Int, 2017. **2017**: p. 7403747.
177. Ouyang, L., et al., *Programmed cell death pathways in cancer: a review of apoptosis, autophagy and programmed necrosis.* Cell Prolif, 2012. **45**(6): p. 487-98.
178. Trejo-Solis, C., et al., *Autophagic and Apoptotic Pathways as Targets for Chemotherapy in Glioblastoma.* Int J Mol Sci, 2018. **19**(12).
179. Chen, C., L.C. Edelstein, and C. Gelinas, *The Rel/NF-kappaB family directly activates expression of the apoptosis inhibitor Bcl-x(L).* Mol Cell Biol, 2000. **20**(8): p. 2687-95.
180. Galloway, M., *CD34 expression in glioblastoma and giant cell glioblastoma.* Clin Neuropathol, 2010. **29**(2): p. 89-93.

181. Plate, K.H., et al., *Vascular endothelial growth factor and glioma angiogenesis: coordinate induction of VEGF receptors, distribution of VEGF protein and possible in vivo regulatory mechanisms.* Int J Cancer, 1994. **59**(4): p. 520-9.
182. Stratmann, A., W. Risau, and K.H. Plate, *Cell type-specific expression of angiopoietin-1 and angiopoietin-2 suggests a role in glioblastoma angiogenesis.* Am J Pathol, 1998. **153**(5): p. 1459-66.
183. Lugano, R., M. Ramachandran, and A. Dimberg, *Tumor angiogenesis: causes, consequences, challenges and opportunities.* Cell Mol Life Sci, 2020. **77**(9): p. 1745-1770.
184. Mastronardi, L., et al., *Relationship between Ki-67 labeling index and survival in high-grade glioma patients treated after surgery with tamoxifen.* J Neurosurg Sci, 1999. **43**(4): p. 263-70.
185. Alkhaibary, A., et al., *Ki-67 labeling index in glioblastoma; does it really matter?* Hematol Oncol Stem Cell Ther, 2019. **12**(2): p. 82-88.
186. Ahmed, A. and S.W.G. Tait, *Targeting immunogenic cell death in cancer.* Mol Oncol, 2020. **14**(12): p. 2994-3006.
187. Vanmeerbeek, I., et al., *Trial watch: chemotherapy-induced immunogenic cell death in immuno-oncology.* Oncoimmunology, 2020. **9**(1): p. 1703449.
188. Galluzzi, L., et al., *Consensus guidelines for the definition, detection and interpretation of immunogenic cell death.* J Immunother Cancer, 2020. **8**(1).
189. Kroemer, G., et al., *Immunogenic cell stress and death.* Nat Immunol, 2022. **23**(4): p. 487-500.
190. Palanivelu, L., C.H. Liu, and L.T. Lin, *Immunogenic cell death: The cornerstone of oncolytic viro-immunotherapy.* Front Immunol, 2022. **13**: p. 1038226.
191. Le Naour, J., et al., *A TLR3 Ligand Reestablishes Chemotherapeutic Responses in the Context of FPR1 Deficiency.* Cancer Discov, 2021. **11**(2): p. 408-423.
192. Vacchelli, E., J. Le Naour, and G. Kroemer, *The ambiguous role of FPR1 in immunity and inflammation.* Oncoimmunology, 2020. **9**(1): p. 1760061.
193. Sztupinszki, Z., et al., *A major genetic accelerator of cancer diagnosis: rs867228 in FPR1.* Oncoimmunology, 2021. **10**(1): p. 1859064.
194. Vacchelli, E., et al., *Chemotherapy-induced antitumor immunity requires formyl peptide receptor 1.* Science, 2015. **350**(6263): p. 972-8.
195. Le Naour, J., et al., *A Chemically Defined TLR3 Agonist with Anticancer Activity.* Oncoimmunology, 2023. **12**(1): p. 2227510.
196. Hanahan, D. and R.A. Weinberg, *Hallmarks of cancer: the next generation.* Cell, 2011. **144**(5): p. 646-74.
197. Sung, H., et al., *Global Cancer Statistics 2020: GLOBOCAN Estimates of Incidence and Mortality Worldwide for 36 Cancers in 185 Countries.* CA Cancer J Clin, 2021. **71**(3): p. 209-249.
198. Zitvogel, L., A. Tesniere, and G. Kroemer, *Cancer despite immunosurveillance: immunoselection and immunosubversion.* Nat Rev Immunol, 2006. **6**(10): p. 715-27.
199. Galon, J., et al., *Type, density, and location of immune cells within human colorectal tumors predict clinical outcome.* Science, 2006. **313**(5795): p. 1960-4.
200. Senovilla, L., et al., *Trial watch: Prognostic and predictive value of the immune infiltrate in cancer.* Oncoimmunology, 2012. **1**(8): p. 1323-1343.
201. Vesely, M.D. and R.D. Schreiber, *Cancer immunoediting: antigens, mechanisms, and implications to cancer immunotherapy.* Ann N Y Acad Sci, 2013. **1284**(1): p. 1-5.
202. Wang, Y.J., et al., *Immunogenic effects of chemotherapy-induced tumor cell death.* Genes Dis, 2018. **5**(3): p. 194-203.
203. Galluzzi, L., et al., *Immunological Effects of Conventional Chemotherapy and Targeted Anticancer Agents.* Cancer Cell, 2015. **28**(6): p. 690-714.
204. Sansone, C., et al., *Natural Compounds of Marine Origin as Inducers of Immunogenic Cell Death (ICD): Potential Role for Cancer Interception and Therapy.* Cells, 2021. **10**(2).

205. Andersson, U. and K.J. Tracey, *HMGB1 is a therapeutic target for sterile inflammation and infection.* Annu Rev Immunol, 2011. **29**: p. 139-62.
206. Apetoh, L., et al., *Toll-like receptor 4-dependent contribution of the immune system to anticancer chemotherapy and radiotherapy.* Nat Med, 2007. **13**(9): p. 1050-9.
207. Kronlage, M., et al., *Autocrine purinergic receptor signalling is essential for macrophage chemotaxis.* Sci Signal, 2010. **3**(132): p. ra55.
208. Viaud, S., et al., *The intestinal microbiota modulates the anticancer immune effects of cyclophosphamide.* Science, 2013. **342**(6161): p. 971-6.
209. Martins, I., et al., *Restoration of the immunogenicity of cisplatin-induced cancer cell death by endoplasmic reticulum stress.* Oncogene, 2011. **30**(10): p. 1147-58.
210. Shalapour, S., et al., *Immunosuppressive plasma cells impede T-cell-dependent immunogenic chemotherapy.* Nature, 2015. **521**(7550): p. 94-8.
211. Lim, S.H., et al., *Effect of neoadjuvant chemoradiation on tumor-infiltrating/associated lymphocytes in locally advanced rectal cancers.* Anticancer Res, 2014. **34**(11): p. 6505-13.
212. Colangelo, T., et al., *The miR-27a-calreticulin axis affects drug-induced immunogenic cell death in human colorectal cancer cells.* Cell Death Dis, 2016. **7**(2): p. e2108.
213. Casares, N., et al., *Caspase-dependent immunogenicity of doxorubicin-induced tumor cell death.* J Exp Med, 2005. **202**(12): p. 1691-701.
214. Liu, M., et al., *G protein-coupled receptor FPR1 as a pharmacologic target in inflammation and human glioblastoma.* Int Immunopharmacol, 2012. **14**(3): p. 283-8.
215. Gerke, V., C.E. Creutz, and S.E. Moss, *Annexins: linking Ca2+ signalling to membrane dynamics.* Nat Rev Mol Cell Biol, 2005. **6**(6): p. 449-61.
216. Lin, R.A., J.K. Lin, and S.Y. Lin, *Mechanisms of immunogenic cell death and immune checkpoint blockade therapy.* Kaohsiung J Med Sci, 2021. **37**(6): p. 448-458.
217. Carbonnier, V., et al., *Rs867228 in FPR1 accelerates the manifestation of luminal B breast cancer.* Oncoimmunology, 2023. **12**(1): p. 2189823.
218. Sameer, A.S. and S. Nissar, *Toll-Like Receptors (TLRs): Structure, Functions, Signalling, and Role of Their Polymorphisms in Colorectal Cancer Susceptibility.* Biomed Res Int, 2021. **2021**: p. 1157023.